A study on applying OpenRiverCam software to determine river discharge levels and the design of a rain radar calibration model in Thailand

Multi-Disciplinary Project Q1 2023

Group: MDP349

Authors:
Willem Toet - 4600428
Luuk van der Plas - 4713834
Dirk van Wijngaarden - 4720199
Niek Aberson - 4591984
Jochem van Lith - 4917634

Supervisors:
Dr.ir. T.A. BOGAARD - TU Delft
Dr.ir. L. VAN BIERT - TU Delft
Dr. D.M.J. TAX - TU Delft
Asst.Prof.Dr. P.P. MAPIAM - Kasetsart University

October 30, 2023

Preface

This report is written as part of a multi-disciplinary project by five master students from the Technical University Delft. This 10-week project gives students the opportunity to conduct research abroad as part of their master's studies. The group consists of master students from Hydraulic Engineering, Marine Technology and Computer Science. The research was in collaboration with the Water Resources Engineering Department of Kasetsart University, where we worked closely with master students from Thailand under the guidance of professors of both the TU Delft and Kasetsart University. The research focuses on testing a new method for analysing river flow with the OpenRiverCam software in the Phetchaburi region in Thailand and improving the model for cleaning up rain gauge data in Thailand to perform a radar calibration.

We want to thank our supervisors Thom Bogaard and Punpim Puttaraksa Mapiam for introducing us to this project and providing us the opportunity to go to Bangkok and work at Kasetsart University. We also want to thank David Tax and Lindert van Biert for the help and guidance along the project and thank all the people at the Royal Irrigation Department who helped us during the fieldwork in Phetchaburi. A special thanks to Poom, Tangkwa, Frong, Toy and Nunu for all the help in the project and for making our stay in Bangkok fun and meaningful.

Introduction

Thailand experiences heavy rainfall during its monsoon period, which generally lasts from mid-May to late October. The rainfall causes problems due to the high intensity of certain events or because of long periods of precipitation. Government organisations, universities, and local parties work closely together to mitigate the negative effects of the rainy season. This collaboration ends up in a national network of rain gauges, rain radars and river monitoring equipment that aims to accurately monitor and follow the rainfall. The goal of this is to be able to take premature measurements in case of an emergency and to efficiently manage the water for the dry period of the year. The monitoring network is the result of decades of hard work and innovations. However, monitoring storm events to prevent flash floods still proves to be difficult, especially in upstream regions. This is a problem that a collaboration between the Water Resources Engineering Department of Kasetsart University (KU) and the Royal Irrigation Department (RID) tries to tackle. During this multidisciplinary project (MDP), a team of Technical University of Delft (TUD) students will assist the national collaboration with this problem.

The group aims to provide a partial solution to this difficult problem in the form of a visual discharge measurement system called OpenRiverCam (ORC). OpenRiverCam presents an innovative open-source modelling software designed to facilitate the establishment and ongoing management of river observation sites dedicated to river flow monitoring using cameras. The software uses technologies such as Large-Scale Particle Image Velocimetry (LSPIV) and geographical ortho projection methods, ensuring accurate and efficient data collection and analysis. With OpenRiverCam, the process of monitoring river flows has been made more accessible and affordable because a single field survey, along with affordable camera equipment, is all that is needed for a river flow monitoring project. The software is user-friendly and can be accessed easily via Github. The processing capabilities rely on a scientific computer vision approach to estimate movements from a video called particle image velocimetry. Patterns undergo frame-to-frame analysis to determine their displacements. These patterns, which may include items like drifting debris or swirling water eddies, are tracked over time. Any unintended or irrelevant movements that do not belong to the mainstream are removed through automated filtering techniques. The computed velocities are subsequently superimposed onto the original movie frame for visualisation. The implementation of OpenRiverCam in Thailand is an interesting initiative due to its cost-effective and accessible approach, offering a practical alternative to the costly sonar river measurement equipment. Presently, the OpenRiverCam approach has primarily been tested in smaller river settings and has only yet undergone testing in Europe and Africa. Therefore, introducing and evaluating the feasibility of this method in Thailand could represent a groundbreaking project. This challenge will assess the viability of the approach in this specific context and identify the challenges that must be addressed.

A second challenge in maintaining a national monitoring network is the coupling of all its parts. Currently, the rain gauges register precipitation that comes from clouds that are in turn registered by the radars. The radars measure the reflectivity of the clouds in dBz to estimate how heavy a rain event will be. However, the reflectivity does not necessarily say something about the amount of precipitation that will fall in millimetres because there are no well-constructed conversion parameters available for the radars in Thailand. These parameters can be learned by coupling rain events to the corresponding radar images after which the parameters to convert reflectivity to millimetres can be estimated more accurately. That is where the MDP group will assist. The goal is to create an end-to-end model[1] that provides the needed events after which a calibration can be done with as output the conversion parameters. Accurate and reliable events are needed to make this estimation. That is why the available rain gauge data from 2006 to 2023 first must be analysed to remove the broken stations for each year. The broken stations can be removed by visually analysing their Double-mass curves. This is generally a long manual process. Therefore, part of the model will be an easy-to-use and streamlined method for analysing a full year of data. The main objective for the group is not to use the model but to finish it and enable Kasetsart University to perform the calibration.

[1] Run the model by following this link.

The collective goal of both OpenRiverCam and radar calibration is to provide a cheaper, streamlined, and more accurate method of predicting and managing precipitation. The findings and results are documented to support this goal. The report starts with a description of the case study and the Phetchaburi region. It will also describe the challenges and common issues that were found during the use of the OpenRiverCam method. The second chapter will provide the OpenRiverCam results from the fieldwork. The third chapter explains the methodology and results of the radar calibration project. The conclusion on both OpenRiverCam and the radar calibration is provided in the fourth chapter. Finally, the appendix contains an extensive but practical manual on how to use OpenRiverCam and RTK.

Contents

List of abbreviations

ADCP	Acoustic Doppler Current Profiler
EWS	Early Warning System
GIS	Geographic Information System
GNSS	Global Navigation Satellite System
GPS	Global Positioning System
HII	Hydro-Informatic Institute
KU	Kasetsart University
LSPIV	Large-Scale Particle Image Velocimetry
MDP	Multi Disciplinary Project
ORC	Open River Cam
RID	Royal Irrigation Department
RTK	Real Time Kinematic
TUD	Technical University Delft

Chapter 1

Case study Phetchaburi District

1.1 The research in Phetchaburi

In pursuit of a comprehensive evaluation of the feasibility of integrating ORC technology within hydrological investigations, a team of students from the Technical University of Delft went on an extensive field research expedition. The primary objective of this inquiry was to assess the practical applicability and effectiveness of ORC across three different river systems located within the Phetchaburi District of Thailand downstream of the Kaeng Krachan Dam. In addition, a river upstream at the Kaeng Krachan Dam in the Kaeng Krachan National Park was examined to investigate whether the ORC could be applied in this remote area. In appendix B a tutorial is written on how the ORC software is used via Google Colab and how it was tested at KU. This gave us knowledge on how to tackle the rivers in Phetchaburi and how to prepare the sites for the ORC measurements.

1.1.1 Phetchaburi District

Nestled within the southwestern district of Thailand, the Phetchaburi District is a province marked by forests and a proximity to the Gulf of Thailand. Its diverse topography gives ecological significance to the region, making it a site of particular interest for environmental studies and conservation efforts. The Phetchaburi District is home to a diverse population that relies on a spectrum of economic activities, ranging from agriculture and fishing to forms of trade. Given its remarkable topographical diversity, the Phetchaburi District assumes a crucial role in the preservation of natural resources and biodiversity. This attitude towards environmental investigations and conservation initiatives makes it an ideal location for this project. Moreover, the presence of the reservoirs and their catchments provides more than enough testing locations. An overview of the map of the Phetchaburi district and the different rivers that have been checked in the field work is visible in Figure 1.1.

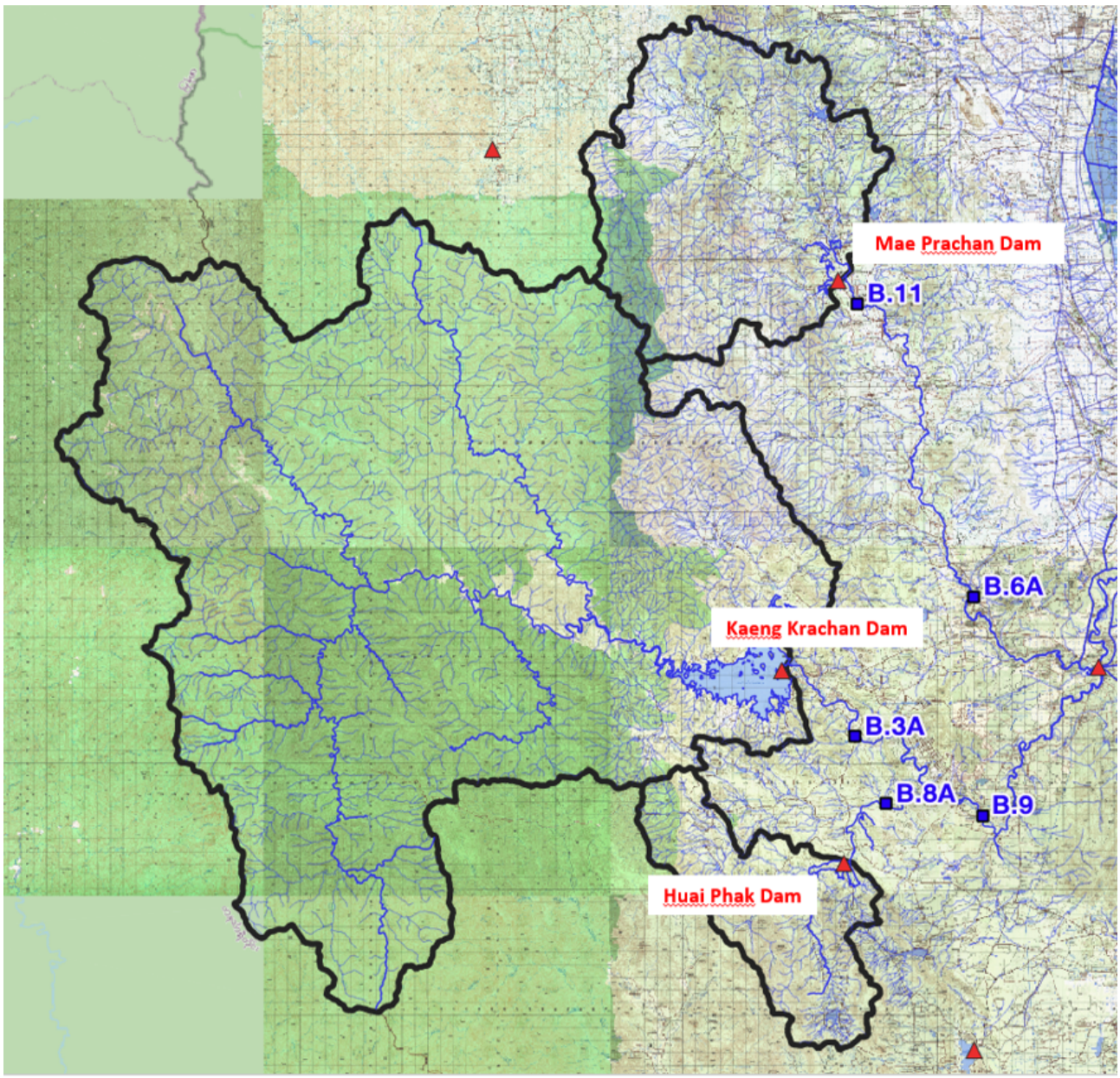

Figure 1.1: Map Phetchaburi District

1.1.2 Rivers in Phetchaburi District

A summary of the four rivers on which ORC is provided to quickly describe the testing subjects. All the important additional information about the rivers can be found in Appendix F. Each of these rivers has its special features and situations. The rivers are briefly described in the following parts of the report.

B.3 River

The B.3 river is a winding river that plays a crucial role in the area's environment. It is an important source of water for farming, which supports local people in their livelihood. B.3 is the second largest river out of the four locations. While it was technically possible to test ORC on such a large river, it had not been tried before. This promised an exciting challenge to the group.

The B.3 river has a width of approximately 30 meters when the reservoir releases 40 m^3 and has a low bridge crossing at our test location. On weekday mornings, the reservoir gate is usually closed, making the river water almost stagnant. When there is heavy rain, the river can change very quickly

because the gates are opened. The water level is therefore mostly dependent on its upstream reservoir. This aspect makes B.3 stand out from the other rivers. The river B.3 can be seen in figure 1.2.

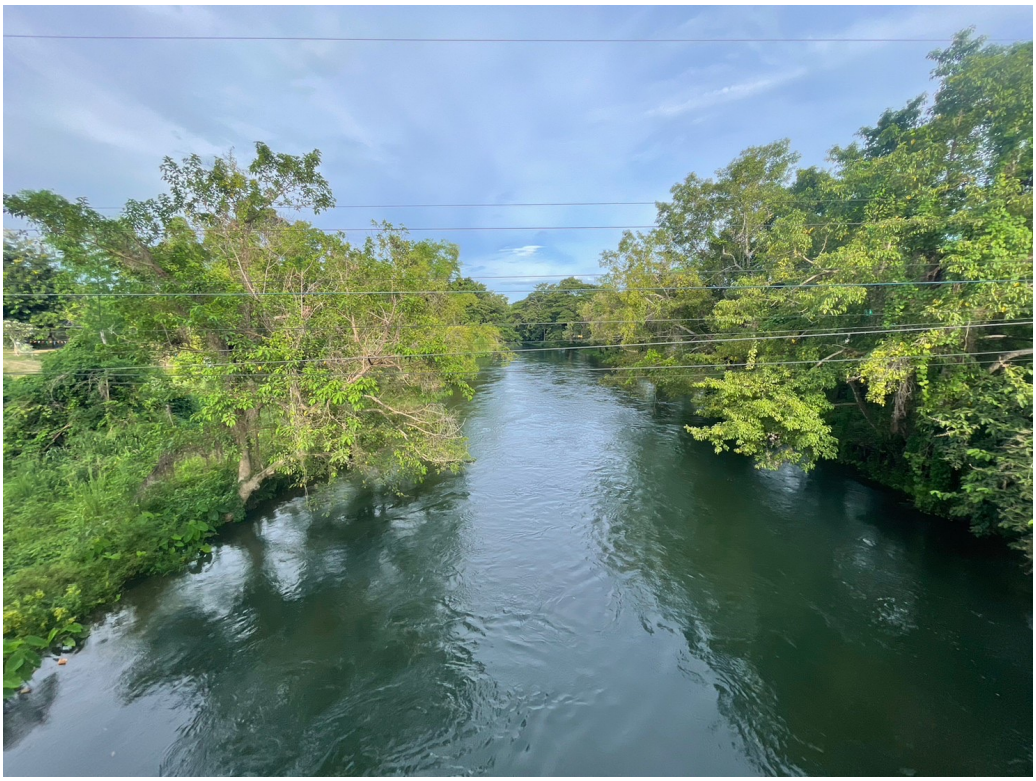

Figure 1.2: River B.3

B.8 River

The B.8 River is a crucial resource for several settlements. It supports irrigation and, for example, has fishing facilities near the bridge where measurements were taken. It is a relatively small and shallow river, but its water level can increase significantly depending on the weather conditions. The Royal Irrigation Department (RID) has installed a weather station and a sonar system to gather real-time data about this river's behaviour. The water is too shallow to use an Acoustic Doppler Current Profiler (ADCP) for measurements but ORC works effectively. The elevation of the bridge is sufficient to capture the entire river within the camera angle. The shallow water allows for manual and GPS RTK-assisted cross-section measurements. The river B.8 can be seen in figure 1.3.

Figure 1.3: River B.8

B.11 River

The B.11 River is downstream from the Mae Prachan Dam. There are still many uncertainties here because it is unclear how the water level in the reservoir influences the outflow through its gates. This is because the expected outflow does not match the measurements. Therefore, it is interesting to understand how much water flows through B.11. This can be measured with the ADCP, but often the water level is too shallow in this part of the river. This is also due to, among other things, the low water level of the reservoir. The sonar installation on the bridge at River B.11 is no longer operational, making the case study of the use of ORC very interesting. The river B.11 can be seen in figure 1.4.

Figure 1.4: River B.11

Upstream River

The last river on which ORC was applied is upstream in the National Forest Park of Kaeng Krachan and therefore upstream of the dam. This river does not have a specific code like the other rivers downstream and will therefore be explained as River Upstream. This was the largest river on which measurements were taken as the discharge was higher than B.3. The use of ORC could be of great value in the future. This location is far away from the normal range of the RID to perform measurements with an ADCP and there is no working Sonar installation yet. Using ORC could provide a solution in this inhospitable area. The journey to this area took no less than 3 hours on an impassable path, especially during heavy rain. It is only possible to get here via 4x4 trucks from the RID. This upstream river is so interesting because a successful application of ORC would mean more insight into the inflow of this river into the reservoir.

Figure 1.5: River Upstream

1.1.3 Research Objectives

This research aims to ascertain the feasibility of integrating ORC technology into the hydrological assessments of these rivers for precise data collection. This enables organisations like the RID to perform near real-time measurements during heavy rain events. This equips those in charge of damage mitigation with an extra tool to prevent disasters from those extreme events. Additionally, it allows them to manage the water in the reservoir more efficiently. ORC technology could therefore serve as an important instrument.

1.1.4 Expected Outcomes

The expected results include a deep understanding of how ORC technology can be used for studying rivers. This can provide important information for future environmental evaluations, conservation projects, and managing resources in a sustainable way in the Phetchaburi District. The ORC technology can offer a cheaper solution to analyse rivers, river flows, and discharge. The method is currently tested on very small rivers in Europe and not yet on this scale of the Phetchaburi District rivers.

An important note is that not all the sonar installations of the RID are working correctly. Some are broken and some deviate a lot. On the other hand, some measurements installation of the RID that measure the water dept, cannot operate correctly because of the low water level. The third important note is that the ADCP can only operate in certain water levels above a certain height. Also, this method has some deviations because it cannot detect the bottom of the river values or some values on the sides. There it gives some dark spots and no values. Even though this deviates, it is a very precise measurement method and is therefore used as the most secure reference data

Other data is only used to compare as reference data if the ADCP was not able to measure in these rivers. Overall the expectation is that the ORC software should come close to the data but there is a possibility it should be optimised. This can be possibly done by adding a factor after a lot of data is collected or when a calibration is done.

Chapter 2

Results OpenRiverCam Phetchaburi District

2.1 Introduction

We were given the chance to stay in the Phetchaburi area and perform measurements at three different stream locations. Transport to each river location was dependent on the driver's availability per day. Yet, we have succeeded in visiting each location at least two times. Additionally, a fourth river location was visited once on October 10th during another trip. GPS coordinates have been obtained using RTK-GPS. In some cases, it was difficult to obtain accurate coordinates because the RTK-GPS sometimes required a minimum of two hours just to reach a deviation below 1.0 meters. Allowing more time to have the RTK calibrate could solve this. However, time was limited given our dependency on the designated drivers in the area. Each river required site preparations and measurements to be performed before taking a video. As an input for the ORC model, different cross-sections of the rivers are required. These have been captured by hand as well. This is because the rivers would only be a couple of centimeters deep and the deviation of the RTK-GPS was often too high (up to around 80 centimeters). In addition, some by-hand measurements would serve as a validity check. A full explanation of the site preparations that have been performed is listed in appendix C. A manual on how to work with RTK-GPS and the corresponding OpenRiverCam software is attached in Appendix A.

Different results have been obtained via OpenRiverCam. Parameters that are discussed for validating the ORC detection are the water flow patterns projected onto the video frame and the discharge values calculated in the ORC model on each cross-section. Because these values are retrieved for each cross-section, accurate values of the depth and the location are very important. The water flow patterns are compared to measurements done by hand with the current velocity meter.

Lastly, the discharge levels measured at different locations using OpenRiverCam software (ORC) are compared with discharge levels calculated by the local Royal Irrigation Department. At most locations, ORC tests have been performed on more than 2 days. However, for each location, the RID has joined only one time to perform their discharge measurements as well. Thus, at locations B.3, B.11 and Upstream it is possible to compare ORC results with RID data - for those days together. For the three aforementioned locations, the RID used an Acoustic Doppler Current Profiler (ADCP) to measure the discharge. Assuming that the ADCP can provide strong estimates of the actual discharge, the ADCP results can be used to validate the ORC results. At location B.8 the draft of the stream was too small for the RID to use the ADCP. Yet, the RID provides telemetry data that estimates the discharge at this location based on their discharge data further upstream. For location B.8 the ORC discharge results are compared with this telemetry data.

2.2 River B.8

River B.8 was the first river to tackle on the field trip. The width of the river (9 m) is considered to be relatively small for this report. This river was comparable to rivers in which ORC software was applied as well in other projects and this site could be easily filmed from different spots on the bridge. Therefore, this was the easiest location to work out the difficulties of the site preparation and working with the RTK GPS.

We shot multiple videos on different days at this location and these videos, combined with the cross-sections and control points of the river, were entered into the ORC software to get discharges of the river. Three video angles were tested, the left, middle, and rightside of the bridge. Because three of the four control points were aligned in the middle video frame, the results from the middle of the bridge were the worst as shown in figure 2.1. Putting three control points on the same line in the video frame made it hard for the ORC software to project the video correctly on the geographical plane. The flow patterns look accurate for the left and right camera angles and are fairly equal to the current measurements. A full overview and analysis of the current velocity measurements done in the field and the ORC results are put in appendix D. The inaccuracy of the GPS points is visible in this image. It shows that the edges of the cross-sections go into the bushes while they have been set at the waterline.

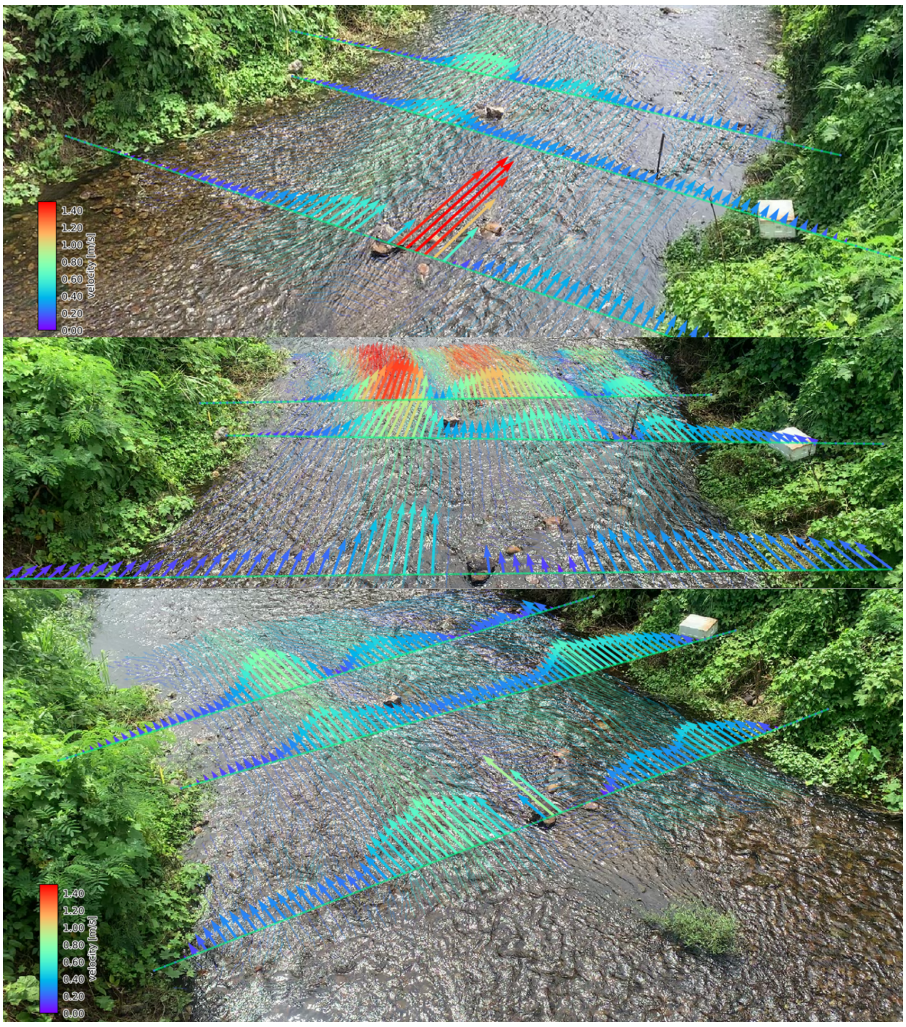

Figure 2.1: B8 Water flow detected by ORC from right, middle and left camera angle

The flow detection in figure 2.1 was shot on September 22. More videos have been taken on other days and compared to the results from the RID. All the results are depicted in Appendix G and the daily averages compared to the RID data are listed below in table 2.1. The discharge values of the different

videos come quite close to each other but are all around 40% lower than the RID values. This could have multiple causes. Among them: the ORC does not take in the flow at each point since it simply does not detect a flow at every point. Additionally, the software may inaccurately link the GPS points and cross-sections to the frames captured. Furthermore, the discharge as measured by the RID using telemetry might be higher than the actual discharge. Unlike ADCP, the telemetering data from the RID is not real-time but calculated using telemetry at nearby locations. It could also be possible that due to the slightly inaccurate GPS points of the cross-sections and the control points the discharge is measured to be lower. In appendix D it is shown how the manual current measurements - taken by us using a small propeller - were slightly higher than the results obtained by ORC.

	21 sep	**22 sep**	**22 sep adv. ORC**	**26 sep**	**av. flow**	**unit**
cross-section 1	0,308	0,348	0,343	0,2275	0,307	m3/s
cross-section 2	0,362	0,361	0,328	0,289	0,335	m3/s
cross-section 3	0,398	0,495	0,426	0,2405	0,390	m3/s
Average CS's	0,356	0,402	0,366	0,252	0,344	m3/s
RID telemetry	0,55	0,58	0,58	0,60	0,575	m3/s
std. deviation	0,061	0,059	0,040	0,051	0,053	m3/s

Table 2.1: B.8 discharges calculated per day compared to RID measurements

ORC provides discharge values in quantiles 0.05, 0.25, 0.5, 0.75, and 0.95. That is why the average discharge is also depicted in figure 2.2 using a box plot. The horizontal line shows the discharge as measured by the RID - for comparison. The RID telemetry-discharge data is shown with a horizontal line for comparison. The figure shows how the ORC detected median discharge values are about 26% to 44% lower compared to the RID data.

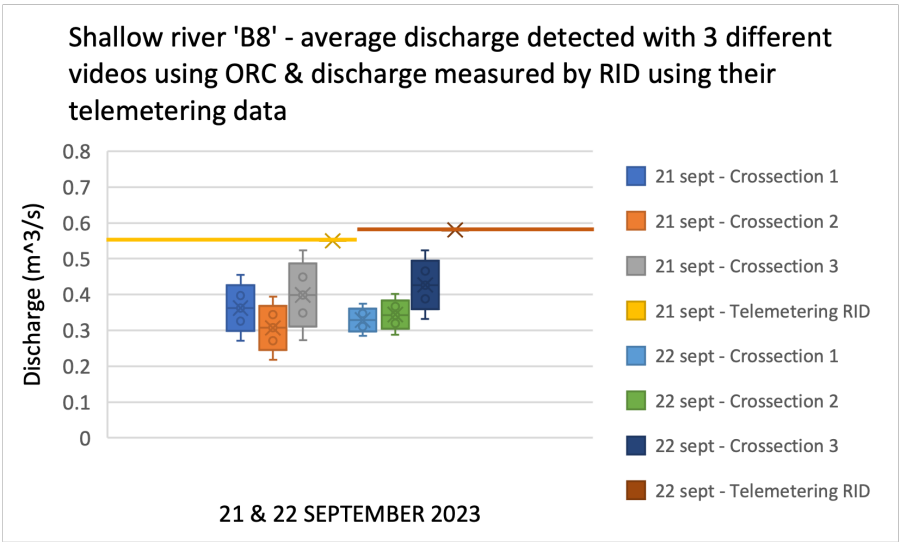

Figure 2.2: Narrow river B.8 - Average flow detected with 3 different videos using ORC & flow measured by RID using their telemetering data

2.3 River B.3

The second river was B.3. This river, with a width of 30 meters, is considered to be 'wide' for this report. Testing ORC on this river brought challenges. The river had an average discharge of 40 m3/s, that is a sixth of the discharge of the Dutch river Maas and a seventh of the discharge of the French river Moesel. The first challenge was to get the whole river into the video frame as the relatively low bridge (7m) and overhanging trees on the left-bank side - see figure 2.3 - made it difficult to capture the whole width of the river. The latter meant a video could only be taken from the right-bank side of the bridge. From this angle the river was best visible and the interference from trees and branches

hanging over the water was the least. A strong current with a depth of up to 2 meters made it difficult to create reference points. As it was only possible to use the ropes to get across, it was chosen to designate two reference points on the right-hand side of the river and to create two hanging reference points on the left side of the river. Because of the two ropes, two cross-sections could be measured. The pink platform in the water was used to move the RTK to the other side. The setup and results are listed in figure 2.4a to 2.5.

Figure 2.3: Choice of reference points B.3

	25-Sep Video 1	25-Sep Video 2	25-Sep Video 3	25-Sep Video 4	25-Sep Video 5	Average	unit
cross-section 1	18.23	15.35	20.63	20.04	26.80	20.21	m3/s
cross-section 2	11.76	5.05	8.46	10.92	15.02	10.24	m3/s
Average discharge	15.00	10.20	14.55	15.48	20.91	15.23	m3/s
std. deviation	33.11	20.67	11.50	11.65	23.88	20.16	m3/s
RID ADCP	30.51	30.51	30.51	30.51	30.51	30.51	m3/s

Table 2.2: River B.3 - discharges calculated using ORC with different videos at the same time

The discharge levels detected using ORC for River B.3 are listed in table 2.2. Also, figure 2.6 shows a boxplot of the ORC detected discharge levels and the RID ADCP measured discharge level.

Some observations about the results: First, both cross-sections 1 and 2 are at a relatively far distance from the bridge and thus the camera. Table 2.2 above shows how the discharge detected at the closest cross-section is higher compared to the cross-section further away. This could be explained when looking at figure 2.4a. ORC detects more discharge at the closer cross-section as it can detect water movement more easily. Second, with reference to the RID discharge values, the levels calculated via cross-section 1 are closer to reality. When examining the average median discharge level of the 2 cross-sections by the ORC it can be noted that these are around $\tilde{3}3\%$ to 67% lower compared to the RID level. Third, figure 2.4a and 2.4b show how the shadow on the left bank has a negative influence on the detect-ability of water movement by the camera. Little water flow is detected on the outer 10 meters on the left bank side - see the left side in figure 2.5. This could explain why the ORC discharge level is lower compared to the RID ADCP value. Fourth, the deviation in results is rather large for this location. These are calculated based on the velocity quantiles that are provided by the ORC software. This is probably due to unclear stream detection as well. .

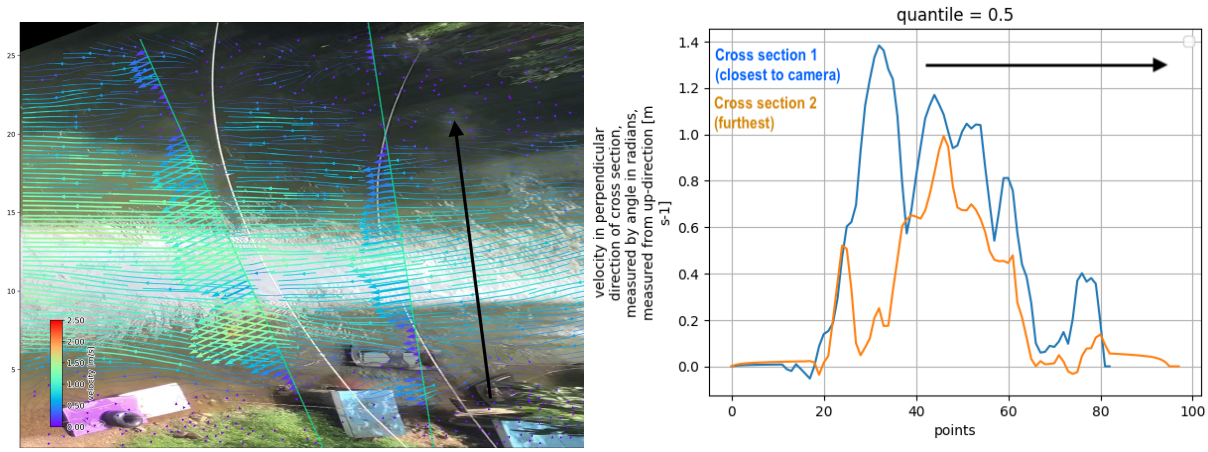

(a) B3 flow visualized from above

(b) Velocity plot B.3

Figure 2.4

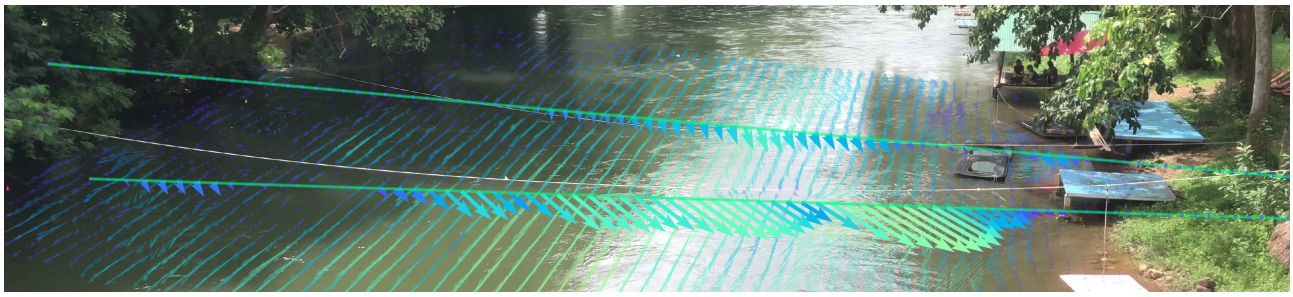

Figure 2.5: B.3 - Flow detected from bridge by ORC

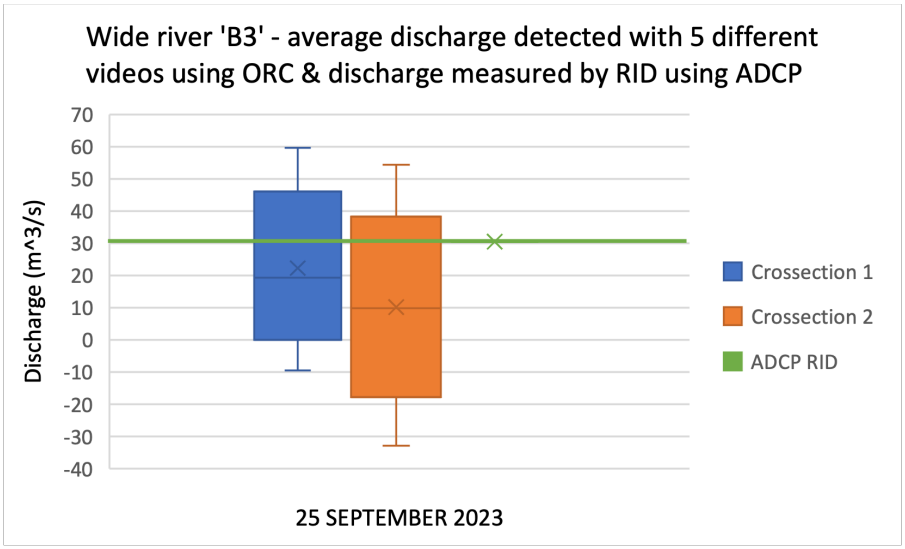

Figure 2.6: Wide River B.3 - Average discharge detected with 5 different videos using ORC & discharge measured by RID using ADCP

2.4 River B.11

The third river in the Phetchaburi area to do measurements was River B.11. The 6-meter width of the river is relatively 'small' like River B.8 - as discussed in section 2.2. Yet, the camera angle should provide a better view of the moving water (more vertical) due to the higher bridge over the river. The site required some extra work as it was harder to access and also many plants and trees had to be

cut away to get an open view of the river. After an extensive site preparation in collaboration with the RID - as shown in figure 2.7, it was possible to realize a clear view of the river from the bridge. The RID performed discharge measurements at the same time using their ADCP rover. After the first visit to B.11, the captured GPS coordinates turned out to be too inaccurate. Coming back another day and resetting the coordinates allowed us to capture valid GPS points after all.

Figure 2.7: River B.11: the plants were cleared and the cross-sections were measured

The discharge levels measured using ORC turned out to be close to the discharge measured by the RID. Four different videos have been taken from slightly different angles. The results of the different ORC discharge values and the corresponding discharge measured by the ADCP from ADCP are listed in table 2.3. These are only the ORC results from 27 September, the results from 28 and 29 September are attached in appendix G. On the other days, the RID did not join us to measure discharge and therefore the ORC values could not be compared with that. However, the water level was around the same height as the water level on the 27th of September. So the actual discharge on September 28th and 29th should be close to that on September 27th.

	27-Sep	27-Sep	27-Sep	27-Sep		
	Video 1	Video 2	Video 3	Video 4	Average	unit
cross-section 1	0.43	0.43	0.41	0.55	0.46	m3/s
cross-section 2	0.54	0.64	0.57	0.60	0.58	m3/s
cross-section 3	0.42	0.51	0.61	0.46	0.50	m3/s
Average 3 CS's	0.46	0.52	0.53	0.53	0.51	m3/s
Std. deviation	0.09	0.11	0.08	0.12	0.10	m3/s
RID ADCP 1	0.434	0.434	0.434	0.434	0.434	m3/s
Std. dev. RID ADCP 1	0.048	0.048	0.048	0.048	0.048	m3/s
RID ADCP 2	0.44	0.44	0.44	0.44	0.44	m3/s
Std. dev. RID ADCP 2	0.027	0.027	0.027	0.027	0.027	m3/s

Table 2.3: River B.11 - discharge results on 27 September

The ORC results are in close proximity to the RID discharge values. The average discharge from the ORC tests was 0,51 m3/s with a std. deviation of 0,10 m3/s. The discharges measured by the RID were 0,434 m3/s with std. deviation of 0.048 m3/s and 0.44 m3/s with a std. deviation of 0.027 m3/s. This means that the average ORC detected discharge is 16,7 % higher than the RID results, which is close. Both ways of measuring the discharge try to achieve a value as close as possible to reality. However, no method is granted to be 100% valid given the uncertainties in the measurements. The ORC results from the B11 river are also compared to the manual current measurements as shown in figure 2.8. Only the 2 right cross-sections were measured by hand and therefore compared. The flow

patterns show the same currents around the same location which is further described in appendix D. This again proves that the ORC results at this location are promising and that the ORC software is well capable of measuring the discharge of this type of river.

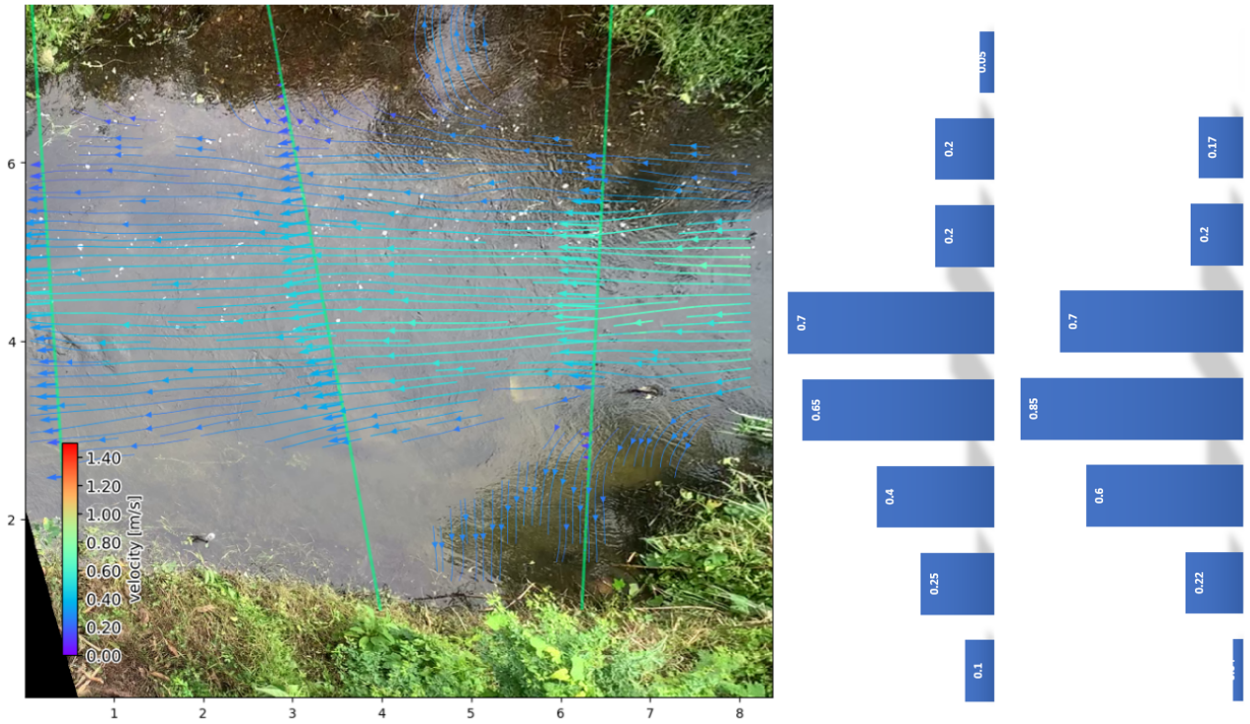

Figure 2.8: 27 sept 2023 measurement 1, ORC results vs. current meter (by hand) measurements

Figure 2.9 shows that at location 'B11' the discharge values measured by the ORC match the RID discharge values strongly.

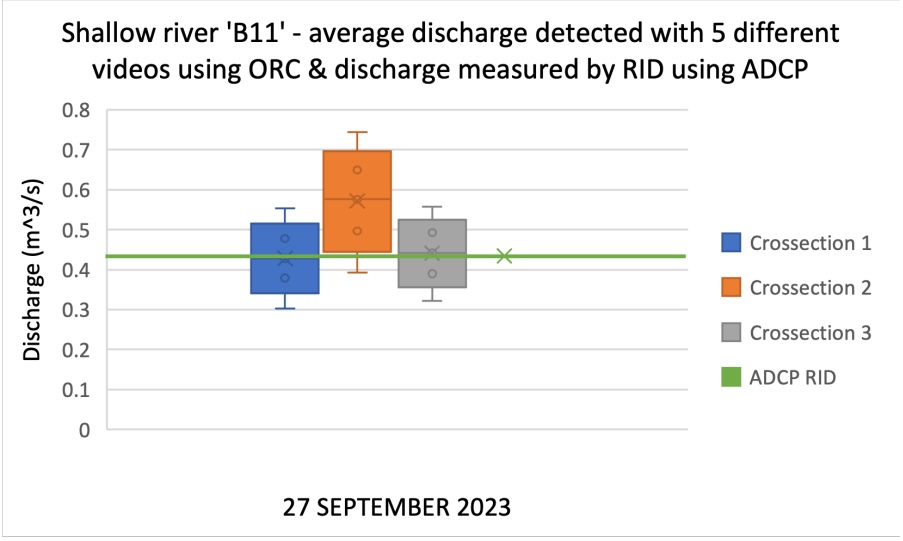

Figure 2.9: Narrow river 'B11' - Average discharge detected with 5 different videos using ORC & discharge measured by RID using ADCP

2.5 River 'upstream'

On October 10th there was one last opportunity to test the ORC software. This last river is - at KU University - called the 'upstream' river and will therefore be referred to as such in this report. This

river is around 30 meters wide and is therefore referred to as 'wide' in this report. For this river, three different cameras with different settings are used to capture the flow. Camera 1 records 3840 x 2160 pixels at 60 fps. Camera 2 records 1920 x 1080 pixels at 30 fps. Camera 3 records 2400 x 1080 at 30 fps. All videos have been captured while standing on a bridge - as this was the only option.

The resulting discharge levels detected using ORC are listed in table 2.4. The table shows the 0.5 quantile velocity for each cross-section per video - for 5 videos. Also, the ADCDP discharge measured by the RID is included in the table for reference. Cross-section 1 is closest to the camera and cross-section 3 is furthest away from the camera.

	10-Oct	10-Oct	10-Oct	10-Oct	10-Oct		
	Camera 1.1	Camera 1.2	Camera 2.1	Camera 2.2	Camera 3	Average	unit
Resolution	3840x2160- 60 fps	3840x2160- 60 fps	1920x1080- 30 fps	1920x1080- 30 fps	2400x1080- 30 fps		
cross-section 1	27.12	15.74	20.46	18.74	20.69	20.55	m3/s
cross-section 2	18.33	19.43	15.98	13.61	17.92	17.05	m3/s
cross-section 3	7.89	9.48	11.87	10.83	12.01	10.42	m3/s
Average 3 CS's	17.78	14.88	16.10	14.39	16.87	16.01	m3/s
Std. deviation	9.92	11.22	8.92	7.93	9.28	9.46	m3/s
ADCP RID	56.70	56.70	56.70	56.70	56.70	56.70	m3/s

Table 2.4: 'Upstream ' discharge levels measured with ORC

Analysing table 2.4 shows that some strong differences between results can be observed. First, the discharge levels as listed above show how cross-section 1 - which is closest to the camera - often provides a discharge level closest to the ADCP level and thus closer to the real level when using ADCP for validity reference. Second, the average discharge level in m^3/s for all cross-sections 1 is still around 64% lower compared to the ADCP discharge level.

To gain insight into the different flow detection for the different cameras a 0.5 quantile velocity plot for each video is depicted in the images below. The corresponding visualized flow detection is listed aside from each velocity plot.

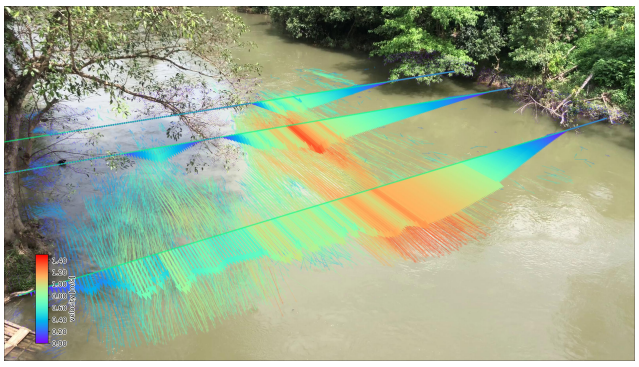

(a) Flow detection from bridge camera 1.1 - 3840 x 2160 pixels at 60 fps

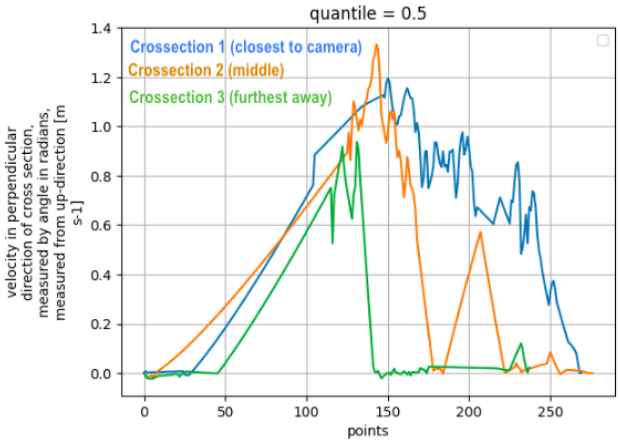

(b) Corresponding velocity plot to flow detected

Figure 2.10

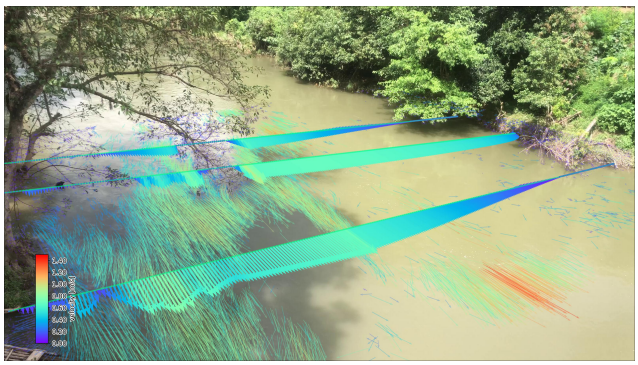

(a) Flow detection from bridge camera 1.2 - 3840 x 2160 pixels at 60 fps

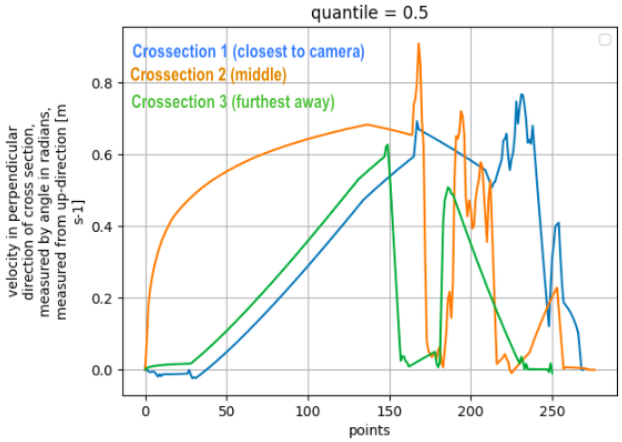

(b) Corresponding velocity plot to flow detected

Figure 2.11

(a) Flow detection from bridge camera 2.1 - 1920 x 1080 pixels at 30 fps

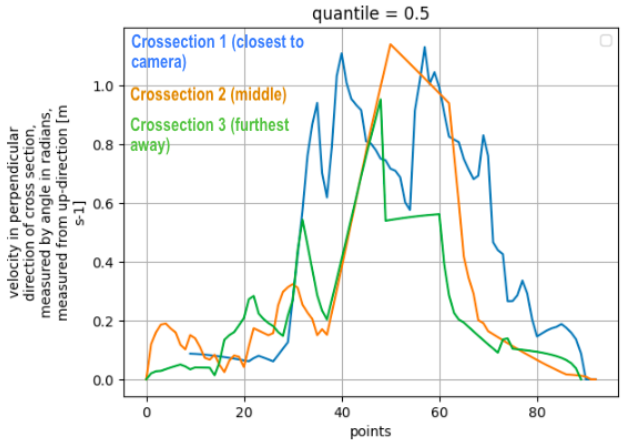

(b) Corresponding velocity plot to flow detected

Figure 2.12

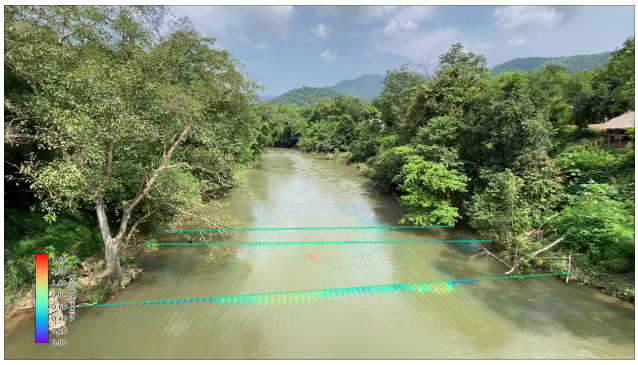

(a) Flow detection from bridge camera 2.1 - 1920 x 1080 pixels at 30 fps

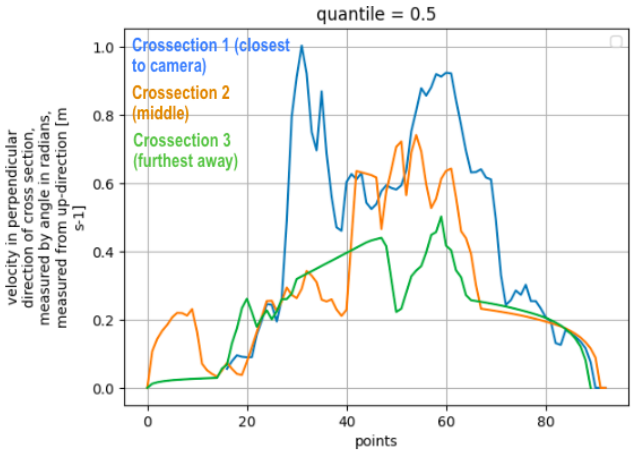

(b) Corresponding velocity plot to flow detected

Figure 2.13

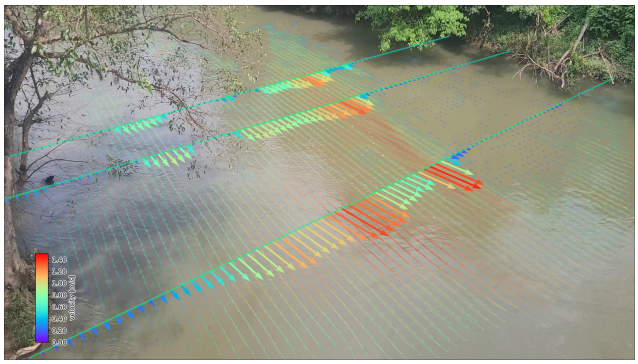

(a) Flow detection from bridge camera 3 - 2400 x 1080 at 30 fps

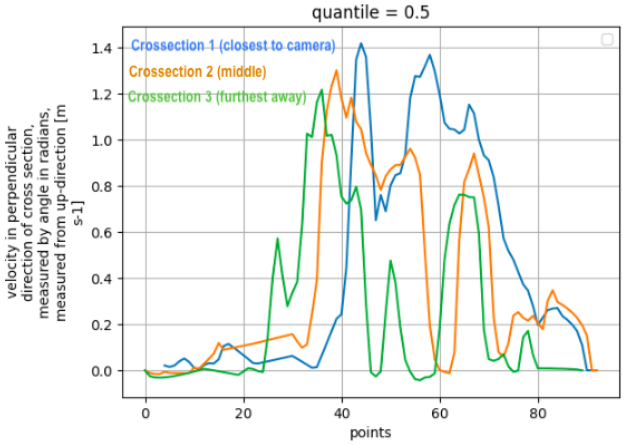

(b) Corresponding velocity plot to flow detected

Figure 2.14

When assessing the flow and velocity visualisations above, it can be noted that there are rather large fluctuations within the different figures. Before elaborating on this, it should be mentioned that the velocity plot is plotted from the right bank to the left bank of the river (as seen from the bridge). First, figure 2.10a and 2.11a show how 2 videos taken with the same camera from the same angle can provide different flow detection as a result of different light caused by clouds, sun and shadow from nearby objects. Second, camera 1 has the highest resolution and therefore a more detailed flow visualisation. However, the results are not considered more accurate as the ORC software returns velocity plots with rather large fluctuations. Third, when taking a video from one side of the bridge it can be noticed that the flow at the bank furthest away from the camera is hardest to detect. In the five examples listed above it hardly detects any flow at a distance of around 50 meters away from the camera. Shadow makes this even more difficult.

Figure 2.15 visualizes how the ORC detects much lower discharge levels compared to the RID ADCP - ~60% to 83% lower. It was difficult to apply ORC software on this river. First, shadow and overhanging trees disturbed the movement detection as can be seen in figures 2.10a to 2.14a. Second, the current in the river was too strong to determine the cross-section ourselves. Therefore, the cross-section - as determined by the ADCP - was used. Third, the view angle from where the video could be taken was again rather far away and at a relatively low angle to the surface.

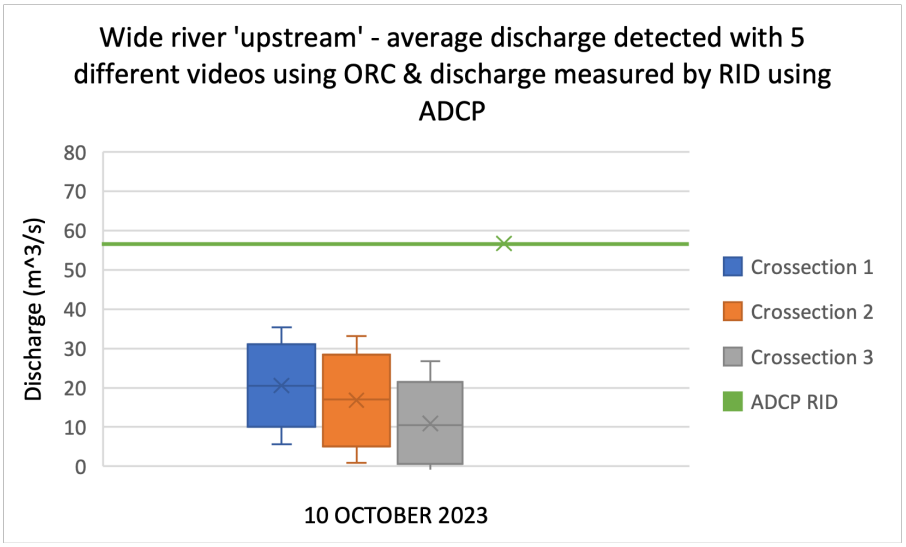

Figure 2.15: Wide river 'upstream' - Average discharge detected with 5 different videos using ORC & discharge measured by RID using ADCP

2.6 Comparing camera settings

The videos taken on each side have all been captured by phones. It is possible to change the resolution and frames-per-second on the settings of your camera. To see whether it makes any difference for the ORC discharge detection a simple comparison has been set up at the river 'upstream' using different settings on the phone. Figure 2.16 shows the velocity quantiles plot for each cross-section using different camera settings. Results do differ among the different settings but there is no clear conclusion to be drawn comparing the different cross-sections. Differences are probably a result of different flow detection as the videos are not taken at exactly the same time. Thus, it is expected not to matter too much whether a video is taken at 1080 p or 4k quality.

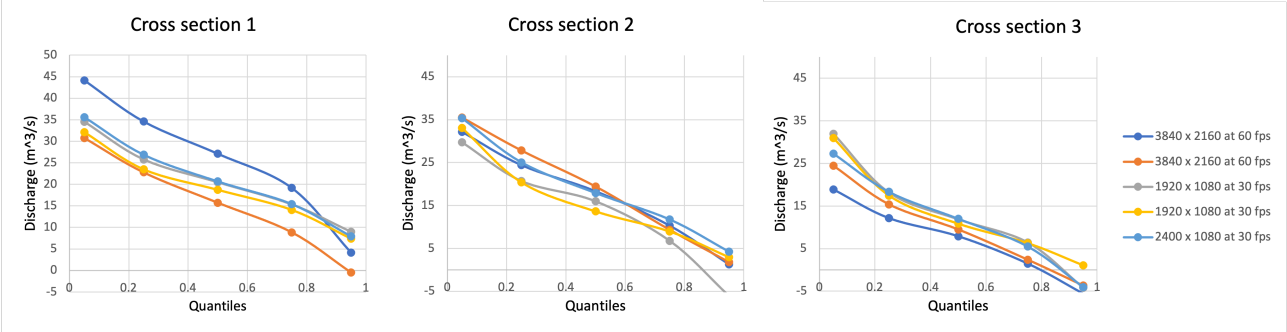

Figure 2.16: Result velocity quantiles using different resolution- and frame-per-second setting on the phone - shot at the river 'Upstream'

2.7 Number of frames per video required for OpenRiverCam analysis

The OpenRiverCam software allows the user to choose the amount of frames to be analysed. In order to discover the minimum amount of frames in a video to be analysed, a comparison has been set up. This is relevant as analysing extra frames requires significantly more running time. Running the software on a 60fps 4k video for just 5 seconds - hence 300 frames - could lead to 30 minutes of running time. This depends on the computer of course. Figure 2.17 shows the discharge detected by the ORC software displayed in quantiles varying the number of frames to be analysed. For rivers B3 and B11 both one video. It can be noted how discharge results converge after analysing a minimum of around 200 frames. Thus, analysing more than 200 frames does not seem to provide better results and would only demand more running time. If one has a camera capturing at 60 fps, one would only need to capture 7 seconds of video.

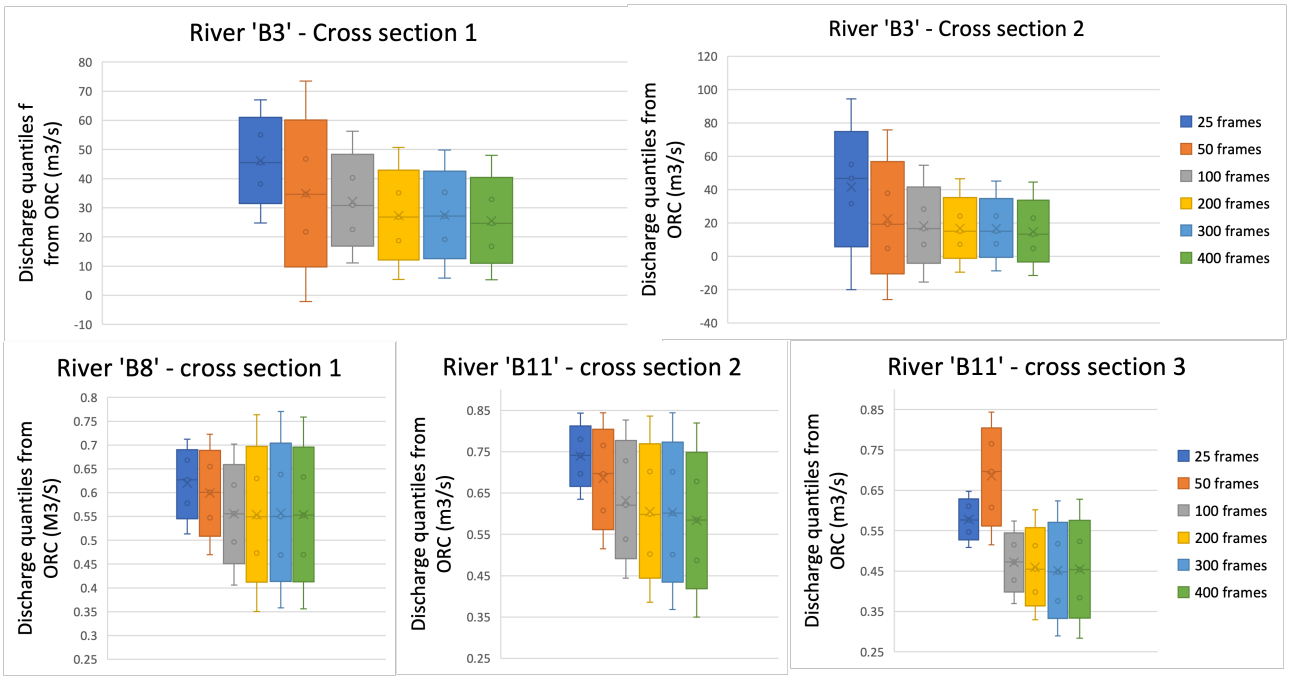

Figure 2.17: Running the OpenRiverCam software on the same video varying the number of frames to be analysed - one video for B3 and one video for B11

Chapter 3

Radar calibration

This chapter will describe the methodology that is used to construct the radar calibration model. The results for 2022 are also reported.

3.1 Introduction

The rain radars in Thailand register reflectivity from clouds and the rain gauges register the precipitation that falls from those clouds. The rain gauges, also referred to as stations, only measure the rain at their specific location, whereas the radars can measure reflectivity across the entire country. To predict the precipitation at any location, the reflectivity measured by the radar (in dBZ) should be converted into expected rain (in mm). With an accurate conversion, it is possible to predict how much rain will fall during storm events and thereby it allows to prepare for the damages that these storms can cause. The second goal of this multidisciplinary project is therefore to construct a model that can learn this conversion from a set of rainfall events. The conversion is described by the formula below:

$$Z = a * R^b \text{ (eq. 3.1)}$$

Where:

- Z = Reflectivity [Z]
- R = Rainfall [mm/hr]
- a = conversion parameter
- b = conversion parameter

The events that must be selected come from the data provided by KU. The data consists of two main sets: the radar data and the rain gauge data. These data sets are the starting point of the calibration. The first step is to clean the rain gauge data available from 2006 to 2023. Each year contains data from stations that were not working or giving unreliable data. Simultaneously, the script to extract the events from the data and eventually learn the parameters is constructed. An overview of this process is given in figure 3.1.

Figure 3.1: Flowchart Radar calibration

3.2 Rain gauge data

The yearly rain gauge data is recorded by two organisations: the Hydro-Informatics Institute (HII) and Early Warning System (EWS). The HII stations measure precipitation every 10 minutes and the EWS gauges every 15 minutes. The data is reshaped to a cumulative hourly amount and then merged before the analysis is performed. Merging is important because it makes both the filtering of the stations and the event selection more streamlined. The filtering of faulty stations starts by removing the stations that had a downtime of more than 60%. The remaining stations have to be visually analysed through a Double-Mass analysis.

3.2.1 Kagan analysis

There are 623 stations in total that record throughout the year. Loading, merging and reshaping this data in the model takes quite some time. That is one of the reasons a distance-correlation calculation is performed. The graph that can be plotted from the calculation, functions as an intermediate step to check whether the data is reshaped properly. The distance-correlation graph should follow a decreasing exponential pattern if this is the case and a scattered pattern when it is not. An example of this is shown in figure 3.2b and figure 3.2a. Because the data from two different types of stations is merged, the graph that follows the exponential pattern is still not completely correct. This will be explained in the next section.

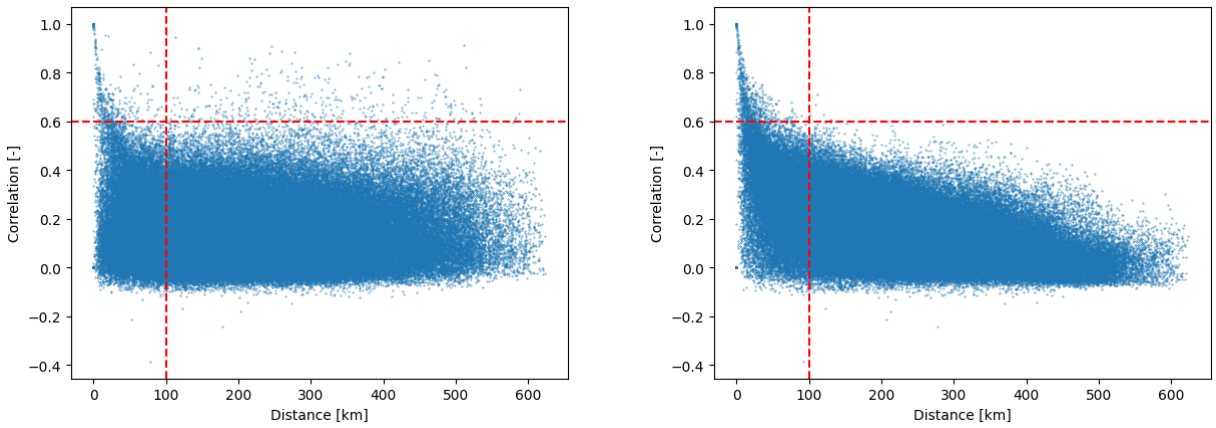

(a) Incorrect

(b) Correct

Figure 3.2: Distance-correlation graphs

The second and main reason for the analysis is to determine the optimal radius in which correlated stations lie. The model provides an optimal set of stations with a maximum radius where a correlation of 0.6 or higher is still reached. If this distance is higher than a predetermined maximum radius, say 30 kilometres, this value is chosen because a too-large radius is unrealistic. If the value is below the predetermined radius, the lower value is chosen because the whole set of distance-correlation points does not contain stations within 30 kilometres that still have a high enough correlation.

3.2.2 Double-Mass analysis

Once the radius for the surrounding stations is determined, the DM-curves can be plotted. The station that is plotted is called the key station. The model runs through all the individual stations and stores the cumulative rainfall of the key station and the average cumulative of the surrounding stations. The names of the surrounding stations are also stored for later use. This creates one large data set that allows the user to perform the DM-analysis in an interactive window with two buttons, *correct* and *defect*, that determine if a station is working or broken. An example of the widget is shown in figure E.1. The widget allows for a fast analysis because it plots the DM-curves automatically instead of plotting each station separately. The output is two lists, one with the working stations and one with

the defect stations. The lists are then used to filter the rain gauge data. The filtered data and the overview of the functionality of the stations for the reviewed year are saved into two Excel files.

The DM-analysis filters out the unreliable data but there are a few side notes. The first is the human aspect. The DM-analysis is a visual analysis and therefore subjective. It is quite clear when a station is working or broken but in some cases, it is difficult to see and the decision to discard the station for that year is entirely up to the person performing the analysis. Examples of a working, broken, and doubtful case are shown in figure 3.3. The examples illustrate the sometimes fine line between broken and working stations.

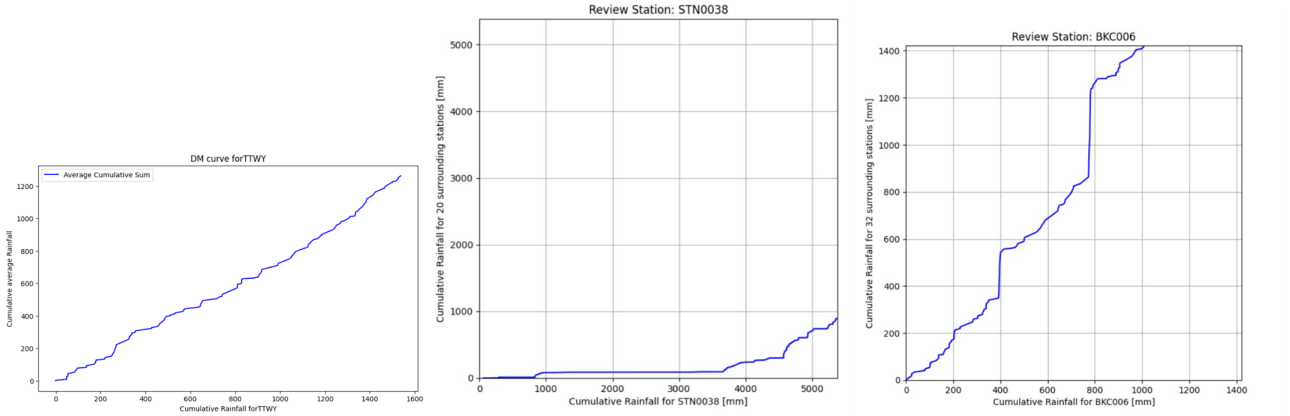

(a) Working (b) Broken (c) Doubtful

Figure 3.3: DM-curves

Secondly, and more importantly, the HII data that is provided at the beginning of the project is different from the EWS data because the HII stations registered a zero when the station was not working whereas the EWS registered a Nan value. This means that missing data is filled with zeros because a station can also record zero precipitation. This causes problems when plotting the DM-curves and while calculating the correlation between the stations. Ideally, the zero values for the key station are located and removed after which the corresponding values in the data of the compared station are also removed. The correlation can then be calculated as the two arrays still have the same length. Additionally, the DM-curve can be plotted without the zero values which gives a better result. However, it is initially impossible to distinguish the actual measurements from those in the period in which the station was broken. Removing the zeros thus causes the unnecessary removal of reliable data. That is why the first analyses on years 2021 and 2022 were done without removing the zeros from the data files. This still gave a reasonably reliable result because it was still obvious when a station was broken in most cases. The result is shown in figure E.2. Because of time restrictions, the remaining years are not reviewed yet.

The difference between the HII and EWS data was known in the beginning. Unfortunately, it only became clear in the final weeks that there is an alternative data set which contains Nan values instead of the zeros for missing data. With this, the stations that have a downtime of more than 60% can already be removed because of the presence of the Nan values. However, this data contained a lot of stations that were not present in the data that was provided at the beginning. Suddenly changing to the newly provided data was not possible as the coordinates of these added stations were not provided. For the future, it is recommended to work with the rain gauge data that contains the Nan values. Especially when HII and EWS data are combined.

3.3 Radar data

The radar images are recorded every 6 minutes and stored as PNG files, where each pixel has a value that represents the reflectivity. Figure 3.4 shows two ways this can be visualised. The images are not from the same moment. Figure 3.4a shows a visualisation that is useful for making near real-time observations about upcoming rainfall. On the contrary, figure 3.4b does not allow for a quick observation but is a more convenient way to store the measurements.

During radar data preparation, noise and hail are filtered out below certain thresholds (default values are 15 dBZ and 53 dBZ respectively). It is recommended to do more data filtering in the future, specifically spikes and beam blocks should be filtered to make the data more accurate. After filtering, rain gauge locations are mapped to pixel locations in the radar images. For each rain gauge, the corresponding pixel values are stored over time.

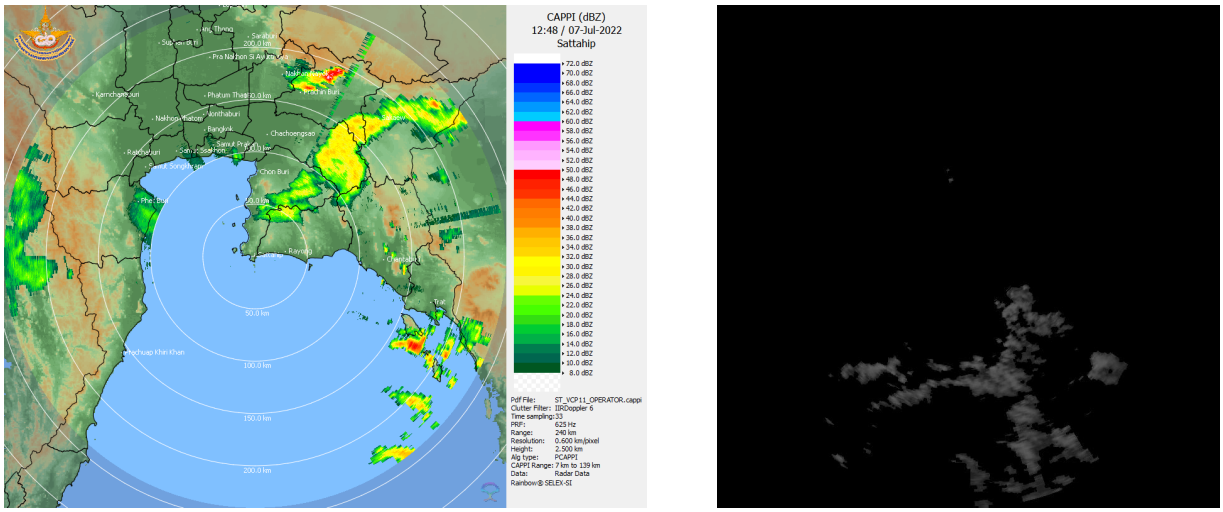

(a) Full radar image

(b) Reduced radar image

Figure 3.4: Radar images Sattahip

3.4 Event selection

With the method for filtering data in place, the event selection can start. The following properties define an event:

- Start/end-time
- Duration [hours]
- Rain intensity [mm/hr]:
  - Minimum intensity
  - Average intensity
  - Maximum intensity
  - Average cumulative intensity
- Stations [-]
- Number of stations in event [-]
- Reflectivity [dBz]:
  - Minimum reflectivity
  - Average reflectivity
  - Maximum reflectivity
- Type

The type is determined based on the average rain intensity. Table 3.1 states all types along with their rain intensity ranges.

Table 3.1: Event types

	Light	Moderate	Heavy	Extreme
Intensity [mm/hr]	0.1 - 5.0	5.1 - 25.0	25.1 - 50.0	> 50

Events are identified by applying the **Peak Over Threshold (POT)** method on the rain gauge data. Given a threshold, this method traverses the measurements of each rain gauge and checks for every measurement if it exceeds this threshold. All the consecutive measurements above the threshold entangle an event. The method also uses a waiting time parameter, which means how many hours there can be no rain within an event. Figure 3.5a displays measurements of station ATG011 in 2022 and how a threshold of 5.0 can identify events.

The POT method identifies events per rain gauge. Events occurring at overlapping times should be merged to get a more complete overview. This merging is done efficiently by first sorting the events on their start time (visualized in figure 3.5) and afterwards examining if the consecutive events overlap.

The most important properties of an event are the start time, end time, and names of the stations. All other properties can be derived from these by consulting the rain gauge and radar data. These other properties are used to summarize an event, but their meaning is limited. For example, the list of stations in an event are not necessarily all measuring rain throughout the entire event. So if more detailed properties are required for your purpose, these should be derived from the main properties in combination with the prepared rain gauge and radar data.

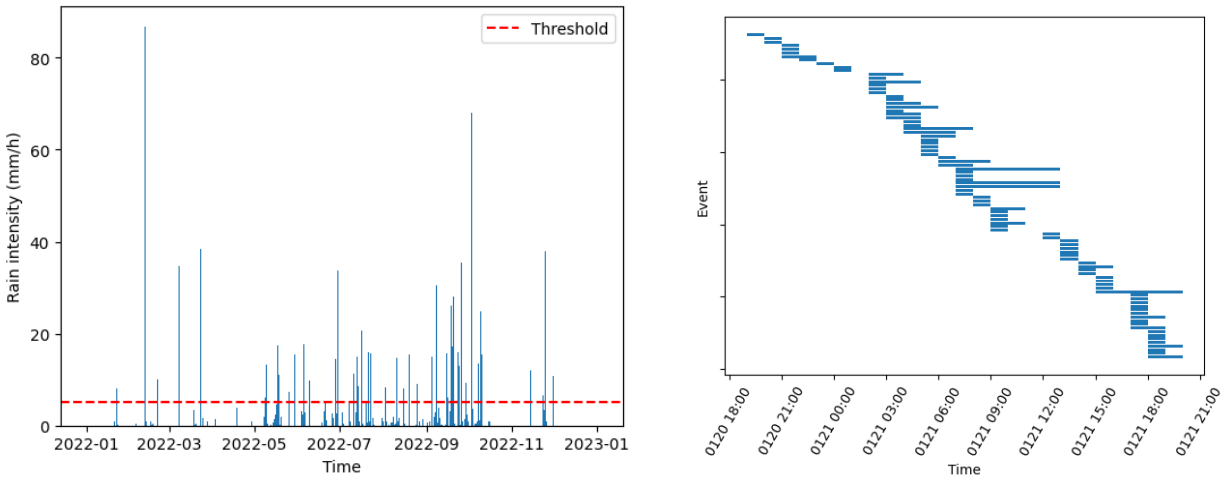

(a) Peak Over Threshold

(b) Unmerged events sorted on start time

Figure 3.5: Examples event selection

3.5 Radar calibration

The event selection provides sets of measured precipitation and reflectivity. The reflectivity can only be provided if there is an image available for that specific moment in time as the reflectivity is derived from those images. There is less radar data available as opposed to the rain gauge data. Five radars in northern and mid-Thailand overlap in the service area as seen in figure 3.6b. Of these five radars, only the Sattahip, whose service area is indicated in orange, has recorded data for over two years. Namely, from 2013 to 2023. That is why the Sattahip radar is used for the calibration process.

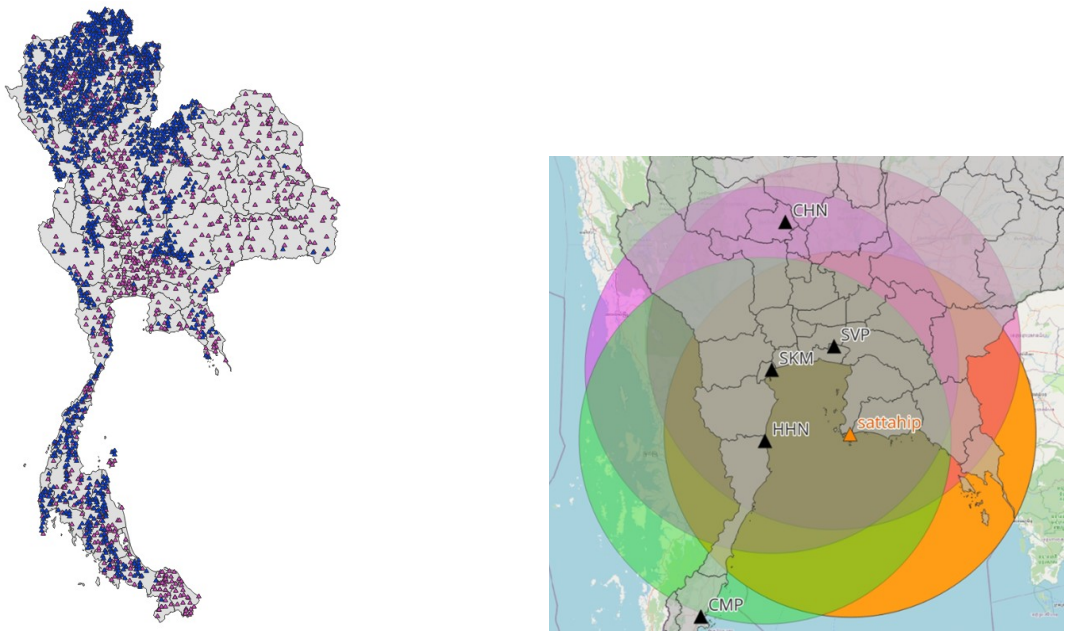

(a) Rain gauges in Thailand

(b) Radars in northern/mid Thailand

Figure 3.6: Service areas radars and gauges

Notice in figure 3.6a that the HII and EWS gauges are spread nationwide. Logically, only the gauges that fall into the service area of the Sattahip are used for the calibration since those have a corresponding reflectivity value. The model excludes the stations that do not fall into the service area.

The reflectivity that coincides with the station pixels does not indicate anything yet. That is because you can accumulate rainfall but not reflectivity. The cumulative reflectivity is dependent on the number of measurements in an hour instead of its value. Averaging the reflectivity is also not possible because this will cause problems with conversion equation 3.1. The reason for this is the nonlinear relationship between the reflectivity and rainfall rate. This can be shown by rewriting eq. 3.1 to solve for R:

$$(\frac{Z}{a})^{\frac{1}{b}} = R \text{ (eq. 3.2)}$$

Equation 3.2 is used to convert the reflectivity (Z) into rainfall intensity (mm/hr). Instead of using an hourly average reflectivity, a cumulative conversion of reflectivity into rain is used. The reflectivity that is measured every 6 minutes is converted with eq. 3.2 and accumulated over the hour. It is assumed that the reflectivity is uniform over the 6 minutes but not over 60 minutes. This is described in equation 3.3. The method where the average reflectivity, and thus an hourly uniform reflectivity, is used is shown on the right-hand side. The left-hand side shows the accumulation method which results in an hourly intensity. The right-hand side results in a different and incorrect rain intensity because of the uniformity assumption that is made when averaging reflectivity over such a long time.

$$\frac{1}{n}\sum_{i=1}^{n}(\frac{Z_n}{a})^{\frac{1}{b}} \neq ((\frac{\frac{1}{n}\sum_{i=1}^{n}Z_n}{a}))^{\frac{1}{b}} \text{ (eq. 3.3)}$$

So reflectivity must first be converted to rain before it can be accumulated using eq. 3.2. Figure 3.7 shows an example of how this is done together with the actual rain measured by the rain gauge in that specific hour. The goal of calibration is to pick conversion parameters a and b that minimize the difference between the values of the blue and red lines at the end of each hour.

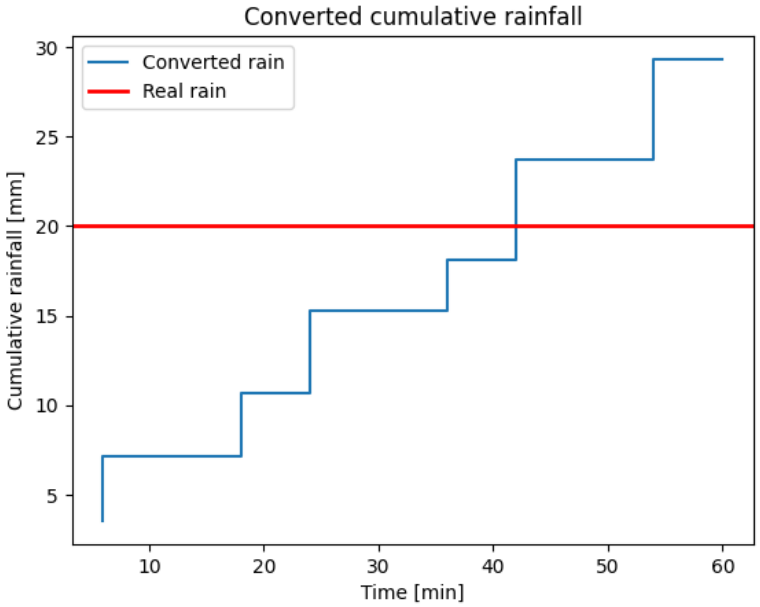

Figure 3.7: Converted reflectivity to cumulative rainfall

To achieve this goal a loss function is minimized. The loss function quantifies the difference between all the reflectivity and rain gauge pairs and is described by equation 3.4. Note that reflectivity and rain gauge pairs are derived from events, but are **not** the same as the average reflectivity and average rain intensity properties. Instead, they are pairs from a single hour and a single rain gauge within an event. So if the duration of an event was two hours and occurred at two stations, the number of pairs will be four. As mentioned before, averaging and accumulating are both not possible for reflectivity values. Therefore, the reflectivity is kept as a vector of 10 values per hour, because measurements were done every 6 minutes.

$$\ell = \frac{1}{n}\sum_{i=1}^{n}\left[\frac{1}{10}\sum_{j=1}^{10}\left(\frac{Z_{ij}}{a}\right)^{\frac{1}{b}} - R_i\right]^2 \quad \text{(eq. 3.4)}$$

3.6 Results and recommendations

Results were achieved by following the full methodology. The data for 2022 was processed entirely which resulted in a few sets of conversion parameters. The first set of points was found by using the cumulative reflectivity rainfall of all events above 5 mm/hr against the actual cumulative rainfall. The second set was fitted only on events above 25 mm/hr. In the last set, the upper bound for b was set to 1.6. The different results can be seen in figure 3.8a, 3.8b, and 3.8c respectfully.

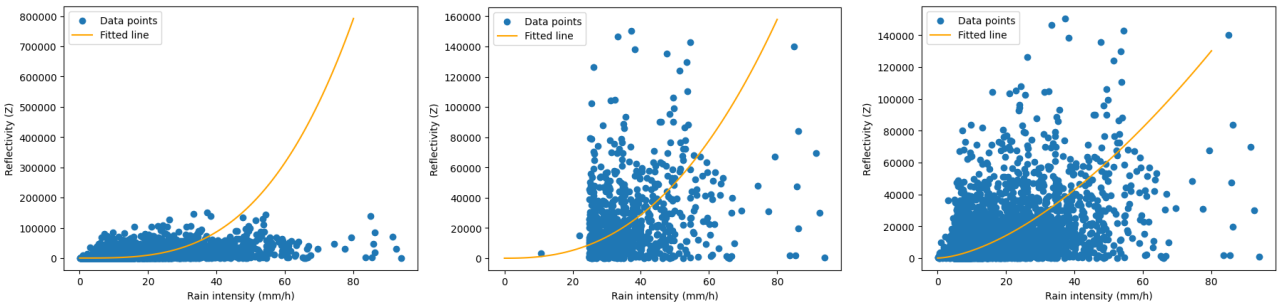

(a) a = 0.6651, b = 3.1927 (b) a = 3.2404, b = 2.4632 (c) a = 117.3207, b = 1.6

Figure 3.8: Calibration results

Figure 3.8a shows overfitting on the lower values. This is because 'light' and 'moderate' events

naturally occur more often than 'heavy' and 'extreme' events. This results in a high value for b.

A possible way to suppress this effect is to set the minimum rain threshold to 25 mm/hr during event selection. Thereby shifting the focus towards heavier events, which is more important in flood forecasting. The resulting a and b already provide a much better-fitted line and logically a tendency towards the larger events.

Another regularization option is to bound b. In the past, KU used to set b to 1.5 or 1.6. The results of using these values as bounds are shown in figure 3.8c. Note that a becomes much larger in this case. The fitted line has a more linear characteristic and better represents the heavier events.

By setting domains for the parameters or by selecting a certain set of events the conversion can be shaped until it complies with the wishes of the user. This means that the parameters are not solely determined by the loss function but also visually. Therefore, there is not one final result for the calibration which is exactly what was expected. It is up to the KU to use the model and interpret the outcomes keeping in mind their preferences. The goal of providing the model is therefore achieved.

Chapter 4

Conclusion and Recommendations

4.1 OpenRiverCam

The time in Phetchaburi and Bangkok served as a good environment to test the OpenRiverCam software in Thailand. The field trips to different size streams and/or rivers provided the opportunity to test the software and take lots of videos which could be used in our research at the university. Sufficient videos have been taken at all locations, when possible at different times and at different angles in an attempt to process results as accurately as possible. In addition, it helped learn about the ideal camera setup and settings for different locations.

The discharge results of the ORC were very good at the smaller rivers. At river B8 the detected water discharge by ORC was 40% lower compared to the RID measurement and at B11 the detected water discharge was only 15% higher compared to the RID measurements. This is promising because these rivers are often too small to measure with the ADCP rover - as the RID does. Moreover, the ORC measurements can be more accurate than the telemetry data. The larger river B3 and the river upstream turned out to be hard to measure due to the width of the river and the horizontal video angle from the bridge. The videos did give good results in the sunny nearby areas of the river, but at the sections of the river that were further away from the camera or in the shadow, flow detection proved to be more difficult. Discharges measured by ORC at these 'wide' rivers were approximately half of the discharge measured by the RID at the same time. Thus, ORC software could not provide realistic discharge data for these rivers given the circumstances and material we had. The ORC model does provide great insight on the velocity profiles of the river. Comparing the current measurements performed by hand with the current profiles received via the ORC model, showed a great resemblance. Because these current profiles are the ones integrated by the ORC model to receive the water discharge, the outcome shows a good representation of the real water discharge. The results from the ORC model show that the ideal video angle is as vertical as possible and that the distance between the camera and the water should be as small as possible.

One can decide upon the number of frames to analyse for one video running the ORC model. A minimum of around two hundred frames is proved to give reliable results. Analysing more frames should not give better results and would only increase the running time of the model. Also, higher quality video's (4k in this report) does bring more detail to the visualization of flow. Yet, it does not provide more reliable results as velocity plots show to be more volatile as a results of small deviations in the stream. This holds especially at the wider rivers. In conclusion, having the model run a 4k high-quality video for a long time will not return more valid results, but will increase your running time significantly

The largest issue in the field was the GPS. It took a long time to calibrate the GPS and the GPS was not very accurate after it finished calibrating. The GPS location points are an important input for the OpenRiverCam model. Unfortunately, RTK GPS - as used in this research - is somewhat outdated and basic. The calibration time was a problem. It took a minimum of 2 to 3 hours to achieve an

average deviation of 70 to 80 centimetres. Furthermore, when finished calibrating, the actual deviation turned out to be higher than the value set. The use of RTK equipment requires an open space to minimise disruptions as much as possible. That is why the base station was always set up next to the river. However, tall trees caused disruptions and bad weather conditions forced the process to be halted sometimes. A base station would ideally calibrate overnight, depending on the range for 24 to 36 hours, which requires a supply of power. When calibrated, an RTK installation can theoretically operate with a distance of 20 to 50 kilometres between the Base station and the Rover. In practice, this turned out to be unfeasible with the installation that was used. In combination with the test locations that were more than 20 kilometres away from the sleeping location, which had a power supply, these deviations had to be accepted. In the ideal scenario, a newer and more accurate RTK installation is used, where the Base station can calibrate overnight to an accuracy of 1 centimetres.

For creating cross sections of the river and getting GPS locations of the control points, an accuracy below 10 centimetres is favourable. An accuracy even lower than 10 centimetres would create better results for the rivers with a very low water level (lower than 10 centimetres). The GPS accuracy achieved in the field in Phetchaburi was between 70 and 80 centimetres, which proved to be too large to create an accurate cross-section of the rivers. Therefore, using a more accurate RTK GPS would provide more accurate cross sections and -reference points and thus better results. Additionally, it would allow one to save time in the field because calibrating the GPS and creating cross sections by hand were the most time-consuming activities at the location. Using colourful poles as control points and using a fixed camera position for each river will also increase efficiency in the fieldwork. The poles will be visible to find in the camera calibration of the ORC model and the fixed camera position will make it unnecessary to create different camera calibrations for each video. In short, a better functioning RTK installation provides better GPS points for both the control reference points and the cross-section so that the results can be optimized and better match reality, which will provide more reliable data.

The documentation of the results and all the measurements in the field could have gone better. It would have been more clear to set documentation rules beforehand on how to write down all the measurements by hand and by the GPS. This could have saved time in processing all the videos and measurements. Getting a clear video of the B3 river and the river upstream was also a challenge. We managed to get all the videos, but the camera angle would have been preferred to be more vertical. This lead to the fact that ORC discharge results at large rivers - where the camera angle is more horizontal when capturing from the bridge, proved to be less valid compared to at small rivers - where the relative camera angle is more vertical to the water surface. A recommendation for future research is to use a drone to shoot the footage. It can get a higher picture than the bridge and it will be able to film open parts of the bridge from a vertical angle. After testing the software with better GPS points and drone videos, the influence of the shadow could be investigated more thoroughly.

4.2 Radar calibration

The radar calibration consisted of three main aspects. Namely, cleaning up the rain gauge data, event selection, and calibrating the conversion parameters. The goal of this part of the project was to streamline the process of calibration and to obtain results for one year. The final model can assist KU in acquiring results in the future and for previous years with enough data.

Starting with the rain gauge data it can be concluded that that goal has been achieved. A robust and self-explanatory model has been delivered that merges HII and EWS data and filters stations that can be identified as broken by their downtime. The remaining stations can then be reviewed by their DM-curve in a streamlined and fast way by using the widget provided in the model. The notebook was fine-tuned in collaboration with the Water Resources Engineering Department. The analysis of the 2022 and 2021 data was done by a MDP student as clean data was needed for the calibration. It is recommended to redo the years 2022 and 2021 and do the remaining years with the new HII data mentioned in section 3.2.2 instead of the previously used data to be more accurate and to involve more stations for the event selection.

The model has shown that it can efficiently select events and obtained results for 2022. The main properties of an event are the start time, end time, and the list of stations where the event occurred. Other properties are also stored, but one should be aware that these are not complete. For a specific purpose, more detailed properties can be derived by consulting the main properties and the prepared rain gauge and radar data.

The model can also calibrate fast allowing for flexible tweaking of hyperparameters. Nevertheless, it is a problem that heavier events are naturally underrepresented in comparison to lighter events. This problem can be suppressed by leaving out lighter events or by bounding the b parameter. In the future, data balancing techniques could be considered to tackle the problem.

In future development, it is recommended to be consistent in the data formatting. Storing the rain gauge data in the same format will make it easier to use in combination with each other. The misalignment between filled missing data in the HII data and the Nan values in the EWS data is an example of this. It could prove to be an unnecessary obstacle in acquiring a much larger data set. Another recommendation is to automate the process of the DM curve analysis. This can be achieved by letting a model learn from a data set of curves accompanied by valid labels. Furthermore, calibration from a radar image pixel to a corresponding rain gauge ignores a lot of external factors. For example, rain can be measured in the air at a specific pixel but due to wind the rain can fall at a different location. Encapsulating more external factors could therefore improve the accuracy of calibration.

Appendix A

Field Guide: RTK-GPS and OpenRiverCam Integration for River Flow Measurements

In this appendix section, we will elucidate the steps involved in utilizing the GPS-RTK system to derive values for implementing OpenRiverCam.

Table of Contents:

A.1 Introduction

One of the essential inputs for the OpenRiverCam software, in addition to videos, consists of GPS coordinates for the river location, reference points, and cross-section coordinates. These GPS coordinates play a crucial role in mapping the video onto geographical maps, enabling the calculation of river flow and discharge. To obtain these GPS points, it is common practice to utilize an RTK GPS system. In the context of this Multi-Disciplinary Project at Kasetsart University in Bangkok, Thailand, the RTK GPS equipment supplied by Professor Dr. Ir. Olivier Hoes, courtesy of the Technical University of Delft, was employed. This manual has been crafted to guide users in the effective utilization of these instruments and equipment.

This GPS manual serves a diverse audience, with its primary focus on users eager to utilize OpenRiverCam software effectively. It caters to a wide spectrum of individuals, including TU Delft students globally who intend to incorporate OpenRiverCam into their projects and research endeavors. Additionally, it extends its support to Kasetsart University students who will be continuing their utilization of OpenRiverCam Software, providing valuable guidance for their studies. Furthermore, this manual offers an English version of the GPS explanation and its practical application, specifically for the Royal Irrigation Department (RID) of Thailand. This inclusion serves as a comprehensive reference and information source, offering insights into the various methods of GPS usage. Ultimately, this manual is a valuable resource for anyone interested in working with OpenRiverCam and who requires

GPS points for their projects. It aims to facilitate access to essential GPS information, enabling users to harness the power of OpenRiverCam for their specific needs and applications.

Real-time kinematic GPS, or RTK-GPS, is a cutting-edge technology recognized for its accuracy in location. By correcting GPS data in real-time using a base station's known location, it achieves centimeter-level accuracy. Surveying, agriculture, construction, and environmental monitoring are all industries where RTK-GPS is used. It is essential for measuring river flow with OpenRiverCam since it gives exact GPS coordinates for video georeferencing, mapping, and discharge calculations. This document explains how to accurately analyze river flow using OpenRiverCam and RTK-GPS. It is very important to read through the entire manual first, as there are many different steps mixed up, certain preparations must be made and everything must be well understood. Therefore, read through everything before starting the work.

A.2 Equipment Overview

The equipment used for the GPS consists of the RTK equipment and laptop software. The idea is to set up a base station, which, with the use of the software U-center, will contact various satellites orbiting the Earth. For this, a maximum deviation can be set on how many cm the location may deviate. In addition, a rover is used that also makes contact with satellites through SW Maps and itself makes contact with the base station through the antennas. SW Maps is an application that registers the GPS points that is used in this manual and will be explained further in Chapter A.4. Because the base and rover know each other's distance, make use of satellites and the base knows its location very accurately, the location of the points to be searched can be registered very accurately. All equipment needed and used is listed below:

- RTK Base + Rover starter kit (Ardus) see figure A.2
- Antennas and Mounting Options Base + Rover
- Data Collector Devices Base + Rover (e.g., Laptop, Tablet, Smartphone)
- Stand for mounting phone or tablet on rover
- USB type Mini to USB type C cable
- USB type Mini to USB cable
- Cables from Antenna to Base + Rover

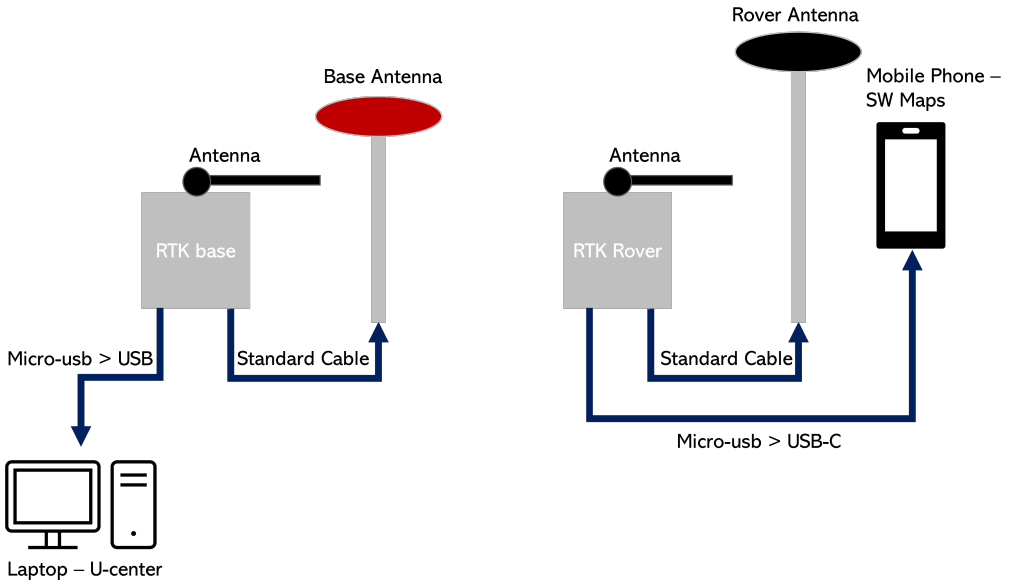

Figure A.1: schematic overview of the equipment

Figure A.2: Ardus RTK rover (left) and RTK base (right)

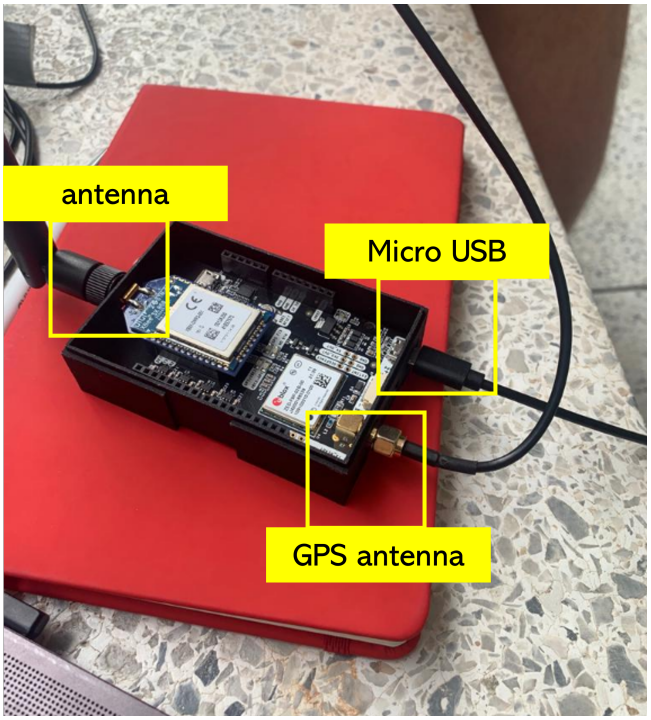

Figure A.3: GPS Rover Antenna

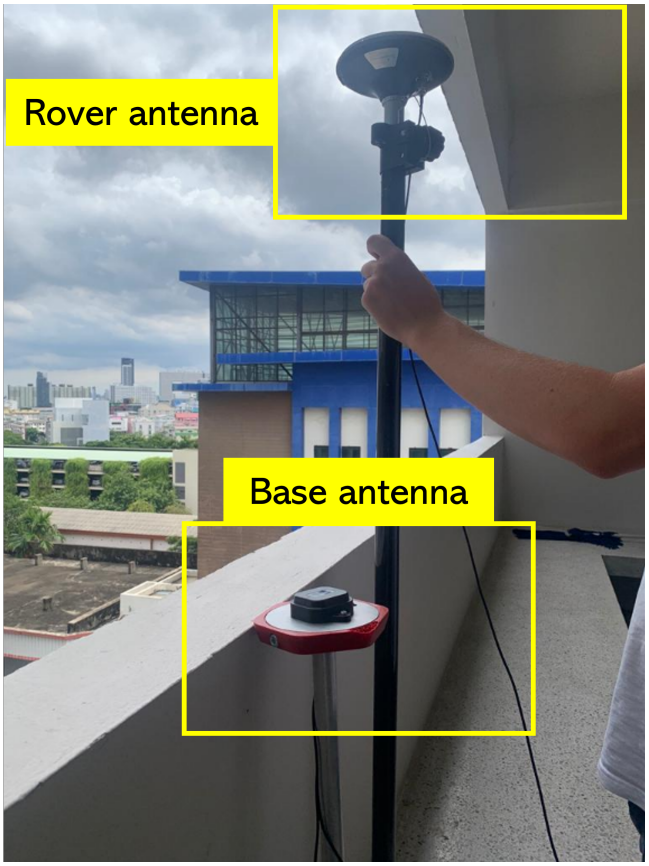

Figure A.4: GPS Rover

A.3 Software Installation and Configuration

To configure the software and install U-center, to calibrate the Base, the following steps should be followed. What is important to note is that U-center is not the only program that can be used, but in the case of the study conducted by the TU-Delft team, this software worked easily with the RTK equipment used. However, there are therefore plenty of other software programs that can be used. For downloading the software go to the next url: `https://www.u-blox.com/en/product/u-center`.

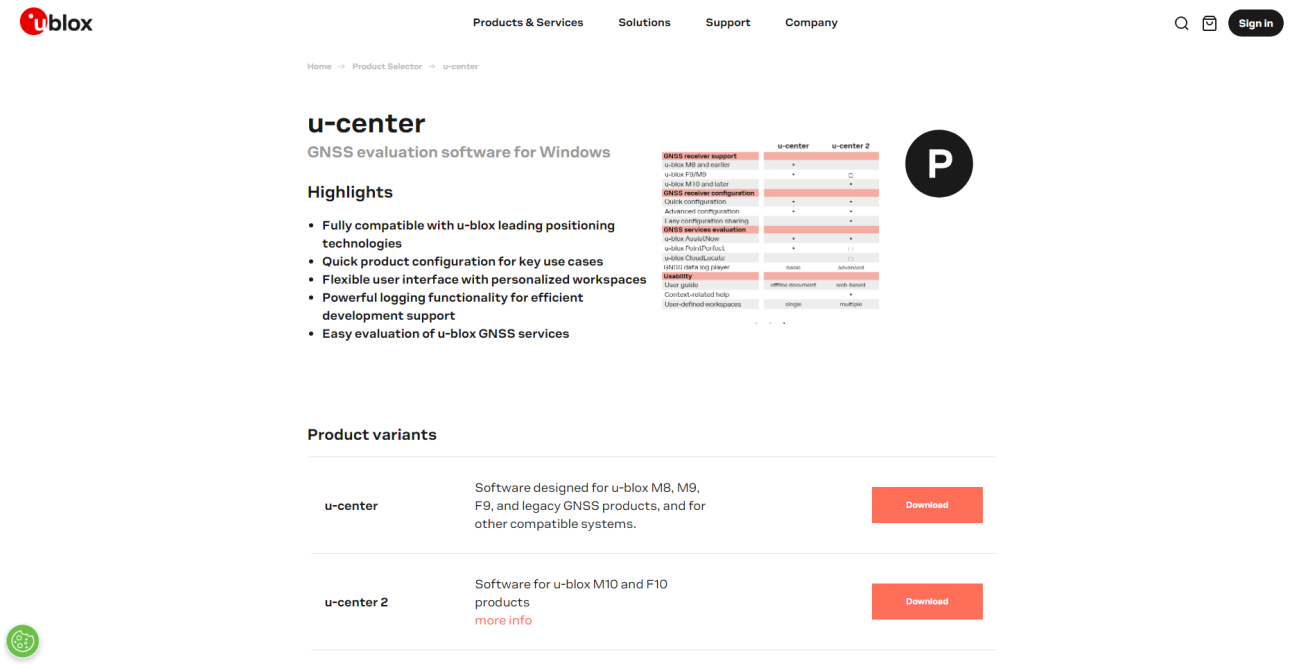

Figure A.5: U-blox website - U-center download

A.3.1 Opening U-center

when U-center has been downloaded, the software program can be opened. The next step to be performed is to configure U-center to install the base station and allow it to contact the satellites. **IMPORTANT: for configuration, the base's antenna must be connected to the laptop**. Openening U-center shows the software's default display as can be seen in figure A.6. In it, open a project with the name of the study in question, via *COMMAND*: **FILE/NEW**.

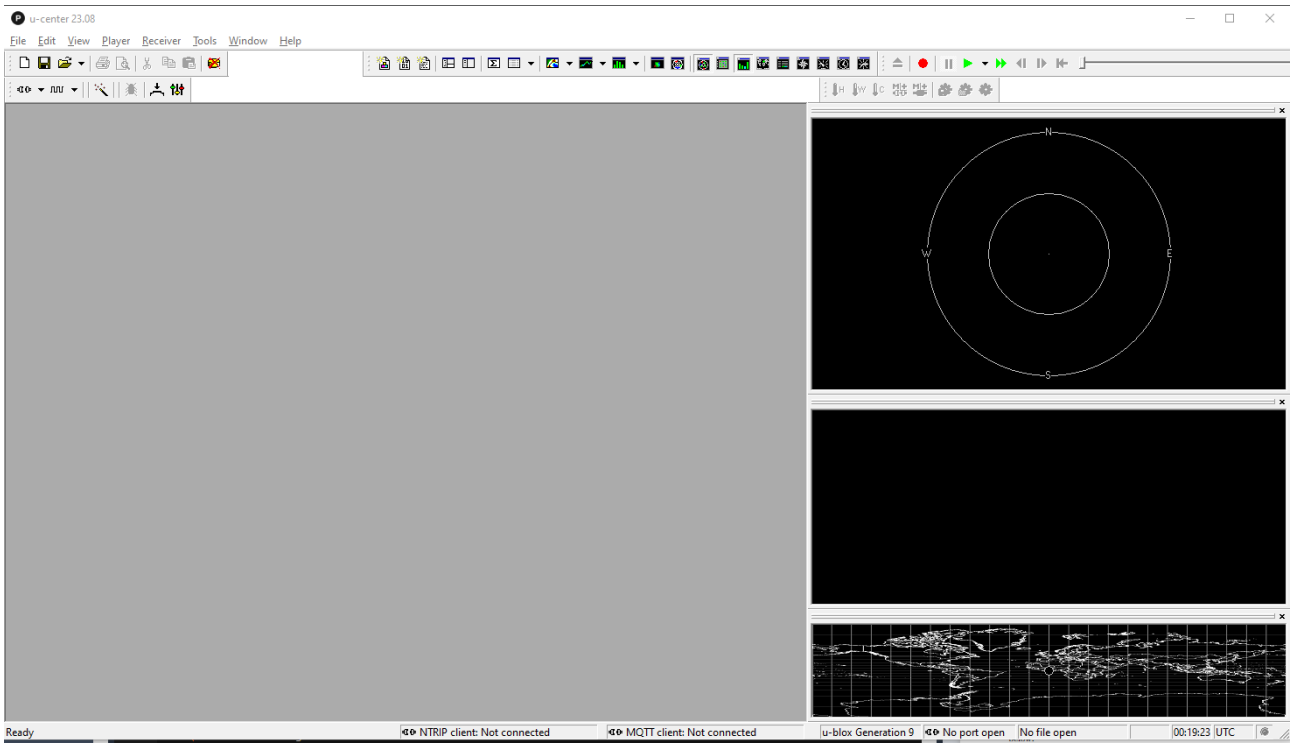

Figure A.6: U-center display

A.3.2 Configuration U-center

Once a file is saved and the opening U-center is successful, configuration can begin. The base station's antenna must be connected, and it must be linked to the software. This can be done through, *COMMAND*: **RECEIVER/CONNECTION/choose the USB port (COM_number)**. The COMP Port Number can be found in Windows by going to Device Manager (Start/Control Panel/Hardware and Sound/Device Manager. Look in the Device Manager list, open the category "Ports, and find the matching COM port. Take the number in the bracket behind the port description. This can be slightly different per laptop type and instructions can be easily found on the internet. This is shown in figure A.7. The laptop may crash and not connect directly. Use the laptop's general settings to find out which port is linked to which COM_number and click it. It should then connect automatically next time, otherwise match the USB port manually one more time.

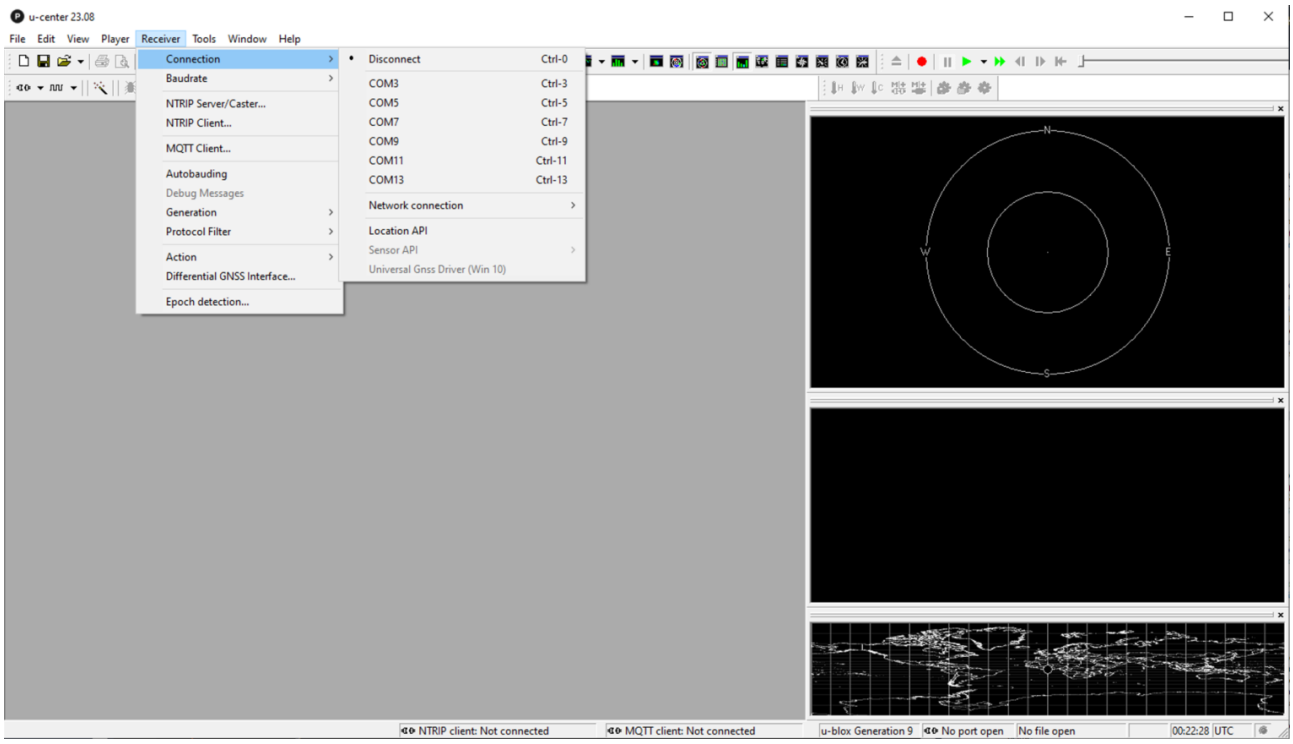

Figure A.7: U-center connection with receiver

The U-center program is only used to support the RTK software and requires no other additional settings. The only two functions used can be found under 'view' and are Messages and Configuration and these can be found in figure A.8.

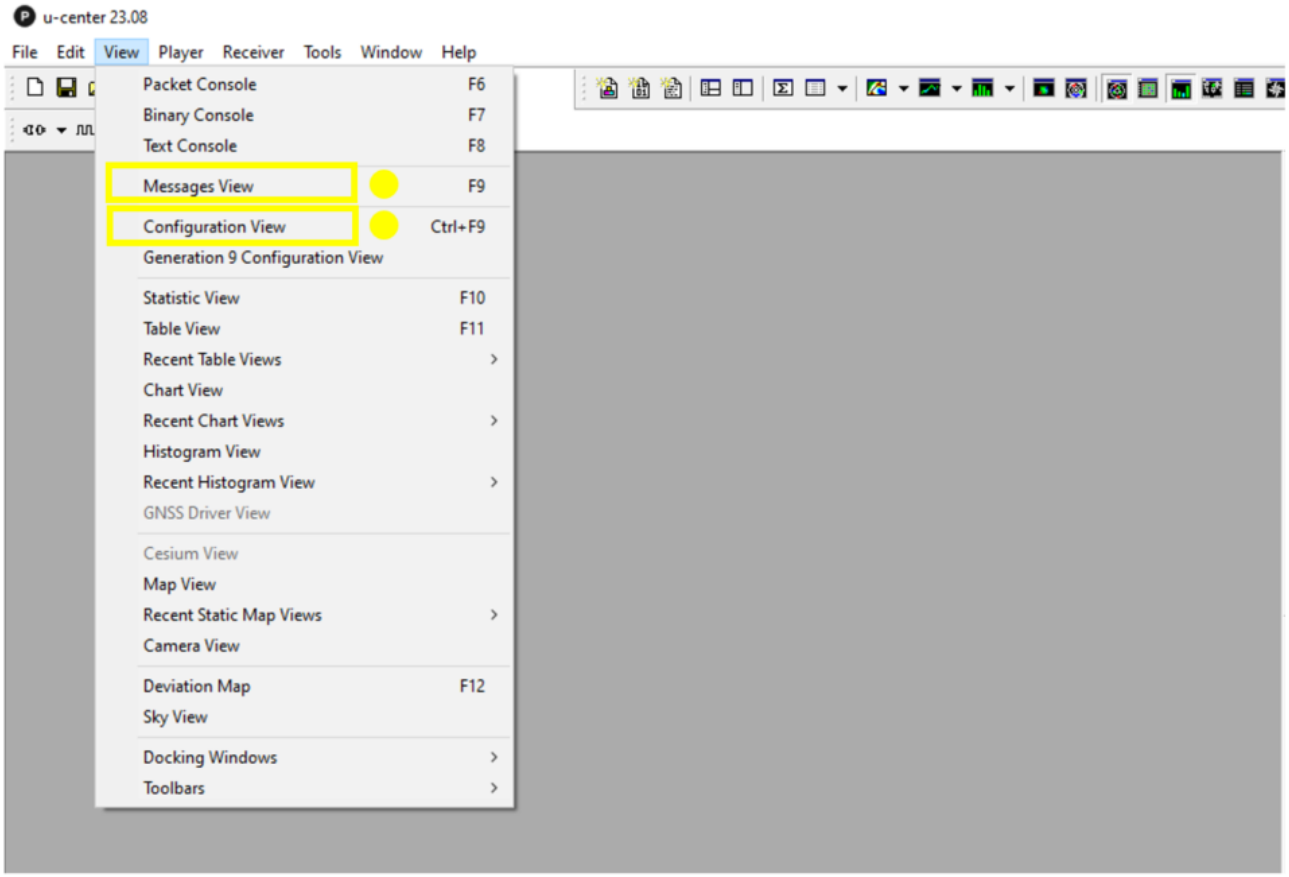

Figure A.8: U-center View: Messages and Configuration

A.3.3 Setting accuracy

The RTK equipment can find the GPS location to a very high degree of accuracy and therefore the desired accuracy must be set. This can be done under configuration at the Required Position Accuracy in meters. The minimum Observation Time is not important and can be left at 60 seconds. The Required Positioning Accuracy can be found via *COMMAND*: **VIEW/CONFIGURE/TMODE3 (time Mode 3)**. When the required accuracy is set, press SEND in the lower left corner of Configure - Time Mode 3 and the time starts running. This can be seen in figure A.10. In figure A.11 is shown that the time is running and the accuracy is set at 1.00 meters. This configuration can take a lot of time depending on the location of measurements and the availability of satellites. In order to reach an accuracy of around 0.01 meters (1 cm) can take between 8 and 48 hours. In order to configure this accuracy it is important that the program of U-center keeps running on a power supply.

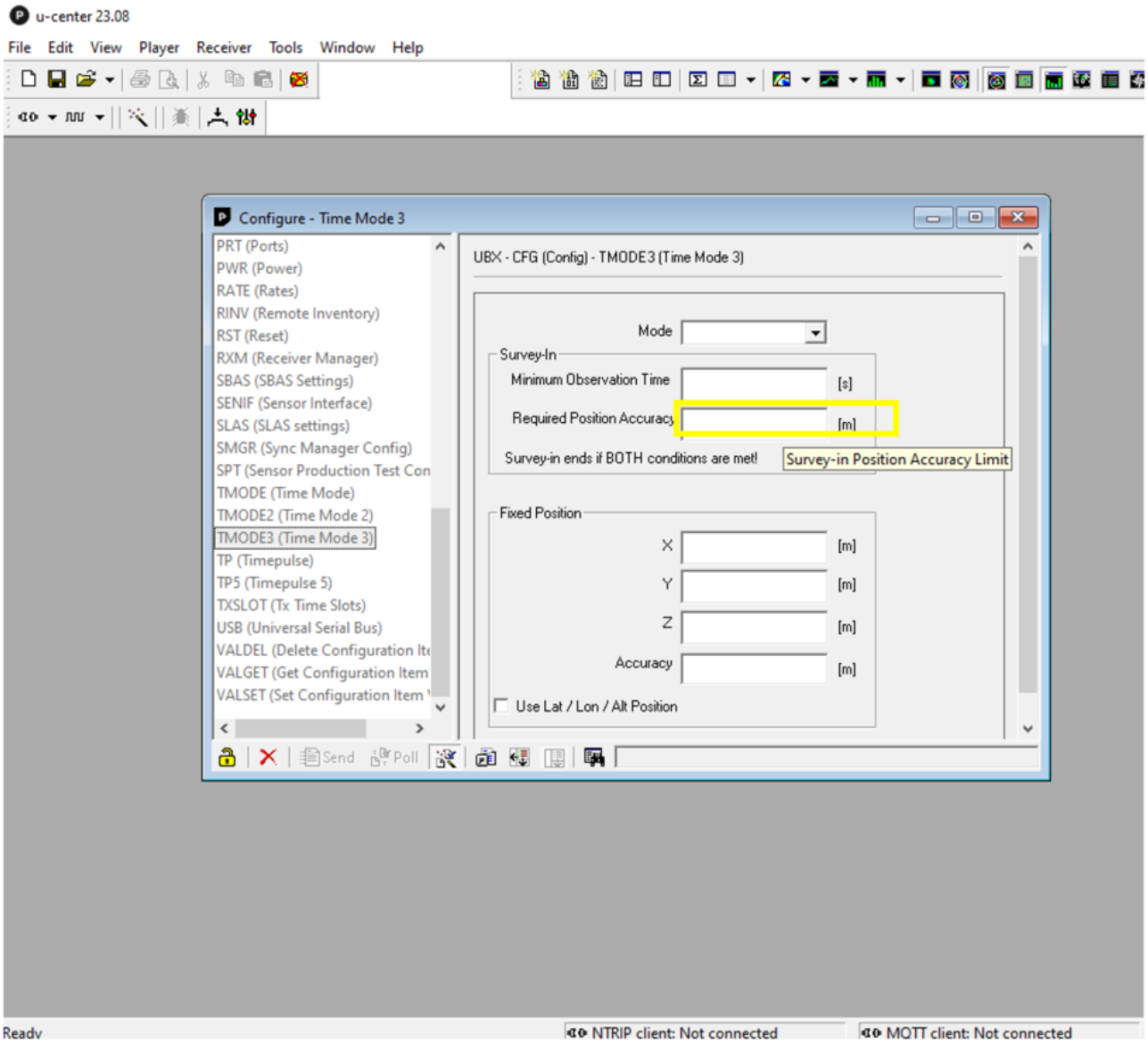

Figure A.9: U-center View: Configure TMODE3

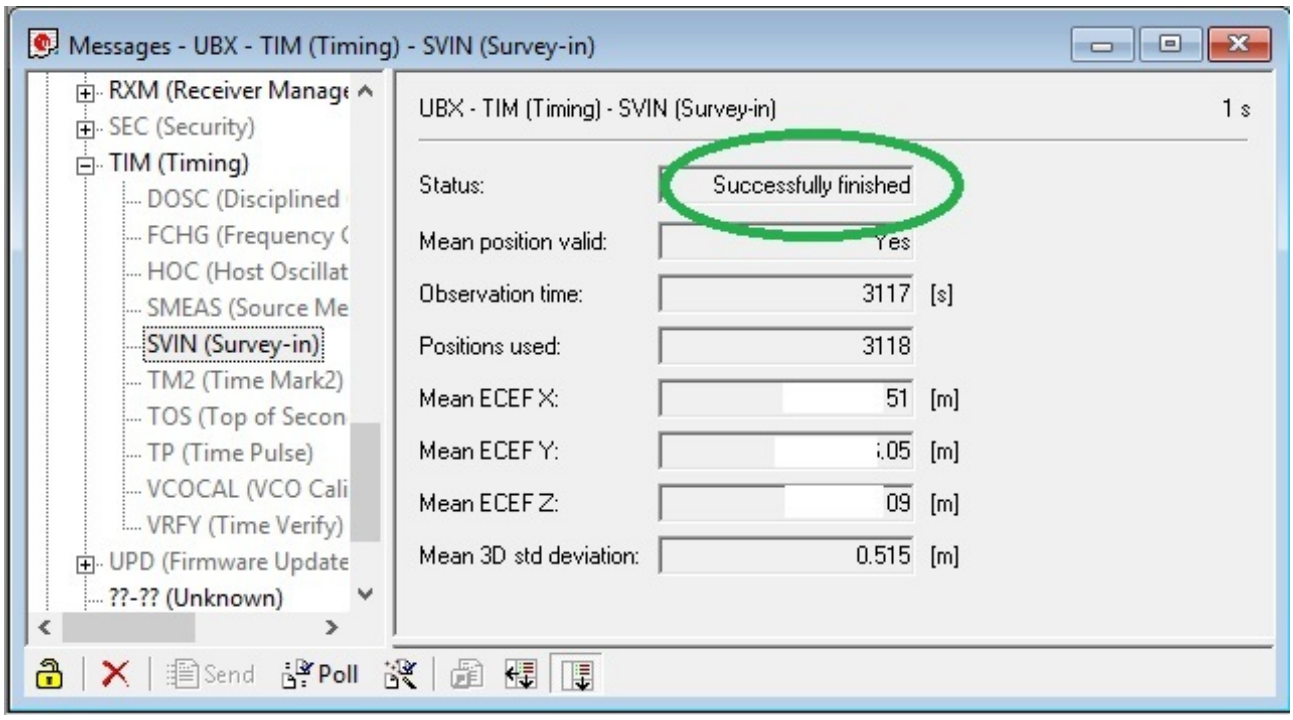

Figure A.10: U-center View: Configure TMODE3 status: Successfully Finished

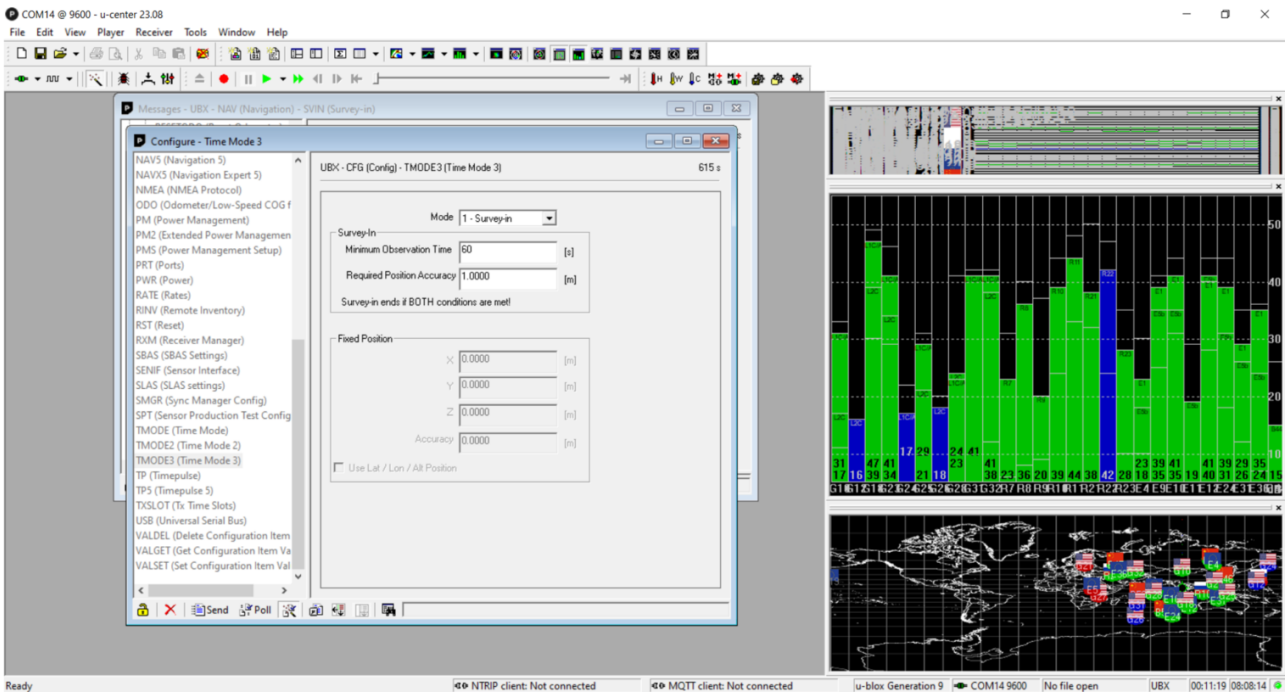

Figure A.11: U-center connection with receiver

A.3.4 Configuring RTK-GPS Software for Field Use

The next function in U-center to be used is the messages menu. This can be found in *VIEW*: **MESSAGES/UBX/NAV (Navigation)/ SVIN (Survey-in)**. In it, the progress of the calibration can be checked. The status shows 'In Progress' during calibration and 'Finished' when it has been fulfilled. The Survey-in display can be seen in figure A.12 and is in this figure still busy with the calibration. After it is fulfilled the calibration is done and the Base station is fixed on the location. **A very important note is that the Base antenna should not be moved and needs to stay in a fixed location!**

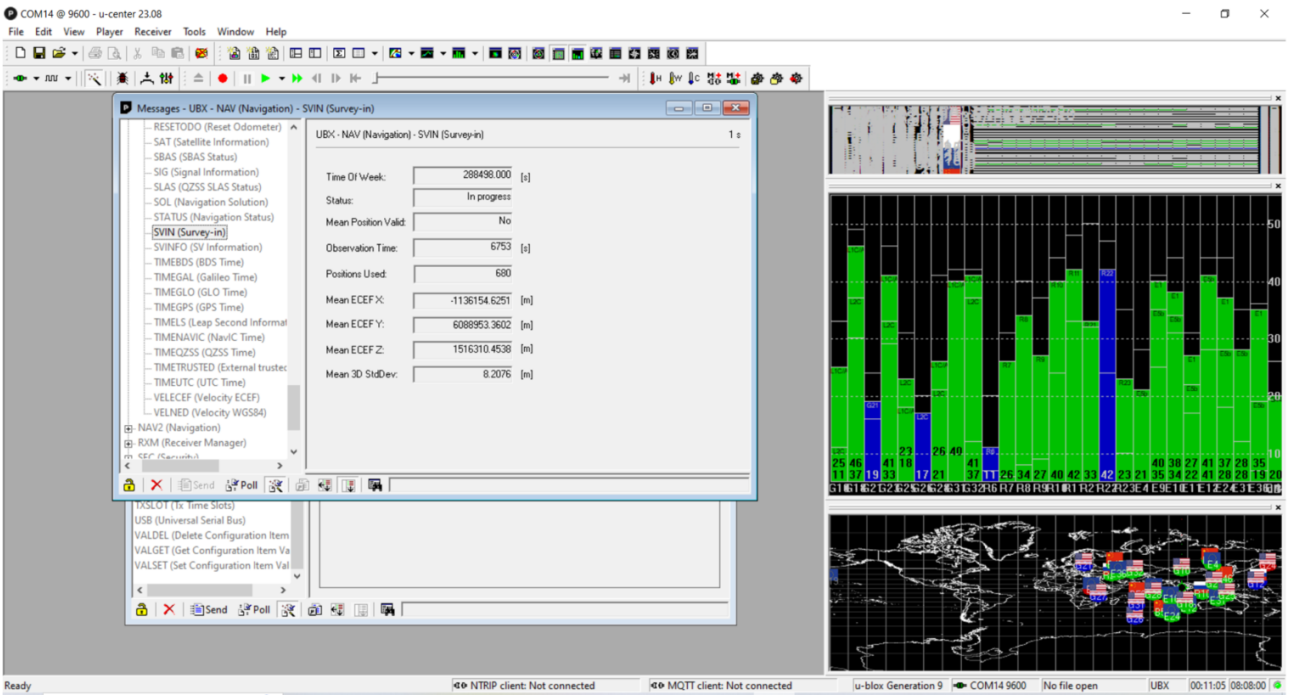

Figure A.12: U-center connection with receiver

A.4 GPS Data Collection using SW Maps

At this juncture, the preparatory phase has reached completion. All requisite pre-field preparations, including the establishment of the RTK Base Station and equipment calibration, have been rigorously addressed and finalized. With the precise determination of reference points and the positioning of cross sections in place, the commencement of field data collection is imminent.

To initiate the data collection process for GPS coordinates, a critical connection must be established between the Base Station and the RTK Rover. It is noteworthy that the RTK equipment integral to the OpenRiverCam system functions in an automatic, streamlined manner, simplifying the connection process.

Furthermore, to effectively register the GPS coordinates and associated data points, the RTK Rover is intricately linked with the SW Maps application, ensuring the seamless integration of geospatial information during the data collection phase.

SW Maps, an open-source mobile Geographic Information System (GIS) application designed for Android devices, functions as a versatile tool for the viewing, editing, and management of diverse geographic data, maps, and spatial information. For downloading the application and more information go to the next url: `https://aviyaantech.com/swmaps/`. At its core, SW Maps is characterized by its open-source framework, granting developers access to its source code for collaborative development. It supports the visualization of various map types, including offline, online, and locally stored maps in formats like MBTiles and GeoPackage. The application integrates seamlessly with the device's GPS, providing real-time location display for navigation and field data collection. Users can create and edit geographic features, encompassing point, line, and polygon geometries. SW Maps also offers offline functionality, allowing users to download maps and data for use in areas with limited internet connectivity. The application facilitates layer management for organized data handling and includes an array of geospatial tools such as distance measurement and area calculation.

SW Maps is accessible for download through the Google Play Store or Apple App Store. For downloading the software go to the next URL: `https://play.google.com/store/apps/details?id=np.com.softwel.swmaps&hl=en_US&pli=1`. While the application is primarily designed for Android devices, it can also be installed on iPhones. It's important to note that the iOS operating system lacks native support for direct cable input of RTK equipment. Enabling this functionality on iOS devices necessitates intricate adjustments to both settings and hardware within the RTK equipment, a process characterized by its complexity. This manual does not provide an in-depth exploration of these adjustments. If a comprehensive understanding of these modifications is required, it is recommended to seek additional resources and guidance available on the internet.

A.4.1 SW Maps run through

Upon initiating the SW Maps application, the user is presented with a choice to either create a new project or resume work on a previously established project. To access the application's menu, one may select the blue SW Maps logo located in the upper-left corner of the interface. This menu encompasses a plethora of options, facilitating the navigation between various projects and layers. For the purpose of employing OpenRiverCam functionality, the most critical features can be accessed via the GNSS header.

To enable the connection between the Android mobile device or tablet, equipped with the SW Maps application, and the USB serial cable, the USB Serial GNSS must be linked with SW Maps. Within the GNSS Status, users can gain insight into diverse data outputs, including longitudinal and latitudinal coordinates, as well as accuracy deviations. The sky plot feature provides a visual representation of satellite visibility and the current position of the rover within the expanse of the Earth's atmosphere.

The initial step involves establishing a connection between the rover and the application, achieved by selecting the "USB Serial GNSS" option. It is essential to note that in instances where the rover antenna is elevated on a pole, and the measurement point is positioned at ground level, it becomes imperative to provide a correction height. Typically, standard rover antennas offer height adjustability, often indicated on the pole structure. In such cases, it is imperative to input the accurate instrument height in meters and subsequently initiate the connection process. This can be done at the instrument height input, where the height is in meters, which can be seen in Figure A.13. Because the correction of Height is only in the vertical direction, the stick of the Rover should always be held perpendicular.

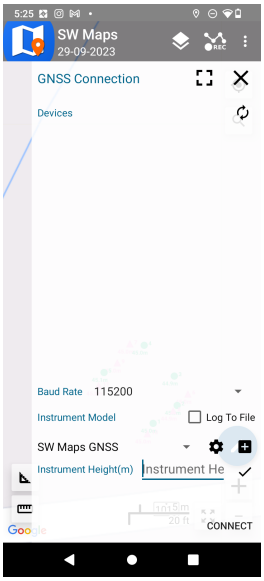

Figure A.13: SW Maps instrument Height

Upon successful establishment of the connection, the "fix type" parameter commences to manifest as

an observable indicator of the positioning status. All significant steps are delineated in Figure A.14.

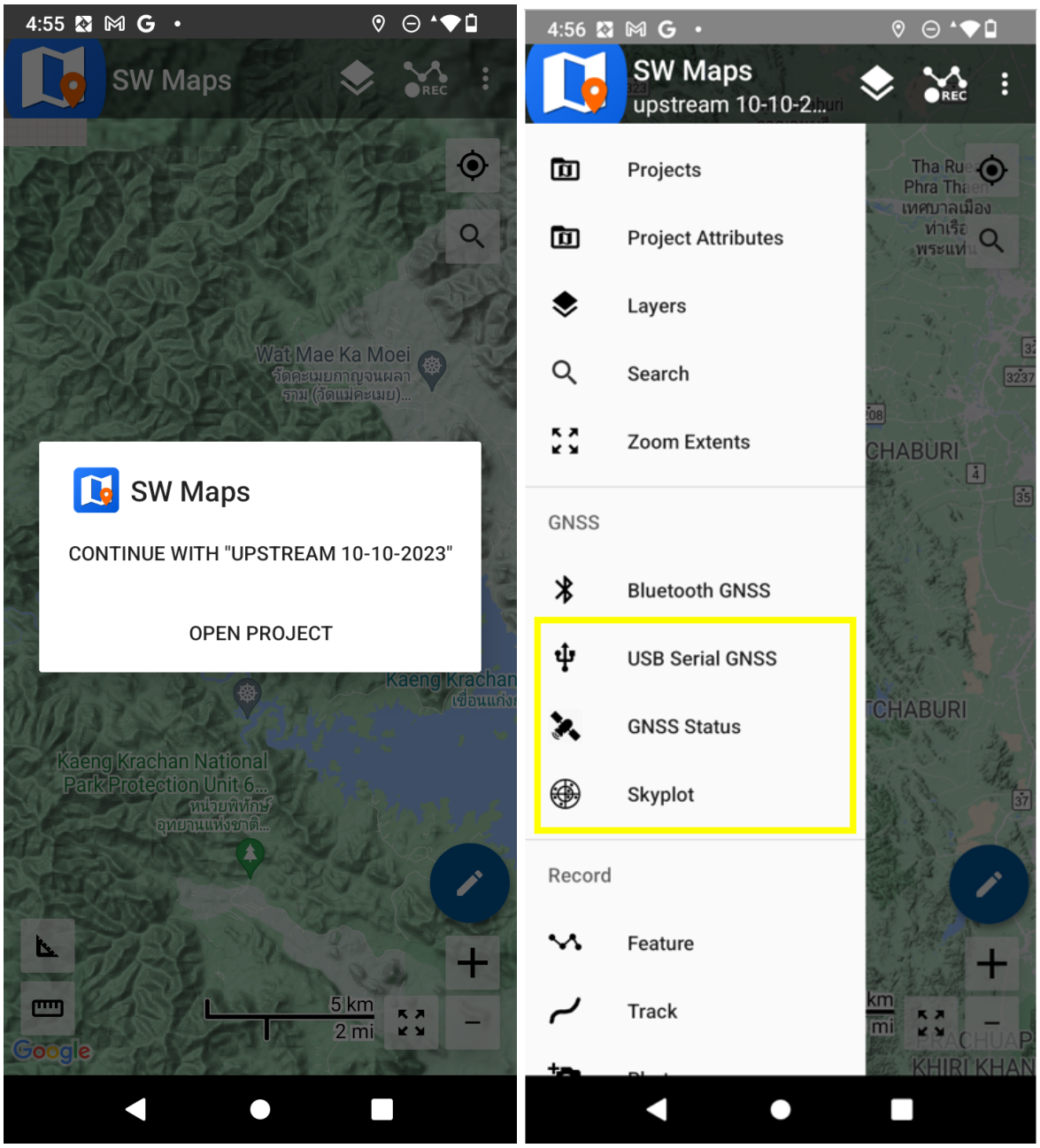

Figure A.14: SW Maps opening app

A.4.2 Record Feature

Upon achieving the "RTK Fixed" status for the rover, it becomes possible to capture and document GPS points and their corresponding coordinates. This action is executed by activating the "REC" function, located in the upper-right section of the application. Upon selecting the "REC" option, the user is presented with two choices: "Record Feature" or "Record Track." In the context of this illustration, the "Record Feature" alternative has been opted for due to its capacity to yield clear and concise output values.

Additionally, the application offers the capability to create distinct layers, thereby facilitating the categorization of reference points and cross-sectional coordinates. Users are afforded the opportunity to input names and descriptions for individual points within the point description interface. To secure a specific point, a simple selection of the designated "balloon" icon suffices, accompanied by a confirmation message indicating the successful fixation of the point. All significant steps are delineated

in Figure A.15.

1. Record Feature
2. Click on the layer desired
3. Fill in the description of the point
4. Click on the balloon to record the point
5. Repeat the entire process for the next point

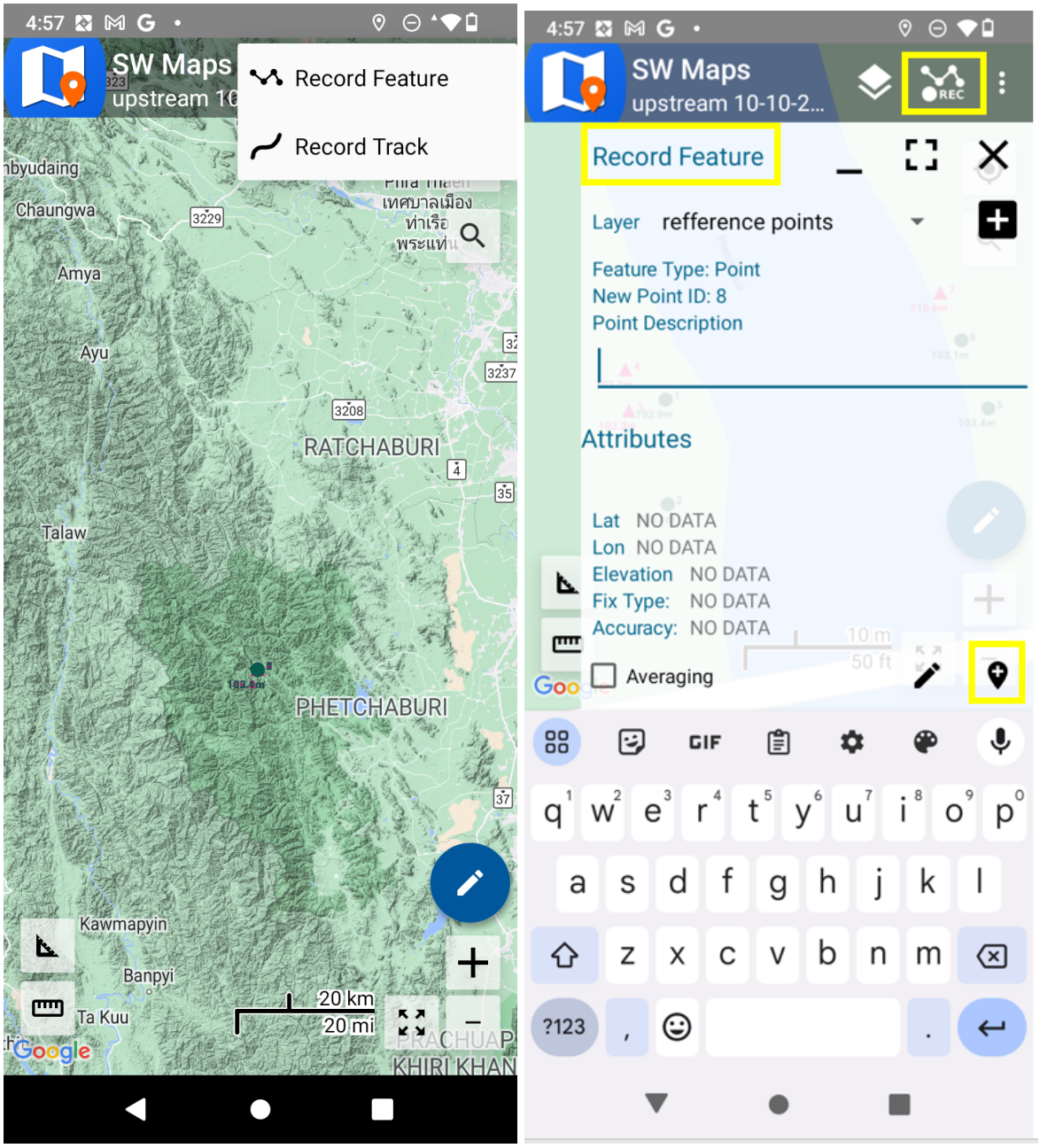

Figure A.15: SW Maps Record Feature

A.4.3 Results and exporting the data points

Upon the successful fixation of GPS location points, these points become conspicuously represented within the application's map interface. Subsequent to the completion of measurements, the acquired data can be extracted and shared to facilitate further analysis and collaboration. This can be accomplished by navigating to the main menu of SW Maps, where a 'Share/Export Project' header is situated. Within this menu, users are provided with the flexibility to upload, share, or export the data, allowing for customization according to individual preferences.

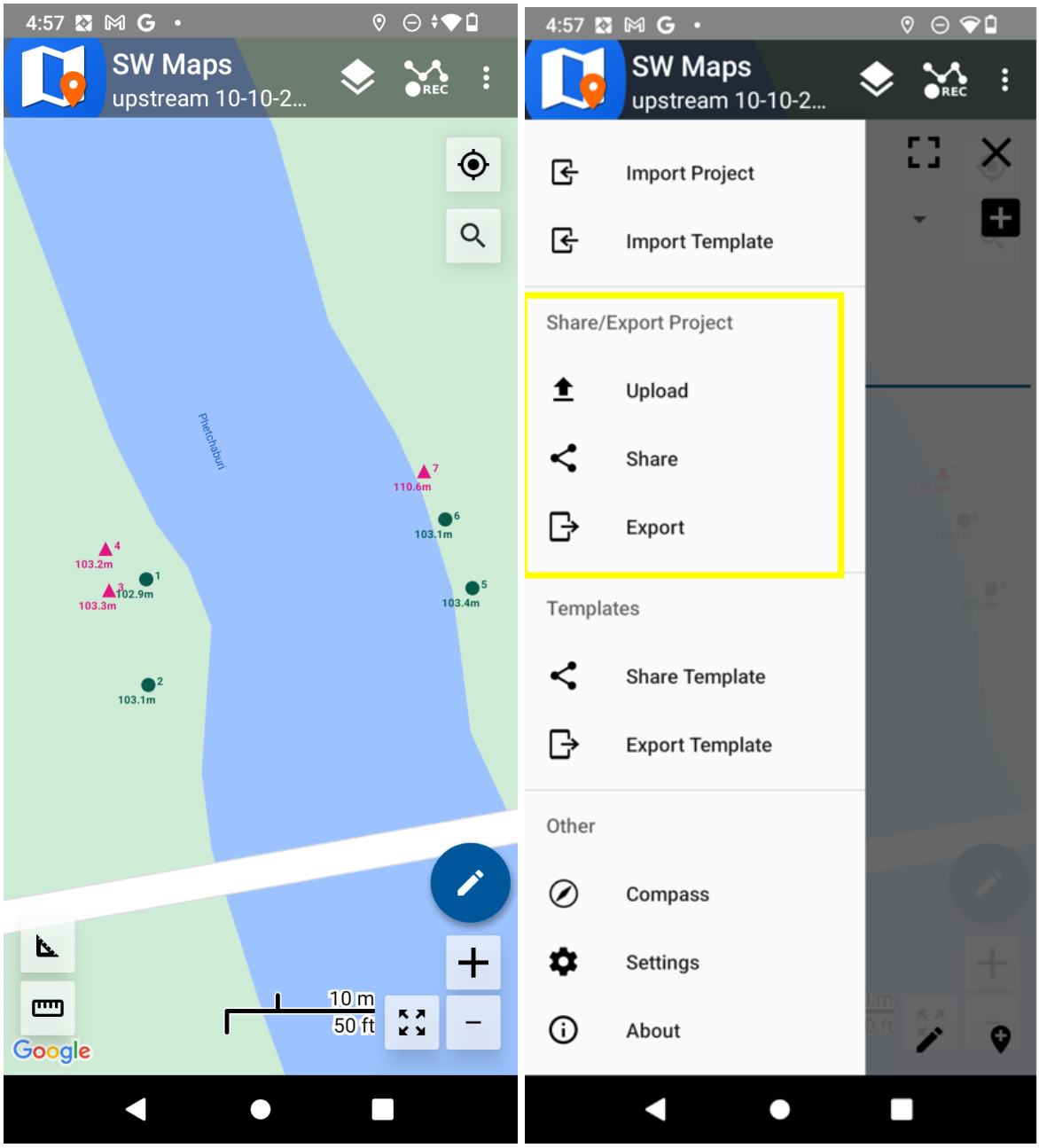

Figure A.16: SW Maps Output and export

If the "Share" option is selected, various choices become available, encompassing distinct file formats that can be utilized for exportation. For OpenRiverCam applications, a CSV file is a requisite. By selecting "Share CSV," a menu of options will appear. It is imperative to designate an export file name, as exemplified in this instance as "upstream 10-10-2023 CSV." Equally crucial is the specification of the appropriate UTM time zone when sharing or exporting the data, as a mismatch with the real-time scenario may occur if this step is omitted. In the present case study, the measurements were conducted in Phetchaburi Thailand, necessitating the selection of "Zone 47" as the relevant time zone in this region. Consequently, it is imperative to ascertain the appropriate time zone associated with the research location and data collection prior to initiating the export process.

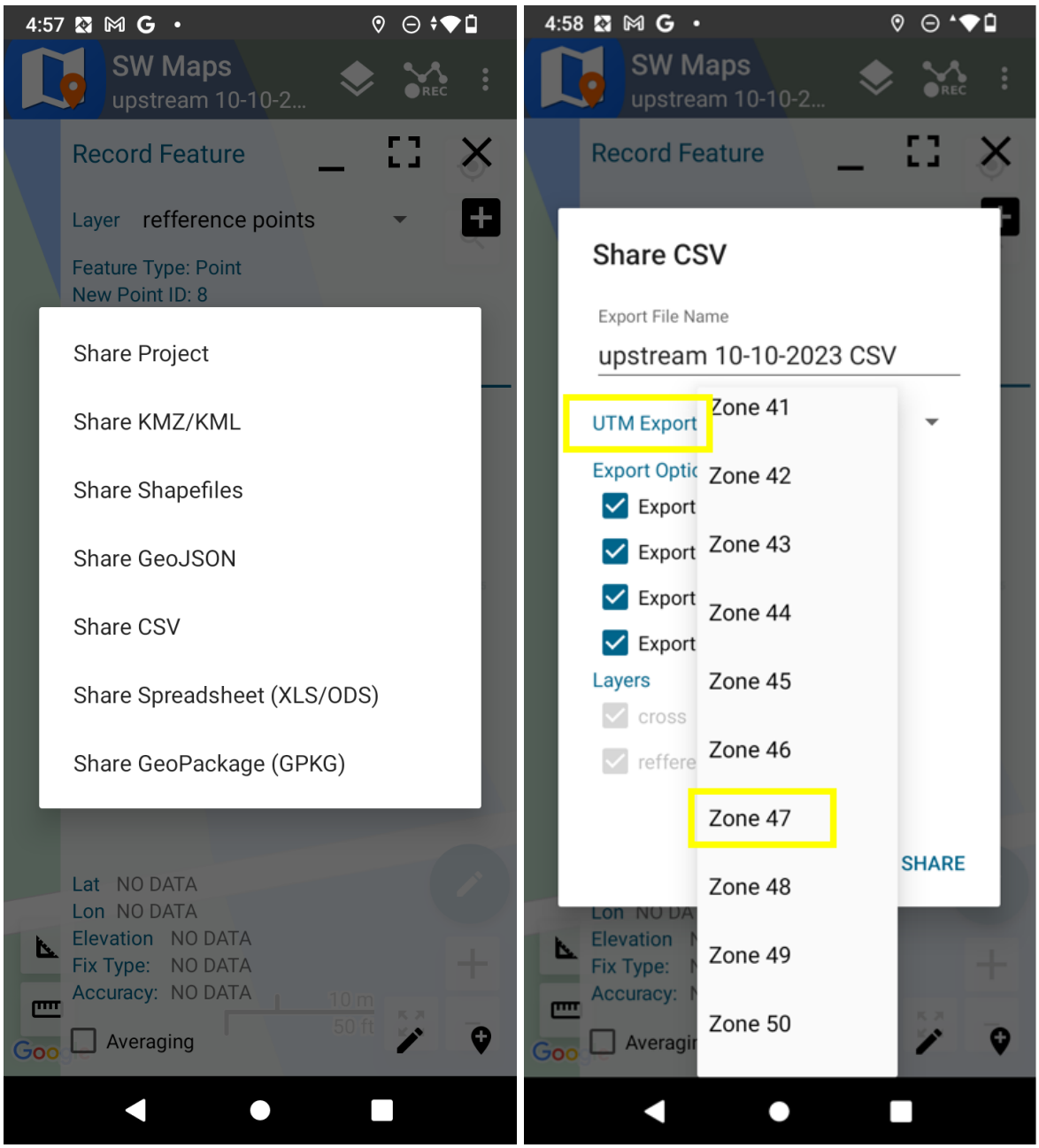

Figure A.17: SW Maps export and UTM time zone

A.5 Data Post-Processing

Subsequent to the export and download of GPS data sheets, the data is poised for transfer. For OpenRiverCam applications, the data is commonly formatted as a CSV file. Before proceeding with the importation of this data into OpenRiverCam, a comprehensive validation and quality control process is essential to enhance accuracy and rectify any potential inaccuracies. This procedure includes scrutinizing data alignment and rectifying any issues arising from practical errors or mislabeling by the data collection researcher. An illustrative representation of a CSV file output containing five reference points, intended for upload into OpenRiverCam, is presented in Figure A.18.

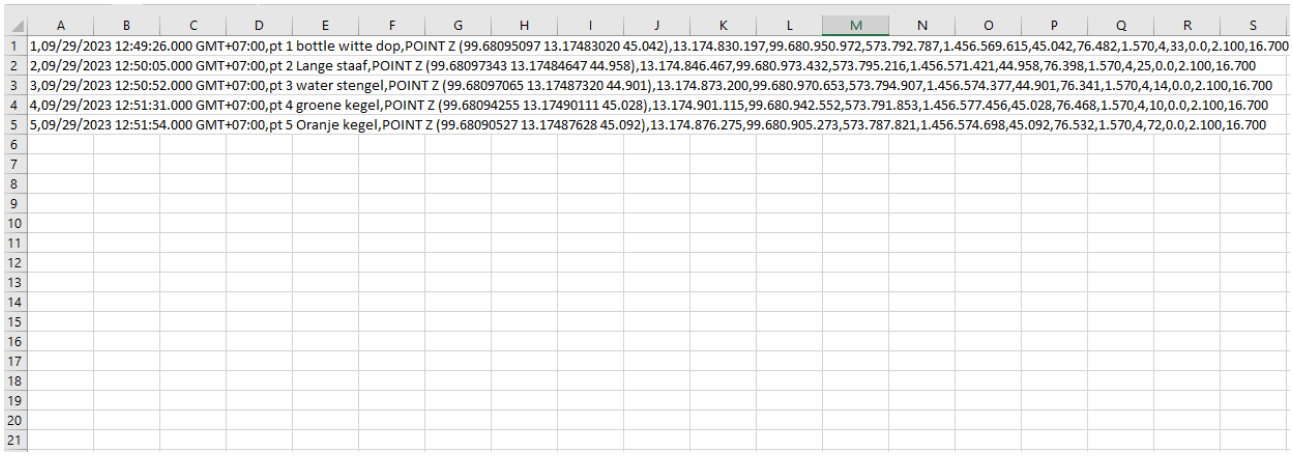

	A	B	C	D	E	F	G	H	I	J	K	L	M	N	O	P	Q	R	S
1	1,09/29/2023 12:49:26.000 GMT+07:00,pt 1 bottle witte dop,POINT Z (99.68095097 13.17483020 45.042),13.174.830.197,99.680.950.972,573.792.787,1.456.569.615,45.042,76.482,1.570,4,33,0.0,2.100,16.700																		
2	2,09/29/2023 12:50:05.000 GMT+07:00,pt 2 Lange staaf,POINT Z (99.68097343 13.17484647 44.958),13.174.846.467,99.680.973.432,573.795.216,1.456.571.421,44.958,76.398,1.570,4,25,0.0,2.100,16.700																		
3	3,09/29/2023 12:50:52.000 GMT+07:00,pt 3 water stengel,POINT Z (99.68097065 13.17487320 44.901),13.174.873.200,99.680.970.653,573.794.907,1.456.574.377,44.901,76.341,1.570,4,14,0.0,2.100,16.700																		
4	4,09/29/2023 12:51:31.000 GMT+07:00,pt 4 groene kegel,POINT Z (99.68094255 13.17490111 45.028),13.174.901.115,99.680.942.552,573.791.853,1.456.577.456,45.028,76.468,1.570,4,10,0.0,2.100,16.700																		
5	5,09/29/2023 12:51:54.000 GMT+07:00,pt 5 Oranje kegel,POINT Z (99.68090527 13.17487628 45.092),13.174.876.275,99.680.905.273,573.787.821,1.456.574.698,45.092,76.532,1.570,4,72,0.0,2.100,16.700																		
6																			
7																			
8																			
9																			
10																			
11																			
12																			
13																			
14																			
15																			
16																			
17																			
18																			
19																			
20																			
21																			

Figure A.18: CSV output file SW Maps

To comprehend the contents of the CSV file, it is imperative to ascertain the significance of each value. These values are consistently arranged in a predefined sequence, ensuring uniform output from SW Maps, as illustrated in this example. Understanding the pertinent information contained within the CSV file is crucial for its effective utilization within the OpenRiverCam application. Each row in the CSV dataset is segmented by commas, and the semantic interpretation of these values is explicated below:

1. Date
2. Time
3. Time Zone
4. Point Number
5. Describtion of points
6. Point Z
7. (Lon°, Lat°, Elv [m])
8. Lat°
9. Lon°
10. Lat [m N/S]
11. Lon [m N/S]
12. Elv [m]
13. Ortho Ht n[m]
14. Instrument Ht [m]
15. Horizontal Accuracy [m]
16. Vertical Accuracy [m]

The requisite input parameters for the OpenRiverCam system comprise the geospatial coordinates, specifically latitude (denoted as value 10) and longitude (denoted as value 11), in conjunction with the elevation (value 12) and orthogonal height (value 13) of a given point. An alternative RTK equipment system may deliver the data in an alternative manner; however, it will yield similar output parameters encompassing these four values.

A.6 Integration with OpenRiverCam

The importation of GPS data into the OpenRiverCam application, as well as subsequent steps, will be elucidated in the following Appendix B. In addition to data importation, the configuration of OpenRiverCam for the purpose of conducting river flow measurements will be detailed. This instructional guidance is predicated on the use of CSV file format, conforming to the specifications outlined in Section A.5 In the event an alternative GPS-RTK system is employed, the sole requisite for initiating OpenRiverCam operation is the availability of a CSV file as the input data format.

Importing GPS Data into OpenRiverCam and the next steps will be explained into the next chapter. Besides the importing of the GPS data the configuring of OpenRiverCam for River Flow Measurements will be explained. This explanation is done from the file format from a CSV file as complies with the output of chapter 4. If another type of GPS-RTK system is used, only an output of a CSV file is needed to start with the OpenRiverCam.

A.7 Troubleshooting and FAQs

- Common Issues Encountered in the Field

- U-Center will not connect: see section A.3.2
- Don't move the Base Antenna while calibrating
- In cities with high buildings, the connecting of the RTK will work less good
- Try to set up the Base Station in an open-air, avoid high trees and buildings
- Calibrate under the electrical power supply of the Base Station Laptop

A.8 References and Resources

Important websites and resources:

- ORC: `https://openrivercam.readthedocs.io/en/latest/`
- U-Center `https://drotek.gitbook.io/rtk-positioning-solutions/`
- U-Center Userguide GNSS evaluation software for windows (or other)
- SW Maps: `https://aviyaantech.com/swmaps/`

Appendix B

Programm Guide: OpenRiverCam software

B.1 Open River Cam tutorial using Google Colab

During this project, we're trying to implement a new method of measuring the water flow in rivers and creeks in the Phetchaburi area. This method was invented in the Netherlands and is called Open River Cam. It uses a short film of a river or a creek and projects the picture and pixels onto a geographical plane. It can do this by using known GPS points in the video frame and converting the pixels that are associated with these known GPS points to the GPS points in the geographical plane. The entire methodology is meant to reduce the required fieldwork for river surveying and flow rating curve management to a minimum. Only a small survey is needed for the bathymetry of the stream and for ortho projection of the camera shots. This can be done during low flow conditions: safely, taking time, without exposure of the equipment.

B.2 Pyorc Software installation

The Open River Cam software (pyorc) is Open Source and is available via GitHub. Although the installation manual uses Docker, we found the software easier to use and access via Google Collab. A short installation manual for Google Collab is shown below. Google Colab uses a remote server where it's easy to import environments and import packages without having to install everything on your computer.

Create a new folder in MyDrive where you put the data files you want to access in your Open RiverCam notebook. In this example, the folder is called pyorc. This will keep your files and notebooks organized and all your files easy to find.

Create a new Google Collab project in the folder and run the following comments to access the pyorc software.

```
!pip install pyopenrivercam            #Installing the packages
!pip install cartopy

import xarray as xr                    #Importing the packages needed
import pyorc
import cartopy
import cartopy.crs as ccrs
import matplotlib.pyplot as plt

from google.colab import drive
drive.mount('/content/drive')
%cd /content/drive/MyDrive/pyorc       #accessing the folder in your drive
```

Now the pyorc environment can be used in the project. The tutorial for the software can be found on the GitHub page of Open River Cam: `https://github.com/localdevices/pyorc`. Open Examples and follow the 5 tutorial notebooks to get an understanding of the pyorc environment.

You can download the notebooks from github and put them in your folder in MyDrive to run them. Don't forget to also download the files from 'camera_calib', 'ngwerere' and 'geul' folders and put them in the pyorc folder in your OneDrive.

You should add the pip install lines on top of the top of the notebook and add the three lines to access the right folder in your drive.

You will now be able to go through the separate tutorial notebooks and will be able to set up your own notebook in the pyorc environment.

B.3 Campus test project

The first test for the Open River Cam method was done at the Campus (Kasetsart University). To determine a GPS location the Base station with a fixed position is connected to a laptop, and the Rover is connected to a mobile phone which can be moved. The Rover is used to determine the GPS location of our control points in the video frame. The use of 2 GPS stations will make sure that the GPS points measured are as accurate as possible.

Figure B.1: Control points shown in video frame

The control points are selected in the video frame by choosing the exact pixel in the frame. Here the pixels are [260, 650],[120, 310],[1460, 365],[825, 200].

For this test, there were some problems with the base station, so the GPS points aren't very accurate because only the rover was used. We still managed to run it through the ORC software and get some results. As shown in Figure B.2 below, you can see that the GPS points aren't really on the edges of the stream like they should be. How better the GPS coordinates of the control points match the location on the geographical plane, and how better the results.

Figure B.2: Measured GPS points projected on geographical plane

Because the GPS points are not accurate, they do not completely match the video. This causes the image to distort in a strange way when placed onto the geographical plane. The flow fields, however, did come through into this distorted frame. It matches how the water was moving in reality and therefore the program registered the right movements. The distorted flow field is shown in Figure B.3.

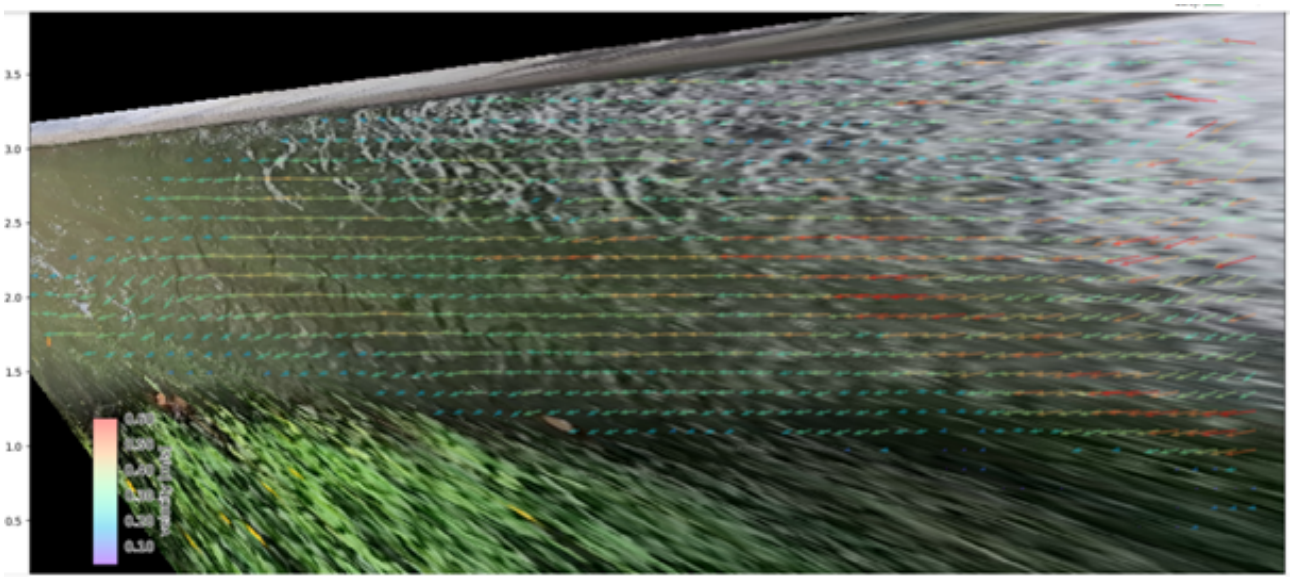

Figure B.3: Distorted picture of water flow field

It was hard to create cross-sections in the creek because of the inaccuracy of the GPS and the fact that we couldn't get into the water. Therefore, the cross-section was simplified with a water depth in the creek of 1.5 m and 2 GPS points on both sides of the creek. The points in between were interpolated. Even though the cross sections were very much simplified, due to the GPS, they didn't match the reality as shown in Figure B.4. Cross section 1 goes in the wrong direction and cross section 2 stretches way to long. Better GPS accuracy will fix this problem and a very accurate could be used to create an entire cross section without interpolating.

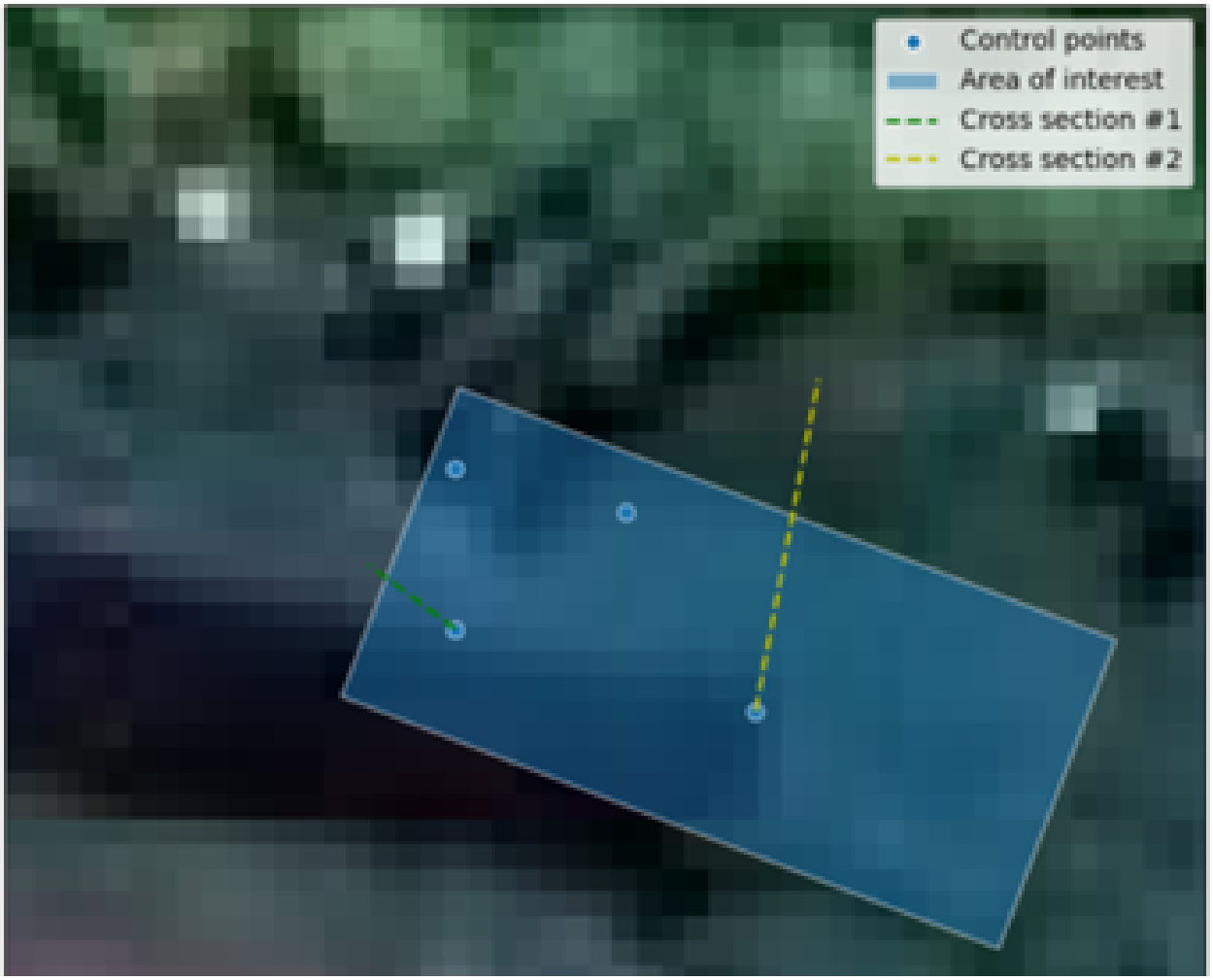

Figure B.4: Cross sections displaced in geographical plane

This resulted in a flow going outside of the creek bounds at cross-section 2 and cross section 1 not useful at all. The results projected in the geographical plane and video frame are shown in figure B.5 5 and figure B.6. It still matches the real flow quite well except for the fact that the field goes out of bounds due to the wrong cross-section. This test shows that an accurate and well calibrated RTK GPS is one of the most important things of the site preparation and that the ORC can already get adequate projections of the water flow with poor inputs.

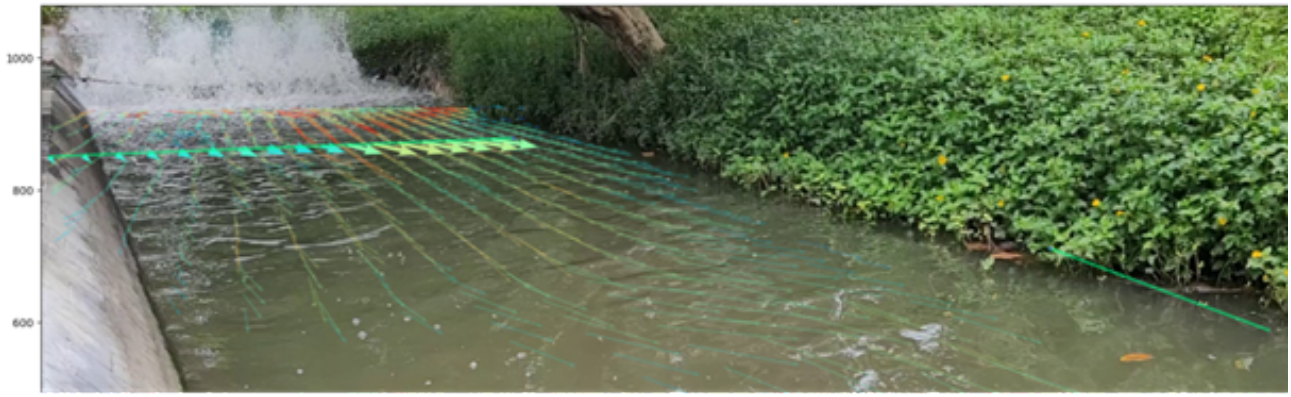

Figure B.5: Cross-sectional flow field in video frame

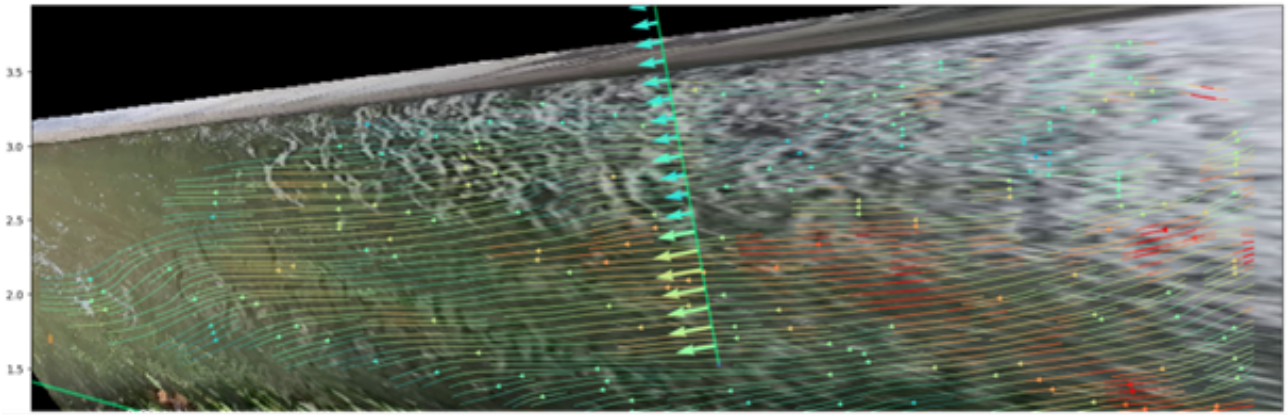

Figure B.6: Cross-sectional flow field in geographical plane

Although the GPS was far off the real location and this caused a lot of distortions, we did manage to get some results and get the Open River Cam software to work. We also received values for the estimations of the discharge as shown below.

```
<xarray.DataArray 'river_flow' (quantile: 5)>
array([2.56409571, 1.34090374, 0.95218255, 0.67806302, 0.15749541])
Coordinates:
    * quantile  (quantile) float64 0.05 0.25 0.5 0.75 0.95
Attributes:
      standard_name:    river_discharge
      long_name:        River Flow
      units:            m3 s-1
```

The quantile values are pretty far apart but the estimation of the discharge as a 50% quantile turned out to be 0.9522 m/s. The quantiles that are given as a result of the water discharge are a prediction of the water flow and also show the accuracy of the test. It gives the value of the discharge with a chance of 5% that it's higher than 2.56 m3/s, the value of the discharge with a chance of 25% that it's higher than 1.34 m3/s, etc.. The outcome of the model is therefore a spread prediction of the discharge with the 0.5 value as its mean discharge predicted by the ORC software.

Appendix C

Site Preparation: Field Trip Phetchaburi

C.1 Open River Cam site preparation Phetchaburi

To use the Open River Cam software in our designated locations preparations needed to be made and data needed to be collected to enter in the software. First, the best viewing point of the river was determined and the control points were chosen. Guidelines and optimal situations were retrieved from the Open River Cam field manual, For the manual go to the next URL: `https://openrivercam.readthedocs.io/en/latest/survey.html#survey`. The first site that was measured at the field trip was B8 and therefore this site will be used as an example.

Figure C.1: River B.8 in Phetchaburi District

C.1.1 Control points and filming locations

A good view of the entire river cross-section is chosen and ideally, the viewing angle is not larger than 45 degrees. The more vertical the viewing angle, the better. Multiple places on the bridge were used to film (left, middle, and right) so it's important that the control points are visible on all videos. We

removed plants and branches to get a clear view from the river bank and get an open view of the complete width of the water flow.

Figure C.2: River B.8 with red crosses on control points

Here the control points are big rocks and a stick we put in the water. Because we were here for only a couple of days we didn't use permanent control points that would be resilient to larger water level fluctuations. If the water level could be checked for a longer period of time, large poles would be more convenient. If the water level rises, the pole will still be visible but the rocks in this example will be underwater and can't be used. Because the water level rise was small between the days we filmed, this method of choosing the control points was determined to be sufficient. The GPS location of the control points was determined with the RTK-GPS. Calibrating the GPS turned out to take a longer time than first predicted and therefore the accuracy was worse. Instead of an accuracy of 10 centimeters an accuracy of 70 centimeters was used.

C.1.2 Cross sections

After the Control points, the cross sections were determined. Because the GPS wasn't accurate enough (height deviation of 2 meters), the depth of the cross-section was determined by hand by using a depth gauge. The outer points of the cross sections were determined by the GPS and between these points, the GPS locations of the cross sections were interpolated. The water level was determined by taking an average of all the GPS measurements. Examples of the cross-section CSV file and the CSV file received from the RTK GPS are shown in Figure C.3. Left is the cross section filled in by hand and GPS data was received from the software.

x	y	z
576079.4	1416794	39.8
576079.3	1416794	39.718
576079.2	1416793	39.69
576079	1416792	39.636
576078.9	1416792	39.628
576078.8	1416791	39.69
576078.7	1416790	39.694
576078.5	1416790	39.654
576078.4	1416789	39.664
576078.3	1416788	39.724
576078.2	1416788	39.684
576078	1416787	39.614
576077.9	1416787	39.654
576077.8	1416786	39.71
576077.7	1416785	39.81

Figure C.3: River B.8 RTK GPS CSV file

We Manually measured the cross sections by pulling strings across the water as shown in Figure C.5 and measuring the depth every 30 cm. The outer GPS points of the strings and the cross sections were still determined by the RTK-GPS. Figure C.4 shows the outcome of uploading the cross-sections into the ORC software. It shows that it matches the places of the control points and the place of the river on the map.

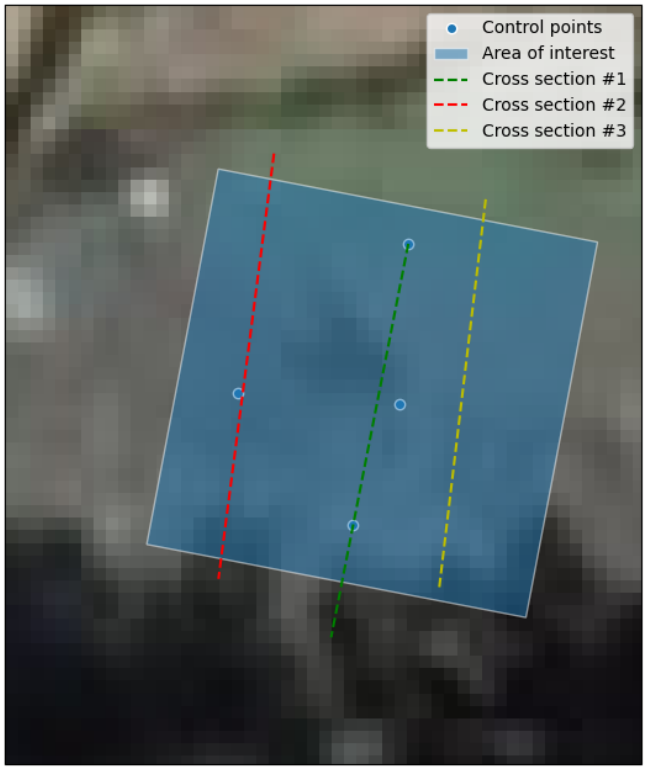

Figure C.4: cross-sections projected on the geographical plane in the ORC model

Figure C.5: River B.8 fieldwork and measurements by the team

C.1.3 Extra measurements

We also tested the water quality using equipment provided by the TU Delft and we manually measured the flow velocity along the cross sections. The flow velocity was measured to check the flow velocity along the cross sections calculated in Open River Cam. If the flow velocity showed high currents in places where we measured low currents and the other way around, it was a sign that something went wrong. It was a way to check our Open River Cam results.

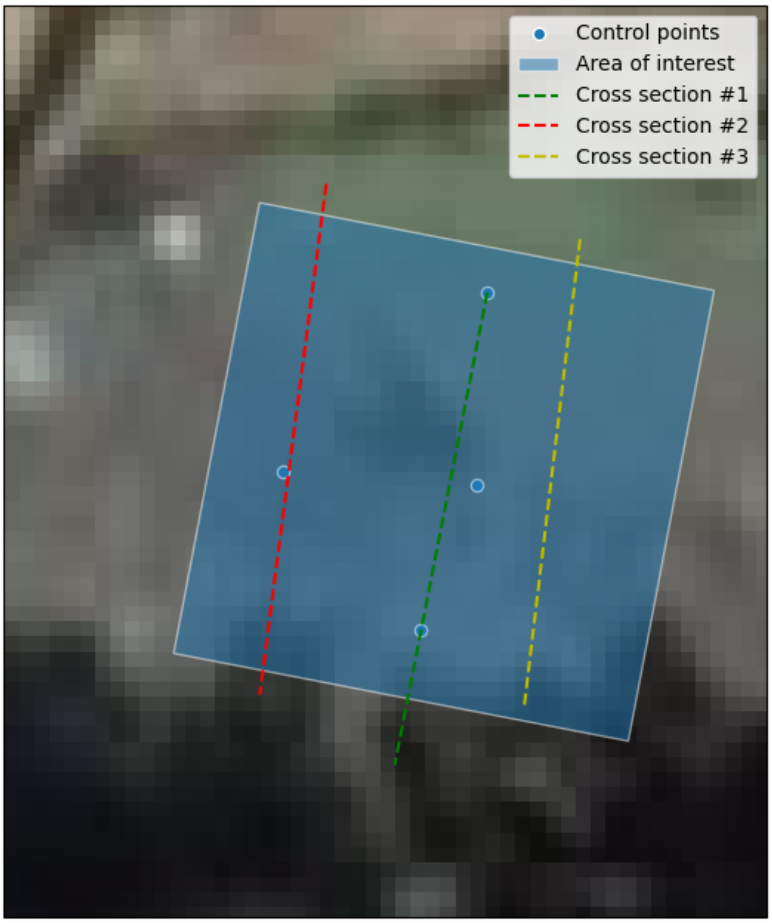

Figure C.6: River B.8 measure dept manually with reference rope

Figure C.7: River B.8 measure dept manually

In this way, the locations were mapped and clear videos could be made. These videos could then be processed in Bangkok and checked next to the values resulting from the stream of measurements and the values measured by the RID.

Appendix D

Current meter versus OpenRiverCam

D.1 Current meter vs ORC

The flow measurements from the current meter are plotted and laid next to the ORC results. This is to check if the places where the water was going faster or slower also show this in the results of the ORC. There are a few flaws with this comparison. For example, the current meter could not detect the speed at small depths because it had to be submerged by at least 10 centimeters. It is also difficult to coordinate the location of the depth measurement and the speed measurement in the same place. Because the GPS had a deviation and fewer current measurements were made, it could be that the comparison shows a mistake in the results while the actual measurements are not at the same location. Therefore, for the small river, it is difficult to say whether it is a reliable comparison, but it at least gives an idea of the magnitude of the water speed. This has been measured in reality and should therefore approximately correspond to the model.

D.1.1 Site 1 B.8 river

For the first flow velocity check, we look at the B8 river. It shows a few flaws as explained before. It doesn't measure the high speed in the most upstream cross-section. This is because the water depth was very low there and no current velocity could be measured. The maximum velocities in the model are a bit lower than in the model, therefore the probable discharge would be a bit higher in reality. The places of the maximum velocity are a bit off when comparing the 2 results, but this is because of the inaccuracy in the GPS and the difference in number of measurements of the current meter and the depth. The maximum in the flow measurements was for the 2 most downstream cross sections 1.4 m/s. The ORS model gave a maximum of around 1 m/s.

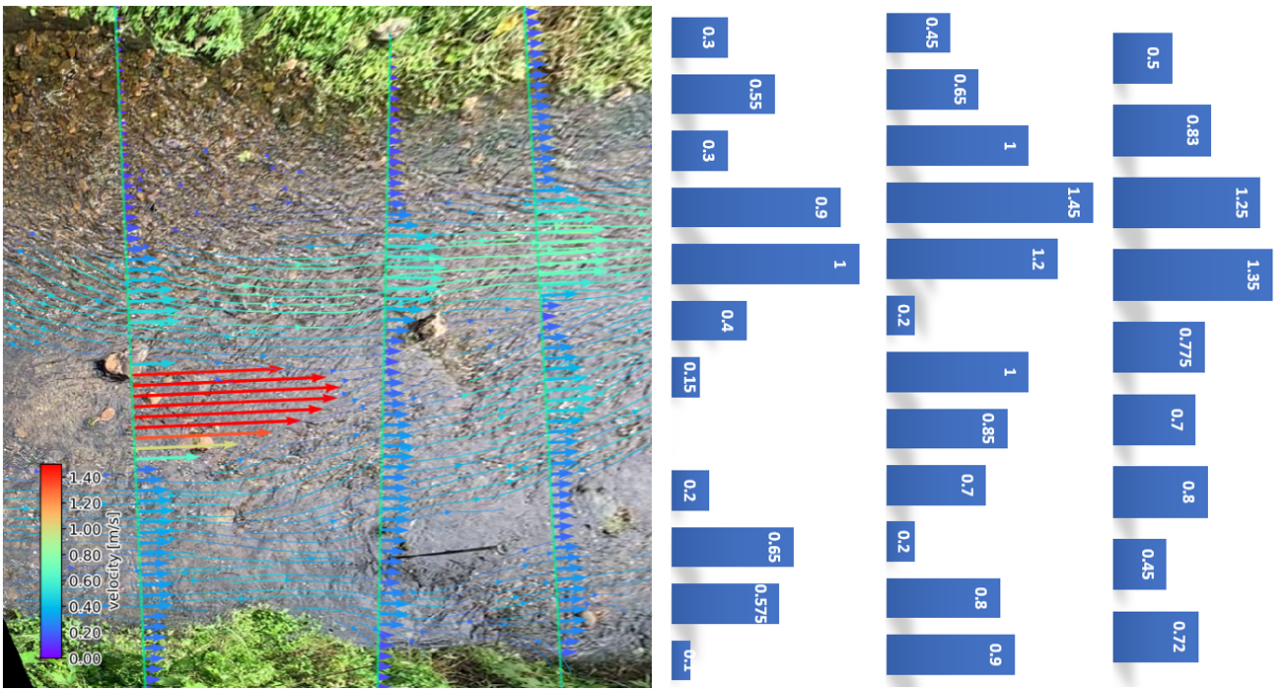

Figure D.1: Right viewing angle vs. current meter results

The water flow profile looks similar but due to the problems with the GPS and the depth of the water, the flow profile isn't very accurate. Hand-measured flow velocities at the places where the water level is very low (¡ 10 cm) aren't possible, but a more accurate GPS and more precise measurements could give better results. The distance between each current measurement should be the same and it would be best if they are at the same locations as the depth measurements.

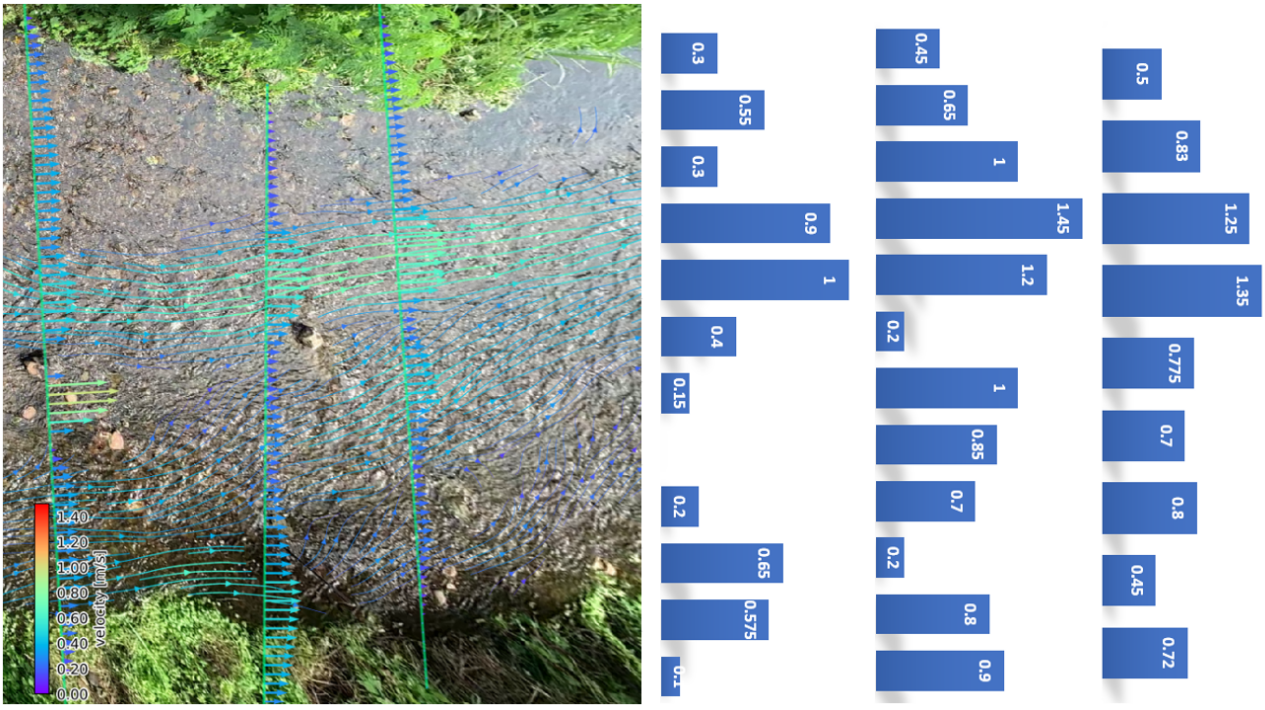

Figure D.2: Left viewing angle vs. current meter results

D.1.2 Site 2 B.3 river

At the B3 river, it was hard to measure the velocity with the current meter. At high water, we did have a raft to get across the river along one cross-section to get flow measurements. At low water we gave it a try to measure the velocity but the water flow was too low to get ORC results and significant current measurements. The ORC couldn't follow the paths of the water because there were too few disturbances in surface water flow.

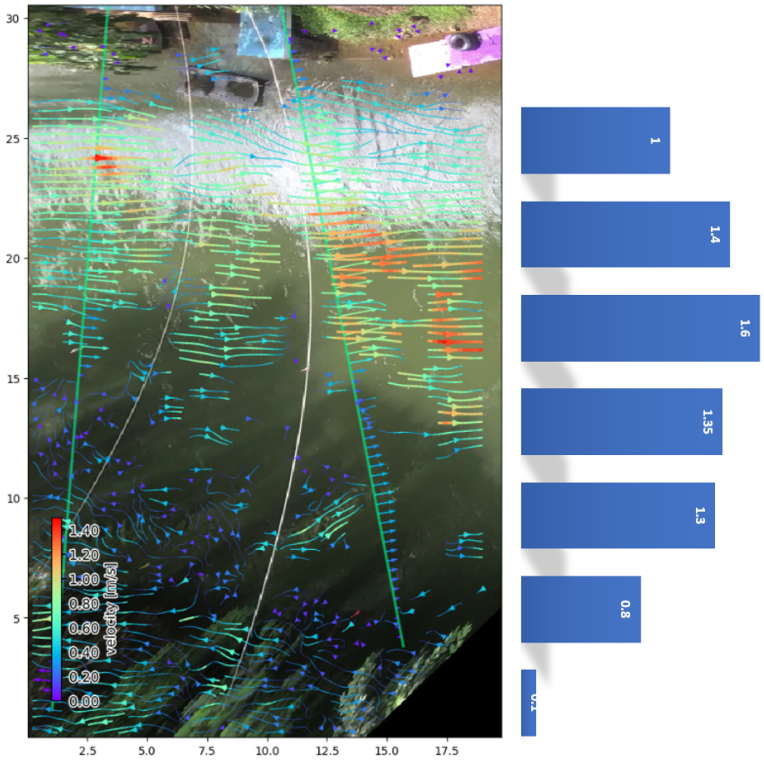

Figure D.3: 25 sept 2023, ORC results vs. current meter measurements

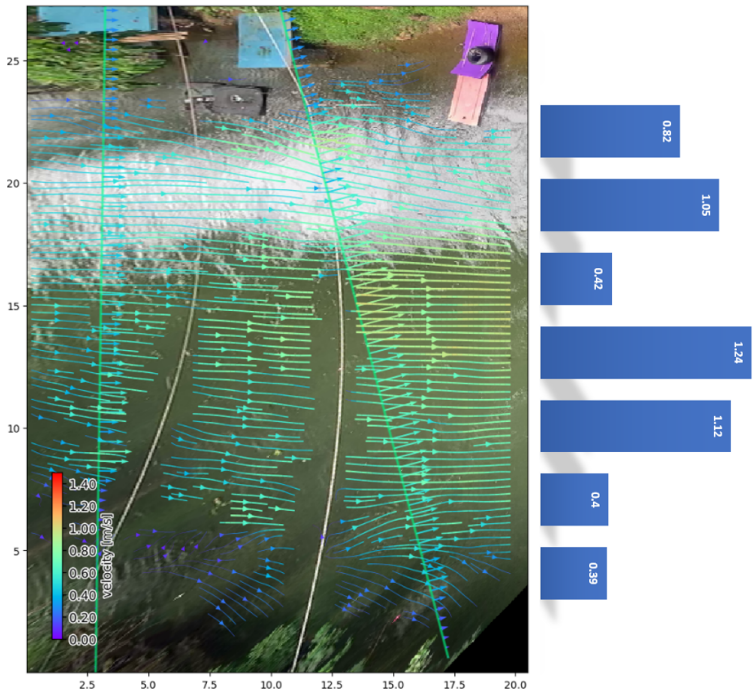

Figure D.4: 26 sept 2023, ORC results vs. current meter measurements

The results are fairly similar for the right cross-section (the left couldn't be measured due to the fast stream). In the shade, the flow isn't detected as well as in the sun and therefore the velocity turned out to be lower. The cross section calculated a discharge of 18.5 m3/s and in reality, it was 31 m3/s for 25 September. This is probably due to the lower velocity detected in the shady area by Open River Cam. On 26 September it was cloudy and the shadow was a smaller issue for the ORC model. The cross-section measured a discharge of 21.4 m3/s while the water velocity was smaller than the day before. This means that the discharge on 26 September was smaller than 31 m3/s and the model got significantly closer to the actual discharge (no measurement was taken that day with the ADCP rover so not sure what the discharge was). Because it was hard to measure the current on the raft and do it exactly per same length step along the cross-section, the actual places of the current along the cross sections could be slightly different.

D.1.3 Site 3 B.11 river

For the third river, we got the best ORC results compared to the RID measurements. This means that the model calculated the discharge very closely compared to the discharge measured by the ADCP rover. We measured two of the 3 cross sections with the current meter as well to determine if the model was also accurate with the flow pattern of the current. We plotted again the current flowmeter measurements besides the results from the ORC model. and the results are shown below.

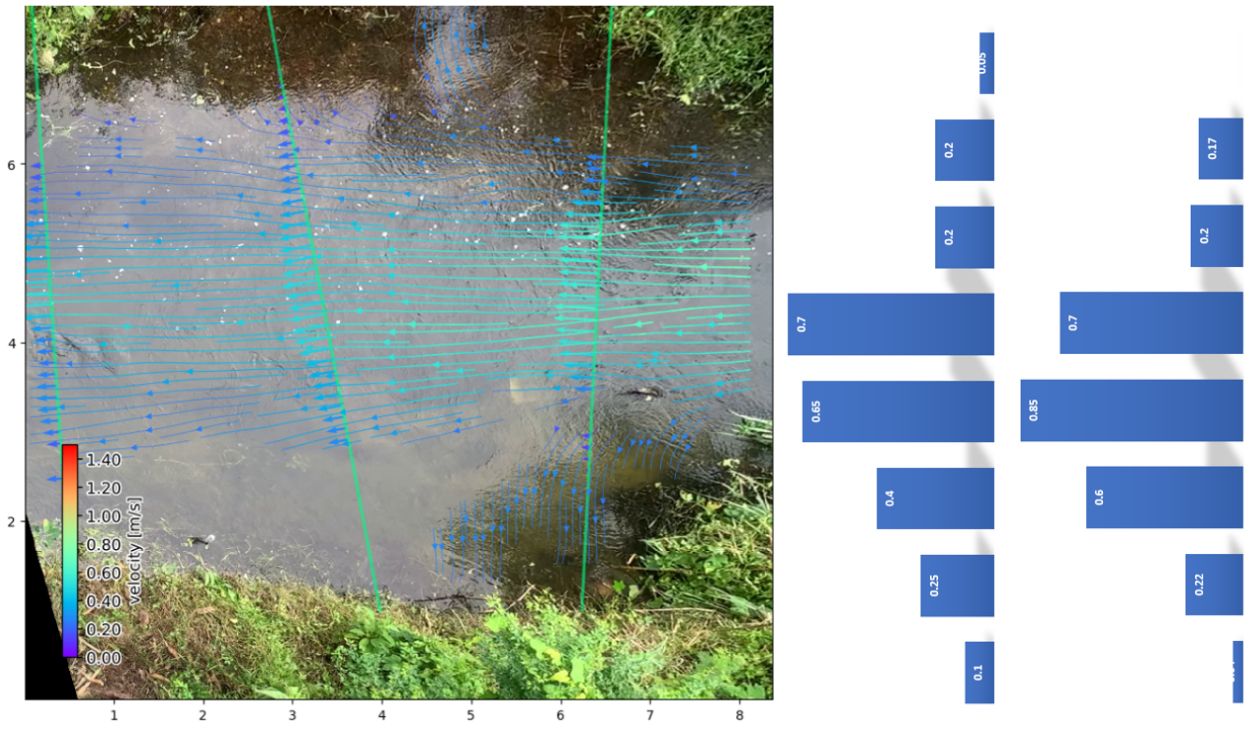

Figure D.5: 27 Sept 2023 measurement 1, ORC results vs. current meter measurements

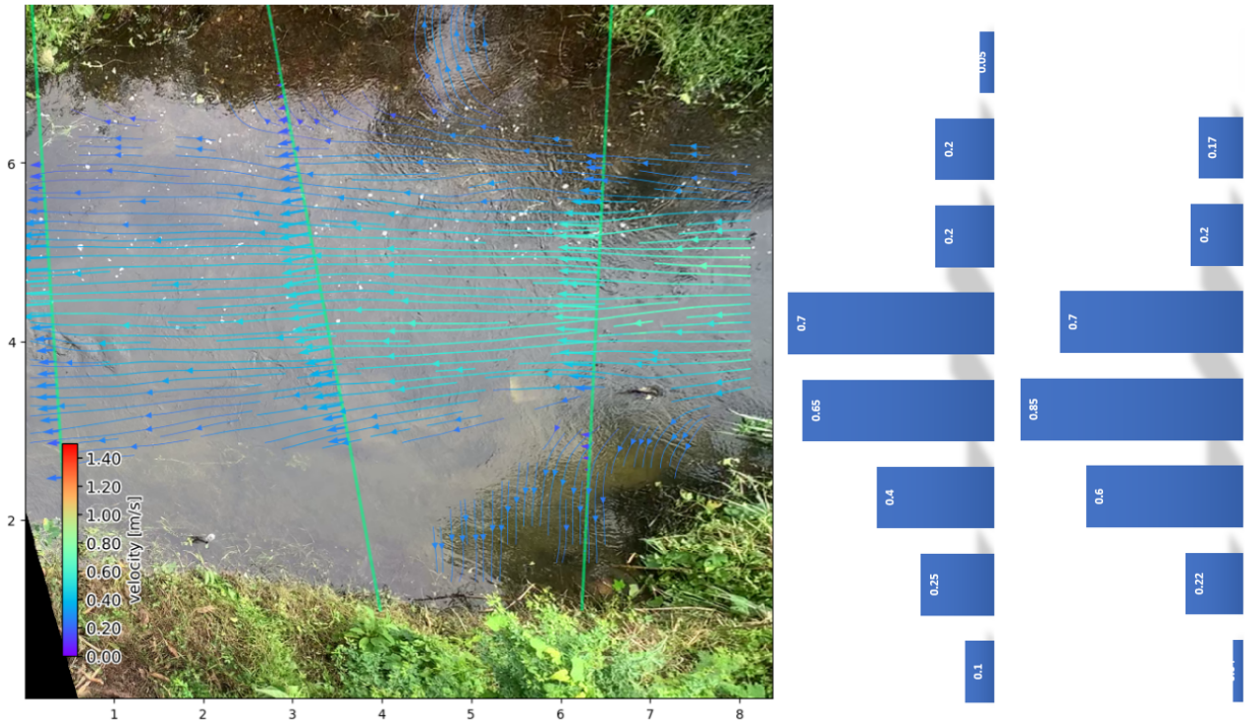

Figure D.6: 27 Sept 2023 measurement 2, ORC results vs. current meter measurements

The 2 cross sections measured and tested are the 2 most upstream sections. The model follows the measurements very accurately and matches the real-world flow of the river/creek. The maximum flow is approximately of the same number and the banks give little to no current. The difference at this river compared to the other rivers is that we get a very vertical view of the flowing water. Here the shadows and reflections are less of a problem and the model works as it best. The GPS locations were also more accurate than the other locations and therefore the cross sections are laid better in the picture frame and on the geographical plane.

Appendix E

Radar calibration

E.1 DM-analysis

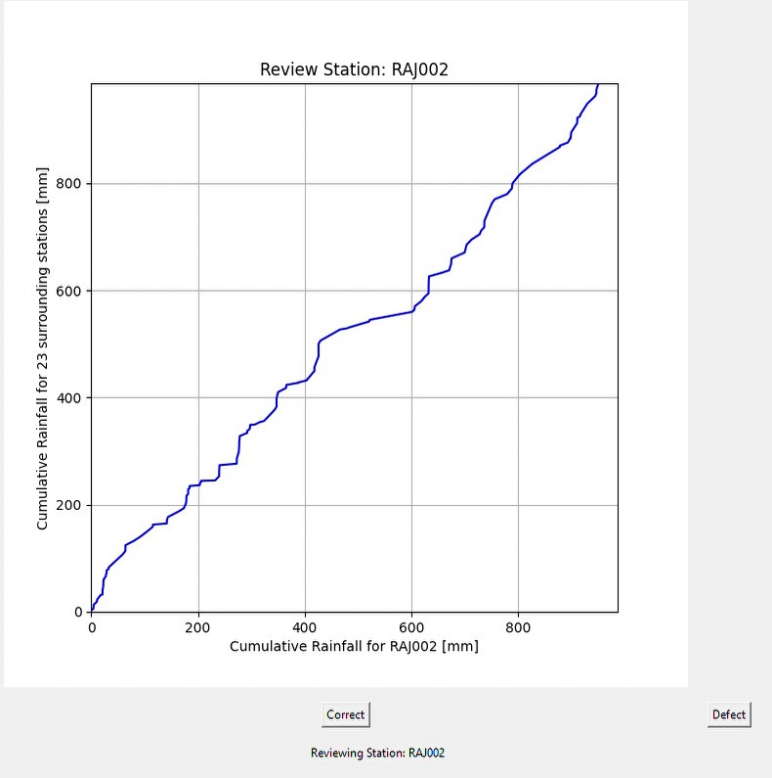

Figure E.1: Example DM-analysis widget

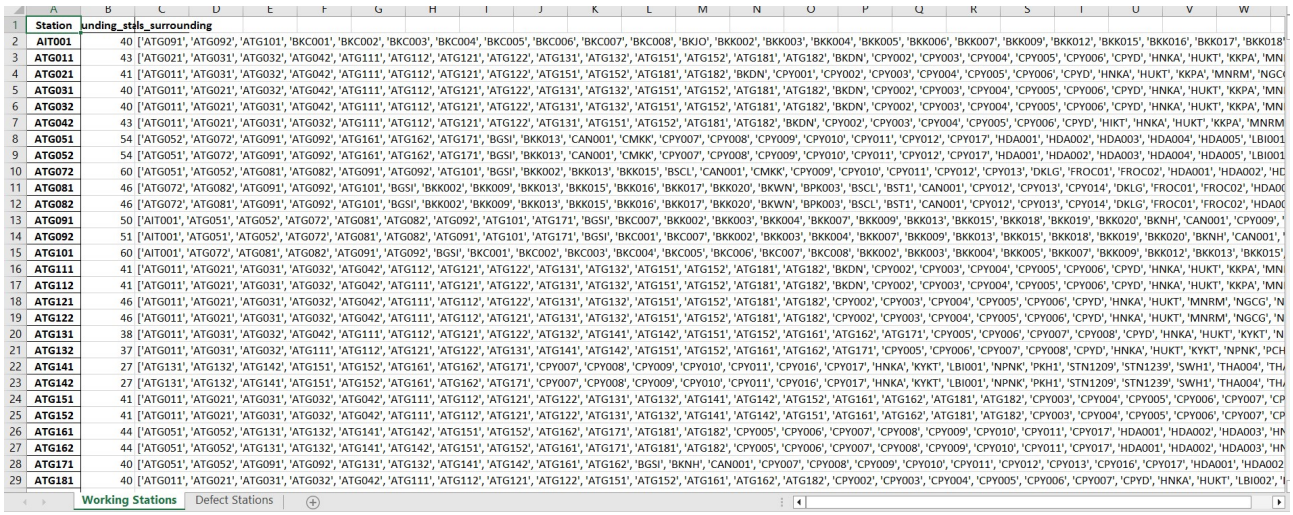

Station	unding_stns_surrounding	
AIT001	40	['ATG091', 'ATG092', 'ATG101', 'BKC001', 'BKC002', 'BKC003', 'BKC004', 'BKC005', 'BKC006', 'BKC007', 'BKC008', 'BKJO', 'BKK002', 'BKK003', 'BKK004', 'BKK005', 'BKK006', 'BKK007', 'BKK009', 'BKK012', 'BKK015', 'BKK016', 'BKK017', 'BKK018'
ATG011	43	['ATG021', 'ATG031', 'ATG032', 'ATG042', 'ATG111', 'ATG112', 'ATG121', 'ATG122', 'ATG131', 'ATG132', 'ATG151', 'ATG152', 'ATG181', 'ATG182', 'BKDN', 'CPY002', 'CPY003', 'CPY004', 'CPY005', 'CPY006', 'CPYD', 'HNKA', 'HUKT', 'KKPA', 'MN
ATG021	41	['ATG011', 'ATG031', 'ATG032', 'ATG042', 'ATG111', 'ATG112', 'ATG121', 'ATG122', 'ATG151', 'ATG152', 'ATG181', 'ATG182', 'BKDN', 'CPY001', 'CPY002', 'CPY003', 'CPY004', 'CPY005', 'CPY006', 'CPYD', 'HNKA', 'HUKT', 'KKPA', 'MNRM', 'NGC
ATG031	40	['ATG011', 'ATG021', 'ATG032', 'ATG042', 'ATG111', 'ATG112', 'ATG121', 'ATG122', 'ATG131', 'ATG132', 'ATG151', 'ATG152', 'ATG181', 'ATG182', 'BKDN', 'CPY002', 'CPY003', 'CPY004', 'CPY005', 'CPY006', 'CPYD', 'HNKA', 'HUKT', 'KKPA', 'MN
ATG032	40	['ATG011', 'ATG021', 'ATG031', 'ATG042', 'ATG111', 'ATG112', 'ATG121', 'ATG122', 'ATG131', 'ATG132', 'ATG151', 'ATG152', 'ATG181', 'ATG182', 'BKDN', 'CPY002', 'CPY003', 'CPY004', 'CPY005', 'CPY006', 'CPYD', 'HNKA', 'HUKT', 'KKPA', 'MN
ATG042	43	['ATG011', 'ATG021', 'ATG031', 'ATG032', 'ATG111', 'ATG112', 'ATG121', 'ATG122', 'ATG131', 'ATG151', 'ATG152', 'ATG181', 'ATG182', 'BKDN', 'CPY002', 'CPY003', 'CPY004', 'CPY005', 'CPY006', 'CPYD', 'HIKT', 'HNKA', 'HUKT', 'KKPA', 'MNRM
ATG051	54	['ATG052', 'ATG072', 'ATG091', 'ATG092', 'ATG161', 'ATG162', 'ATG171', 'BGSI', 'BKK013', 'CAN001', 'CMKK', 'CPY007', 'CPY008', 'CPY009', 'CPY010', 'CPY011', 'CPY012', 'CPY017', 'HDA001', 'HDA002', 'HDA003', 'HDA004', 'HDA005', 'LBI001
ATG052	54	['ATG051', 'ATG072', 'ATG091', 'ATG092', 'ATG161', 'ATG162', 'ATG171', 'BGSI', 'BKK013', 'CAN001', 'CMKK', 'CPY007', 'CPY008', 'CPY009', 'CPY010', 'CPY011', 'CPY012', 'CPY017', 'HDA001', 'HDA002', 'HDA003', 'HDA004', 'HDA005', 'LBI001
ATG072	60	['ATG051', 'ATG052', 'ATG081', 'ATG082', 'ATG091', 'ATG092', 'ATG101', 'BGSI', 'BKK002', 'BKK013', 'BKK015', 'BSCL', 'CAN001', 'CMKK', 'CPY009', 'CPY010', 'CPY011', 'CPY012', 'CPY013', 'DKLG', 'FROC01', 'FROC02', 'HDA001', 'HDA002', 'HD
ATG081	46	['ATG072', 'ATG082', 'ATG091', 'ATG092', 'ATG101', 'BGSI', 'BKK002', 'BKK009', 'BKK013', 'BKK015', 'BKK016', 'BKK017', 'BKK020', 'BKWN', 'BPK003', 'BSCL', 'BST1', 'CAN001', 'CPY012', 'CPY013', 'CPY014', 'DKLG', 'FROC01', 'FROC02', 'HDA0
ATG082	46	['ATG072', 'ATG081', 'ATG091', 'ATG092', 'ATG101', 'BGSI', 'BKK002', 'BKK009', 'BKK013', 'BKK015', 'BKK016', 'BKK017', 'BKK020', 'BKWN', 'BPK003', 'BSCL', 'BST1', 'CAN001', 'CPY012', 'CPY013', 'CPY014', 'DKLG', 'FROC01', 'FROC02', 'HDA0
ATG091	50	['AIT001', 'ATG051', 'ATG052', 'ATG072', 'ATG081', 'ATG082', 'ATG092', 'ATG101', 'ATG171', 'BGSI', 'BKC007', 'BKK002', 'BKK003', 'BKK004', 'BKK007', 'BKK009', 'BKK013', 'BKK015', 'BKK018', 'BKK019', 'BKK020', 'BKNH', 'CAN001', 'CPY009', '
ATG092	51	['AIT001', 'ATG051', 'ATG052', 'ATG072', 'ATG081', 'ATG082', 'ATG091', 'ATG101', 'ATG171', 'BGSI', 'BKC001', 'BKC007', 'BKK002', 'BKK003', 'BKK004', 'BKK007', 'BKK009', 'BKK013', 'BKK015', 'BKK018', 'BKK019', 'BKK020', 'BKNH', 'CAN001', '
ATG101	60	['AIT001', 'ATG072', 'ATG081', 'ATG082', 'ATG091', 'ATG092', 'BGSI', 'BKC001', 'BKC002', 'BKC003', 'BKC004', 'BKC005', 'BKC006', 'BKC007', 'BKC008', 'BKK002', 'BKK003', 'BKK004', 'BKK005', 'BKK007', 'BKK009', 'BKK012', 'BKK013', 'BKK015',
ATG111	41	['ATG011', 'ATG021', 'ATG031', 'ATG032', 'ATG042', 'ATG112', 'ATG121', 'ATG122', 'ATG131', 'ATG132', 'ATG151', 'ATG152', 'ATG181', 'ATG182', 'BKDN', 'CPY002', 'CPY003', 'CPY004', 'CPY005', 'CPY006', 'CPYD', 'HNKA', 'HUKT', 'KKPA', 'MN
ATG112	41	['ATG011', 'ATG021', 'ATG031', 'ATG032', 'ATG042', 'ATG111', 'ATG121', 'ATG122', 'ATG131', 'ATG132', 'ATG151', 'ATG152', 'ATG181', 'ATG182', 'BKDN', 'CPY002', 'CPY003', 'CPY004', 'CPY005', 'CPY006', 'CPYD', 'HNKA', 'HUKT', 'KKPA', 'MN
ATG121	46	['ATG011', 'ATG021', 'ATG031', 'ATG032', 'ATG042', 'ATG111', 'ATG112', 'ATG122', 'ATG131', 'ATG132', 'ATG151', 'ATG152', 'ATG181', 'ATG182', 'CPY002', 'CPY003', 'CPY004', 'CPY005', 'CPY006', 'CPYD', 'HNKA', 'HUKT', 'MNRM', 'NGCG', 'N
ATG122	46	['ATG011', 'ATG021', 'ATG031', 'ATG032', 'ATG042', 'ATG111', 'ATG112', 'ATG121', 'ATG131', 'ATG132', 'ATG151', 'ATG152', 'ATG181', 'ATG182', 'CPY002', 'CPY003', 'CPY004', 'CPY005', 'CPY006', 'CPYD', 'HNKA', 'HUKT', 'MNRM', 'NGCG', 'N
ATG131	38	['ATG011', 'ATG031', 'ATG032', 'ATG042', 'ATG111', 'ATG112', 'ATG121', 'ATG122', 'ATG132', 'ATG141', 'ATG142', 'ATG151', 'ATG152', 'ATG161', 'ATG162', 'ATG171', 'CPY005', 'CPY006', 'CPY007', 'CPY008', 'CPYD', 'HNKA', 'HUKT', 'KYKT', 'N
ATG132	37	['ATG011', 'ATG031', 'ATG032', 'ATG111', 'ATG112', 'ATG121', 'ATG122', 'ATG131', 'ATG141', 'ATG142', 'ATG151', 'ATG152', 'ATG161', 'ATG162', 'ATG171', 'CPY005', 'CPY006', 'CPY007', 'CPY008', 'CPYD', 'HNKA', 'HUKT', 'KYKT', 'NPNK', 'PCH
ATG141	27	['ATG131', 'ATG132', 'ATG142', 'ATG151', 'ATG152', 'ATG161', 'ATG162', 'ATG171', 'CPY007', 'CPY008', 'CPY009', 'CPY010', 'CPY011', 'CPY016', 'CPY017', 'HNKA', 'KYKT', 'LBI001', 'NPNK', 'PKH1', 'STN1209', 'STN1239', 'SWH1', 'THA004', 'TH
ATG142	27	['ATG131', 'ATG132', 'ATG141', 'ATG151', 'ATG152', 'ATG161', 'ATG162', 'ATG171', 'CPY007', 'CPY008', 'CPY009', 'CPY010', 'CPY011', 'CPY016', 'CPY017', 'HNKA', 'KYKT', 'LBI001', 'NPNK', 'PKH1', 'STN1209', 'STN1239', 'SWH1', 'THA004', 'TH
ATG151	41	['ATG011', 'ATG021', 'ATG031', 'ATG032', 'ATG042', 'ATG111', 'ATG112', 'ATG121', 'ATG122', 'ATG131', 'ATG132', 'ATG141', 'ATG142', 'ATG152', 'ATG161', 'ATG162', 'ATG181', 'ATG182', 'CPY003', 'CPY004', 'CPY005', 'CPY006', 'CPY007', 'CP
ATG152	41	['ATG011', 'ATG021', 'ATG031', 'ATG032', 'ATG042', 'ATG111', 'ATG112', 'ATG121', 'ATG122', 'ATG131', 'ATG132', 'ATG141', 'ATG142', 'ATG151', 'ATG161', 'ATG162', 'ATG181', 'ATG182', 'CPY003', 'CPY004', 'CPY005', 'CPY006', 'CPY007', 'CP
ATG161	44	['ATG051', 'ATG052', 'ATG131', 'ATG132', 'ATG141', 'ATG142', 'ATG151', 'ATG152', 'ATG162', 'ATG171', 'ATG181', 'ATG182', 'CPY005', 'CPY006', 'CPY007', 'CPY008', 'CPY009', 'CPY010', 'CPY011', 'CPY017', 'HDA001', 'HDA002', 'HDA003', 'HN
ATG162	44	['ATG051', 'ATG052', 'ATG131', 'ATG132', 'ATG141', 'ATG142', 'ATG151', 'ATG152', 'ATG161', 'ATG171', 'ATG181', 'ATG182', 'CPY005', 'CPY006', 'CPY007', 'CPY008', 'CPY009', 'CPY010', 'CPY011', 'CPY017', 'HDA001', 'HDA002', 'HDA003', 'HN
ATG171	40	['ATG051', 'ATG052', 'ATG091', 'ATG092', 'ATG131', 'ATG132', 'ATG141', 'ATG142', 'ATG161', 'ATG162', 'BGSI', 'BKNH', 'CAN001', 'CPY007', 'CPY008', 'CPY009', 'CPY010', 'CPY011', 'CPY012', 'CPY013', 'CPY016', 'CPY017', 'HDA001', 'HDA002
ATG181	40	['ATG011', 'ATG021', 'ATG031', 'ATG032', 'ATG042', 'ATG111', 'ATG112', 'ATG121', 'ATG122', 'ATG151', 'ATG152', 'ATG161', 'ATG162', 'ATG182', 'CPY002', 'CPY003', 'CPY004', 'CPY005', 'CPY006', 'CPY007', 'CPYD', 'HNKA', 'HUKT', 'LBI002', '

Working Stations | Defect Stations

Figure E.2: Result DM-analysis

Appendix F

Background information field trip rivers Phetchaburi

F.1 River B.3

x (m)	y (m MSL)	remark
-30	48,647	
-20	48,72	
-10	48,684	Left Bank
-5	47,969	
0	46,399	
5	44,702	
10	43,426	
15	43,189	
20	43,025	
25	42,905	
30	41,603	
35	40,903	
40	40,663	
45	40,533	Bed
50	40,903	
55	41,25	
60	43,062	
65	45,239	
70	45,757	
75	46,375	
80	47,219	
85	47,899	
90	48,339	Right Bank
100	48,214	
110	48,229	

Table F.1: Cross section river B.3 data set

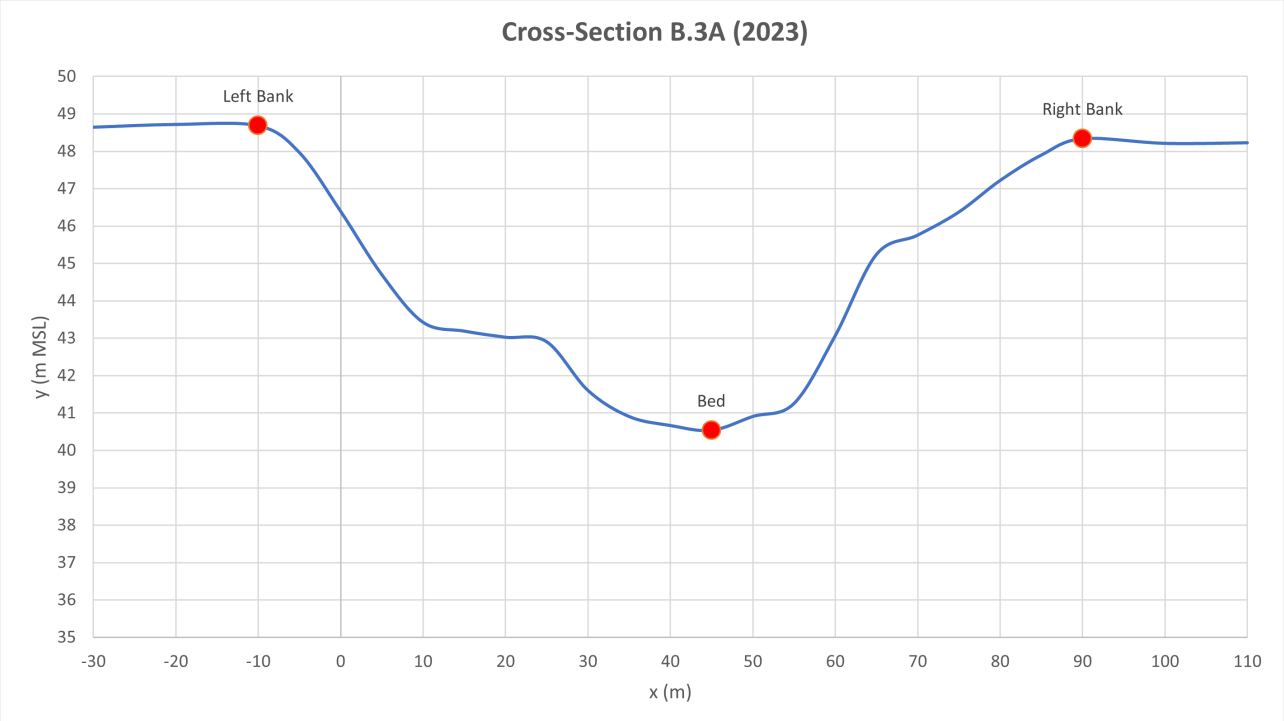

Figure F.1: Cross section river B.3

รูปตัดขวางลำน้ำ ปีน้ำ 2023

สถานี B.3A (ภาพถ่าย เหนือแนวสำรวจสะพาน) แม่น้ำเพชรบุรี อ.แก่งกระจาน จ.เพชรบุรี

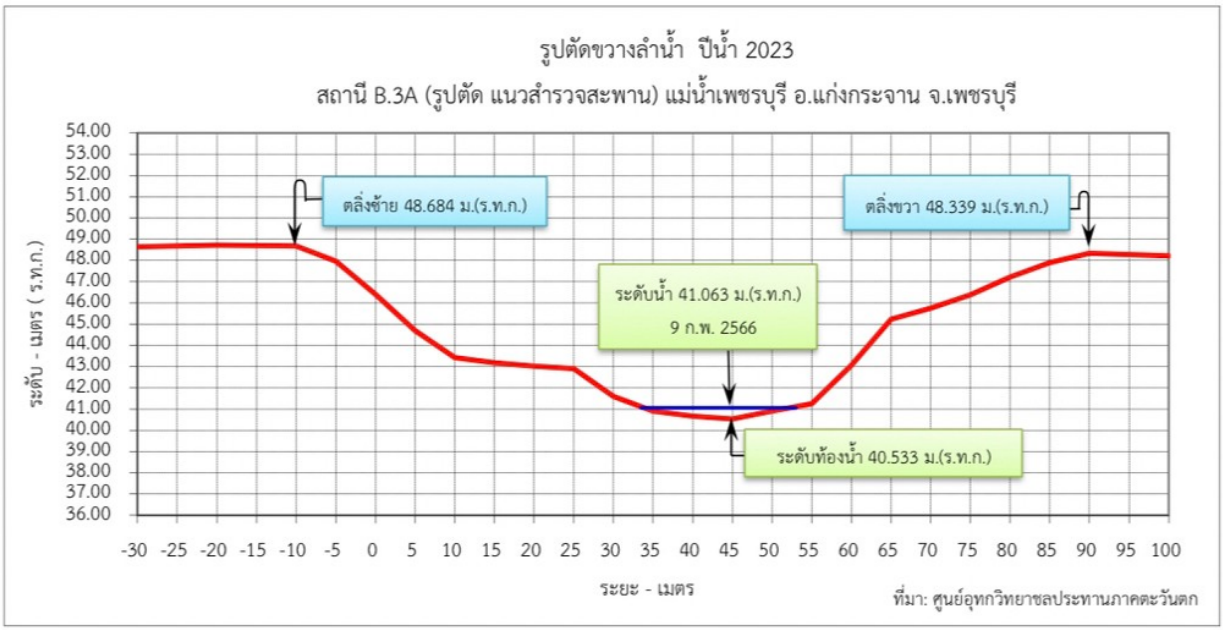

ระยะ	-30	-20	-10	-5	0	5	10	15	20	25	30	35	40	45	50	55	60
ระดับ	48.647	48.720	48.684	47.969	46.399	44.702	43.426	43.189	43.025	42.905	41.603	40.903	40.663	40.533	40.903	41.250	43.062
ระยะ	65	70	75	80	85	90	100	110									
ระดับ	45.239	45.757	46.375	47.219	47.899	48.339	48.214	48.229									

A.S.D.01B	49.188 ม. (ร.ท.ก.)	ศูนย์เสาระดับ	41.000 ม. (ร.ท.ก.)	ระดับท้องน้ำ	40.533 ม. (ร.ท.ก.)
ตลิ่งฝั่งซ้าย	48.684 ม. (ร.ท.ก.)	ตลิ่งฝั่งขวา	48.339 ม. (ร.ท.ก.)	สำรวจเมื่อวันที่	9 กุมภาพันธ์ 2566
ผู้สำรวจ	นายพงษ์ศิริ จิตตรัตน์	ผู้ตรวจ		บันทึกข้อมูล	นายพงษ์ศิริ จิตตรัตน์

Figure F.2: Information river B.3

F.2 River B.8

x (m)	y (m MSL)	remark
-40	47,192	
-30	46,429	
-20	45,806	
-10	45,39	
0	45,089	Left Bank
0	42,63	
2	41,472	
4	41,723	
6	41,936	
8	41,726	
10	41,163	
12	39,399	
14	39,302	
16	39,338	
18	39,209	
20	39,161	Bed
22	39,404	
24	39,618	
26	40,224	
28	40,713	
30	41,047	
32	41,476	
34	41,888	
36	42,236	
38	42,411	
40	42,443	
45	43,643	Right Bank
50	44,039	
60	44,703	
70	45,151	
80	45,475	

Table F.2: Cross section river B.8 data set

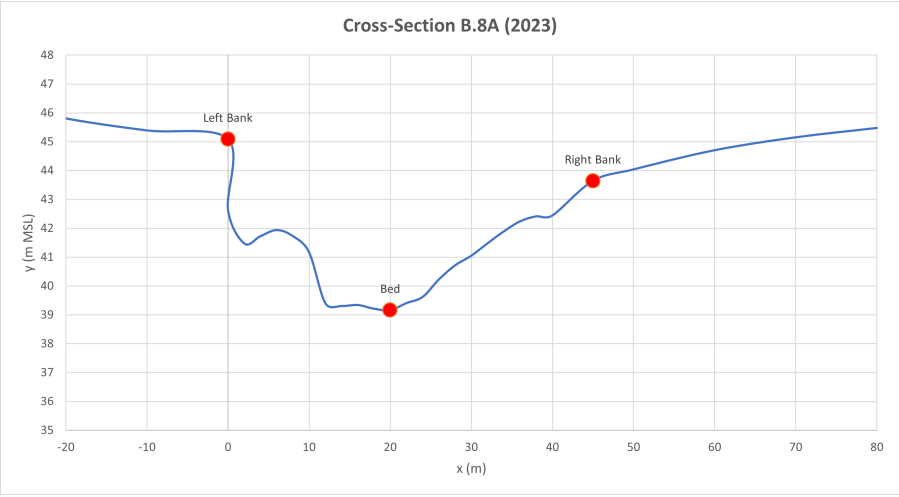

Figure F.3: Cross section river B.8

รูปตัดขวางลำน้ำ ปีน้ำ 2022

สถานี B.8A (ภาพถ่าย เหนือแนวสำรวจสะพาน) ห้วยผาก อ.ท่ายาง จ.เพชรบุรี

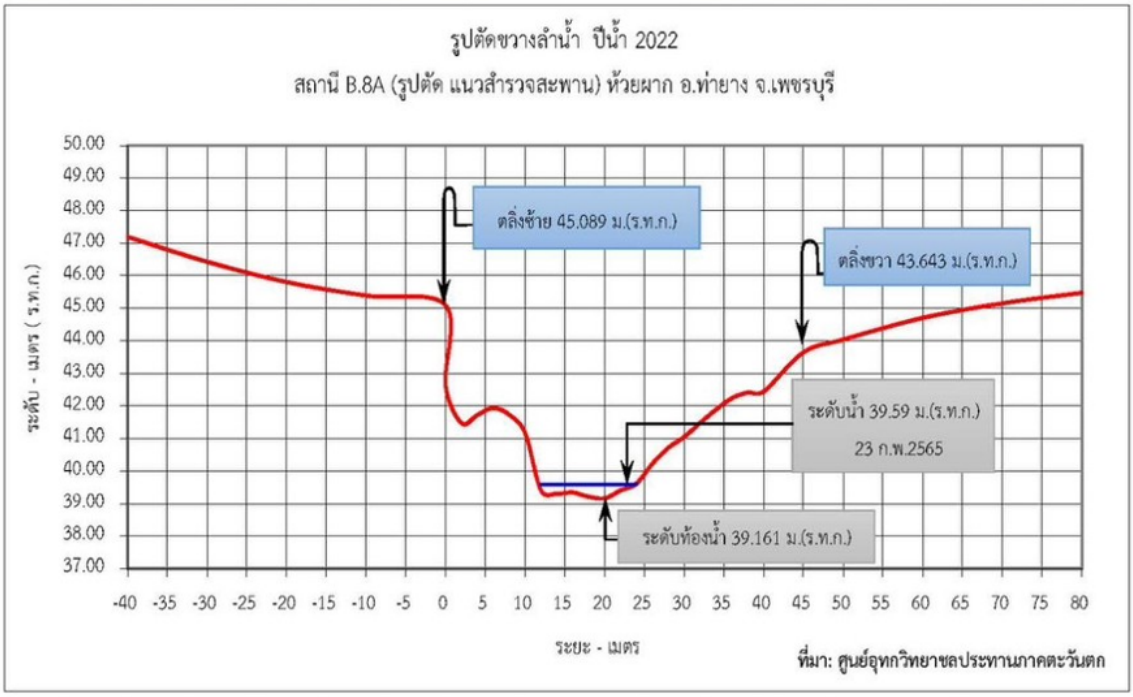

ระยะ	-40	-30	-20	-10	0	0	2	4	6	8	10	12	14	16	18	20	22
ระดับ	47.192	46.429	45.806	45.390	45.089	42.630	41.472	41.723	41.936	41.726	41.163	39.399	39.302	39.338	39.209	39.161	39.404
ระยะ	24	26	28	30	32	34	36	38	40	45	50	60	70	80			
ระดับ	39.618	40.224	40.713	41.047	41.476	41.888	42.236	42.411	42.443	43.643	44.039	44.703	45.151	45.475			

RID.GPS.7119 45.056 ม. (ร.ท.ก.) ศูนย์เสาระดับ 39.100 ม. (ร.ท.ก.) ระดับท้องน้ำ 39.161 ม. (ร.ท.ก.)

ตลิ่งฝั่งซ้าย 45.089 ม. (ร.ท.ก.) ตลิ่งฝั่งขวา 43.643 ม. (ร.ท.ก.)

ผู้สำรวจ นายพงษ์ศิริ จิตต์รัตน์ ผู้ตรวจ นายคทาวุธ สุรินทร์ชมพู บันทึกข้อมูล นายพงษ์ศักดิ์ เปี่ยมท่าน

x (m)	y (m MSL)	remark
-20	80,202	
-10	80,026	
0	79,971	Left Bank
0	79,846	
5	77,631	
10	76,537	
15	75,577	
20	73,885	
25	72,53	
30	71,391	
35	71,031	Bed
40	71,19	
45	71,225	
50	71,787	
55	71,886	
60	71,723	
65	72,879	
70	72,484	
75	72,791	
80	76,182	
85	76,341	
90	78,134	
95	78,591	
100	78,783	
105	79,21	
105	80,012	Right Bank
110	80,001	
120	79,937	
130	79,911	
140	79,722	

Table F.3: Cross section river B.11 data set

F.3 River B.11

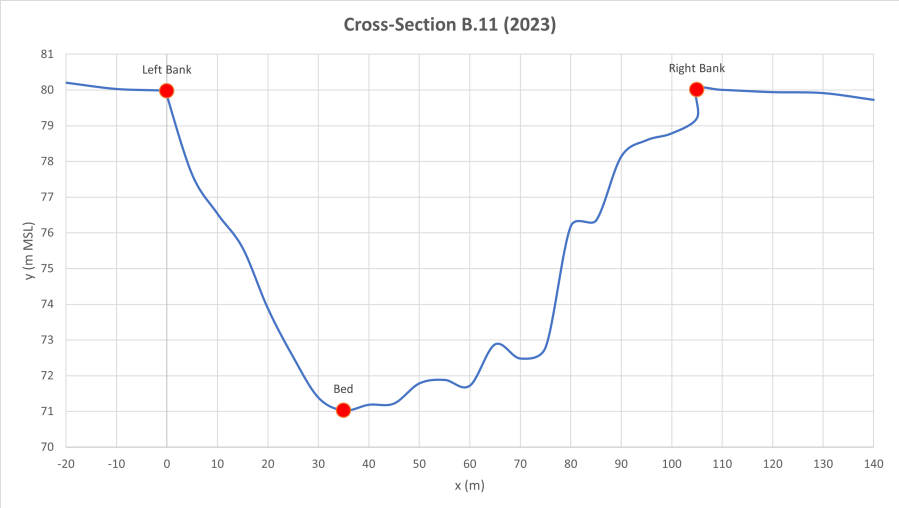

Figure F.5: Cross section river B.11

รูปตัดขวางลำน้ำ ปีน้ำ 2023

สถานี B.11 (ภาพถ่าย เหนือแนวสำรวจสะพาน) ห้วยแม่ประจันต์ อ.หนองหญ้าปล้อง จ.เพชรบุรี

ระยะ	-20	-10	0	0	5	10	15	20	25	30	35	40	45	50	55	60	65
ระดับ	80.202	80.026	79.971	79.846	77.631	76.537	75.577	73.885	72.530	71.391	71.031	71.190	71.225	71.787	71.886	71.723	72.879
ระยะ	70	75	80	85	90	95	100	105	105	110	120	130	140				
ระดับ	72.484	72.791	76.182	76.341	78.134	78.591	78.783	79.210	80.012	80.001	79.937	79.911	79.722				

หมุด RID.GPS.1686	80.214 ม. (ร.ท.ก.)	ศูนย์เสาระดับ	73.000 ม. (ร.ท.ก.)	ระดับท้องน้ำ	71.031 ม. (ร.ท.ก.)
ตลิ่งฝั่งซ้าย	79.971 ม. (ร.ท.ก.)	ตลิ่งฝั่งขวา	80.012 ม. (ร.ท.ก.)	สำรวจเมื่อวันที่	6 กุมภาพันธ์ 2566
ผู้สำรวจ	นายพงษ์ศิริ จิตตรัตน์	ผู้ตรวจ		บันทึกข้อมูล	นายพงษ์ศิริ จิตตรัตน์

Figure F.6: Information river B.11

Appendix G

Appendix Results

B8

Discharge measured by the ORC model and the RID in m3/s

cross-section	21 sep left	21 sep right	21 sep middle	gem. cross	RID
1	0,324	0,2474	0,353	0,308	0,55
2	0,3803	0,41	0,295	0,362	0,55
3	0,3485	0,3518	0,495	0,398	0,55
avarage	0,351	0,3364	0,381	0,356	0,55

21 sep left	quantiles: 5%-25%-50%-75%-95%	std.dev of the quantiles
0.1929527 , 0.	26972204, 0.32398258, 0.37365201, 0.4397473	0,078
0.24960412, 0.	33023262, 0.38032933, 0.42811076, 0.511583	0,073
0.18083515, 0.	2838256 , 0.34853607, 0.41274961, 0.5100011	0,097
		0,083

21 sep right	quantiles: 5%-25%-50%-75%-95%	
0.17092318, 0.	21829698, 0.24739868, 0.27726679, 0.324836	0,044
0.30598551, 0.	36773918, 0.41002688, 0.45158735, 0.515102	0,063
0.2350696 , 0.	30573835, 0.35181762, 0.40185109, 0.4773679	0,072
		0,060

21 sep middle	quantiles: 5%-25%-50%-75%-95%	
0.2886174 , 0.	32624594, 0.35252983, 0.37939689, 0.4183330	0,04
0.25769849, 0.	27858877, 0.29489035, 0.31269608, 0.337404	0,026
0.40280457, 0.	45669555, 0.49488048, 0.53084373, 0.583661	0,056
		0,04

cross-section	26 sep test 2	26 sep test 3	26 sep test 4	26 sep test 5	gem. cross	RID
1	0,243	0,195	0,213	0,259	0,2275	0,6
2	0,3	0,26	0,328	0,268	0,289	0,6
3	0,262	0,193	0,188	0,319	0,2405	0,6
avarage	0,268	0,216	0,243	0,282	0,252	0,6

26 sep test 2	quantiles: 5%-25%-50%-75%-95%	std.dev of the quantiles
0.15773053, 0.	20711955, 0.24329777, 0.27962813, 0.334010	0,054
0.23182812, 0.	27202994, 0.30026107, 0.33001941, 0.369163	0,043
0.14091536, 0.	21456398, 0.26174313, 0.31006054, 0.383175	0,072
		0,056

26 sep test 3	quantiles: 5%-25%-50%-75%-95%	
0.12679005, 0.	16864269, 0.19511219, 0.22122924, 0.259428	0,039
0.15288062, 0.	21464138, 0.25959807, 0.3032121 , 0.3688524	0,066
0.10779085, 0.	15928468, 0.19309429, 0.22617687, 0.273767	0,050
		0,052

26 sep test 4	quantiles: 5%-25%-50%-75%-95%	
0.14449176, 0.	18823702, 0.21255895, 0.23667687, 0.271829	0,036
0.22618924, 0.	2862989 , 0.32841736, 0.37084169, 0.4299616	0,063
0.10426524, 0.	15501002, 0.18797195, 0.22148315, 0.273198	0,05
		0,050

26 sep test 5	quantiles: 5%-25%-50%-75%-95%	
0.19273194, 0.	23247872, 0.25873391, 0.28880547, 0.336508	0,042
0.21798242, 0.	24712088, 0.26819002, 0.28904808, 0.319942	0,031
0.21155593, 0.	27504076, 0.31850596, 0.36743177, 0.437254	0,069
		0,047

new method, where the models standard paramteres are slightly changed

	22 sep left	22 sep right	sep middle	gem. cross	RID
	0,334	0,269	0,425	0,343	0,58
	0,405	0,313	0,267	0,328	0,58
	0,294	0,305	0,68	0,426	0,58
	0,344	0,296	0,457	0,366	0,58

22 sep left	quantiles: 5%-25%-50%-75%-95%	std.dev of the quantiles
0.28769932, 0.	31600225, 0.33421536, 0.35383424, 0.3819159	0,028
0.35182462, 0.	38391795, 0.40517167, 0.42671952, 0.4572298	0,032
0.23531221, 0.	26946556, 0.29397849, 0.31712824, 0.3506501	0,036
		0,032

22 sep right	quantiles: 5%-25%-50%-75%-95%	
0.22310536, 0.	249369 , 0.26911374, 0.28926568, 0.32246637	0,03
0.26198765, 0.	29206272, 0.31299637, 0.33339648, 0.3670140	0,031
0.23107415, 0.	27584742, 0.30503201, 0.3347491 , 0.3776092	0,044
		0,035

22 sep middle	quantiles: 5%-25%-50%-75%-95%	
0.35178149, 0.	39509462, 0.42519972, 0.45624801, 0.5006562	0,046
0.23845327, 0.	25429256, 0.26690963, 0.28106856, 0.3002014	0,02
0.52945399, 0.	61804623, 0.68017988, 0.74480153, 0.8395799	0,095
		0,054

old method, where the same parameters of the tutorial notebook are used

	22 sep left	22 sep right	sep middle	gem. cross	
	0,365	0,286	0,394	0,348	0,58
	0,422	0,378	0,284	0,361	0,58
	0,345	0,347	0,794	0,495	0,58
	0,377	0,337	0,491	0,402	0,58

22 sep left	quantiles: 5%-25%-50%-75%-95%	std.dev of the quantiles
0.26976059, 0.	33344651, 0.36530878, 0.39940108, 0.4423474	0,049
0.32668212, 0.	38248331, 0.42171251, 0.46023642, 0.5175864	0,058
0.2563821 , 0.	30948071, 0.34494463, 0.37754478, 0.4305562	0,051
		0,053

22 sep right	quantiles: 5%-25%-50%-75%-95%	
0.20900174, 0.	25295133, 0.28630519, 0.31870703, 0.3741581	0,049
0.28742762, 0.	34285073, 0.37836613, 0.41739022, 0.4740546	0,056
0.25185686, 0.	30809235, 0.34653213, 0.38718959, 0.4538549	0,059
		0,055

22 sep middle	quantiles: 5%-25%-50%-75%-95%	
0.29689913, 0.	35358067, 0.39418177, 0.42896871, 0.4838410	0,056
0.23805646, 0.	26310487, 0.28441699, 0.30322899, 0.3313028	0,03
0.57534386, 0.	7103178 , 0.79383053, 0.8749965 , 1.00461971	0,124
		0,07

B3

Discharge measured by the ORC model and the RID in m 13:45

cross-section	25 sep test 1	25 sep test 2	25 sep test 3	25 sep test 4	25 sep test 5	gem. cross	RID ADCP	RID
1	18,23	20,07	14,04	17,56	30,85	20,15	31	37,65
2	11,76	10,92	4,75	6,69	16,58	10,14	31	37,65
average	14,995	15,495	9,395	12,125	23,715	15,145	31	37,65

25 sep test 1	quantiles: 5%-25%-50%-75%-95%	std dev of the quantiles
-41.78018452, 1.	36980583, 18.23026666, 40.3737265 , 93.805	29,25
-70.37370048, -14.	00149228, 11.76373929, 35.27747212, 95.	36,96
		33,105

25 sep test 2	quantiles: 5%-25%-50%-75%-95%	
-9.31778433, 9.	80269438, 20.07023442, 33.54899637, 60.849	17,81
-43.5895204 , -5.	07466663, 10.92394058, 26.28972087, 59.24	23,52
		20,665

25 sep test 3	quantiles: 5%-25%-50%-75%-95%	
45.90487705, 24.	72150958, 14.042543 , 7.3680822 , -1.49005	13,02
43.06158916, 12.	00193873, 4.75446745, -1.28886068, -30.40	9,97
		11,495

25 sep test 4	quantiles: 5%-25%-50%-75%-95%	
46.75951358, 27.	95112249, 17.56077809, 9.73784179, 0.1345	13,66
27.34415634, 13.	38273329, 6.69347041, 0.52503903, -10.662	9,64
		11,65

25 sep test 5	quantiles: 5%-25%-50%-75%-95%	
56.31432936, 40.	35261535, 30.85004868, 22.60455703, 11.06	13,31
54.73061784, 28.	3818385 , 16.5788755 , 7.04347146, -15.450	16
		14,655

cross-secti	26 sep test 1	RID
1	21,35	37,65
2	12,9	37,65
average	17,125	37,65

26 sep test	quantiles: 5%-25%-50%-75%-95%	std dev of the quantiles
8.16184848, 16.	77916067, 21.35370493, 25.68517812, 36.38841	6,68
1.14982402, 8.	68890388, 12.89655233, 18.54718996, 32.743917	7,39
		7,035

cross-secti	28 sep test 1	RID
1	21,46	37
2	15,15	37
average	18,305	37

28 sep test	quantiles: 5%-25%-50%-75%-95%	std dev of the quantiles
9.60377219, 16.	65373779, 21.46102924, 26.70630992, 40.15264	7,54
-4.65429276, 8.	42428004, 15.14960465, 24.22822178, 56.15397	11,85
		9,695

B11

Discharge measured by the ORC model and the RID in m3/s

First GPS coordinates used which turned out to be far off

cross-section	27 sep test 1	27 sep test 2	gem. cross
1	0,324	0,311	0,3175
2	0,38	0,44	0,41
3	0,35	0,901	0,6255
avarage	0,351	0,551	0,451

second GPS coordinates used who were more accurate

cross-section	27 sep test 1	27 sep test 2	27 sep test 3	gem. cross	RID mean std = 0,434
1	0,4313	0,4305	0,4145	0,425	0,434
2	0,5355	0,6375	0,5671	0,580	0,434
3	0,4218	0,505	0,6124	0,513	0,434
avarage	0,463	0,524	0,531	0,506	0,434

27 sep test 1	quantiles: 5%-25%-50%-75%-95%	std dev of the quantiles
0.57767021,	0.49067338, 0.43125877, 0.37355363	0,088
0.68845673,	0.60241093, 0.53553685, 0.4598678	0,107
0.53322062,	0.4713631 , 0.42178372, 0.37182596	0,075
		0,09

27 sep test 2	quantiles: 5%-25%-50%-75%-95%	
0.57778214,	0.48639619, 0.43048282, 0.37283265	0,085
0.84035814,	0.72250361, 0.63752306, 0.54055451	0,136
0.67950391,	0.57977132, 0.50504174, 0.43094598	0,112
		0,111

27 sep test 3	quantiles: 5%-25%-50%-75%-95%	
0.48761462,	0.44343747, 0.41447858, 0.38370075	0,045
0.70442248,	0.6276009 , 0.56711912, 0.50628427	0,091
0.74845411,	0.67815334, 0.61240362, 0.54915195	0,097
		0,078

second GPS coordinates used who were more accurate

cross-section	28 sep test 1
1	0,3865
2	0,5402
3	0,3055
avarage	0,411

28 sep test 1	quantiles: 5%-25%-50%-75%-95%	std dev of t
0.47441805,	0.42426374, 0.38654595, 0.3527413	0,072
0.91771686,	0.7323603 , 0.54022801, 0.34233193	0,293
0.36181963,	0.33462778, 0.30554284, 0.2719291	0,047
		0,137

First GPS coordinates used which turned out to be far off

cross-section	29 sep test 1
1	0
2	0,9
3	0
avarage	0,300

second GPS coordinates used who were more accurate

cross-section	29 sep test 1	29 sep test 2	gem. cross
1	0,47	0,4729	0,47
2	0,513	0,6242	0,5686
3	0,43	0,5354	0,4827
avarage	0,471	0,544	0,508

29 sep test 1	quantiles: 5%-25%-50%-75%-95%	std dev of the quantiles
0.88962663,	0.64716033, 0.46997593, 0.32732963, 0.	0,24
0.99863602,	0.70472946, 0.51297893, 0.33091422, 0.	0,28
0.62096494,	0.52473297, 0.43576313, 0.36585008, 0.	0,119
		0,213

29 sep test 2	quantiles: 5%-25%-50%-75%-95%	
0.59214615,	0.52153567, 0.47289314, 0.42439075, 0.	0,073
0.86012365,	0.73998784, 0.62417695, 0.50441046, 0.	0,177
0.69237266,	0.60271305, 0.53538748, 0.46584694, 0.	0,103
		0,118